VARIATION OF CRANIAL BONE SCULPTURING IN GEKKOTA

_____

A Thesis

Presented to

The Faculty of the Department of Biological Sciences

Sam Houston State University

_____

In Partial Fulfillment

of the Requirements for the Degree of

Master of Science

_____

by

Elizabeth Glynne Sullivan

August, 2018

VARIATION OF CRANIAL BONE SCULPTURING IN GEKKOTA

by

Elizabeth Glynne Sullivan

_____

APPROVED:

Juan D. Daza , PhD
Thesis Director

Aaron M. Bauer, PhD
Committee Member

Sibyl R. Bucheli, PhD
Committee Member

Monte L. Thies, PhD
Committee Member

John B. Pascarella, PhD
Dean, College of Science and Engineering Technology

DEDICATION

To my friends and family who have helped make this dream a reality, do you know how wonderful it is to have you? I hope you do.

I love you.

Elizabeth

ABSTRACT

Sullivan, Elizabeth Glynne, *Variation of cranial bone sculpturing in Gekkota*. Master of Science (Biology), August, 2018, Sam Houston State University, Huntsville, Texas.

Cranial bone sculpturing has not been evaluated in Gekkota. The first aim of this study was to identify the presence of cranial bone sculpturing by completion of a bone by bone analysis and then optimizing the character information onto a known molecular tree from Gamble et al. (2012). All three identified types of cranial bone sculpturing were identified in at least one member of Gekkota. It was found to occur almost exclusively on the dermatocranium, except for *Chondrodactylus bibronii*. Upon optimization of the character, there was only one family found to be entirely smooth (Pygopodidae), while the remaining have at least one occurrence of cranial bone sculpturing. Regardless, the predominant character state for cranial bones remains to be smooth. The second aim of this study was to investigate the relationship between cranial size and bone sculpturing, in both an intra- and interspecific context. Smooth and grooved cranial bone sculpturing can be found on any skull size, whereas pitted and grooved cranial bone sculpturing is found on the medium to larger sized skulls, excluding *Matoatoa*. Rugose cranial bone sculpturing develops from an almost smooth cranial surface to the extreme morphology seen in the skeletally mature individual. Pitted cranial bone sculpturing develops comparably to that observed in crocodiles, grooved sculpturing that progresses to the extreme morphology observed in the skeletally mature individual. Confirming variation of cranial bone sculpturing in Gekkota.

KEY WORDS: Cranial bone sculpturing, Gekkota, Dermal bones, Sam Houston State University

ACKNOWLEDGEMENTS

I would like to thank my advisor, Dr. Juan Diego Daza, for bringing me into the scientific world. I would also like to thank my committee members, for their continued patience and effort in helping me accomplish this thesis work. To my lab mates and academic siblings, both here at Sam Houston State University and those at their respective universities, thank you for the thought-provoking conversations and continued support.

TABLE OF CONTENTS

Page

LIST OF FIGURES

CHAPTER I

Background

Ornamentation and sculpturing

Textured bone surfaces have been described using several names, including but not limited to: ornamentation (e.g., de Buffrenil, 1982), cranial ossification (e.g., Boulenger, 1885), and sculpture or sculpturing (e.g., Witzmann, 2009). It is necessary to distinguish bone sculpturing from bone ornamentation, as the latter is known to produce extreme morphologies (e.g., large frills seen in triceraptopsian dinosaurs or the parietal horns of the phyrynsomatid lizards). In this thesis, I propose to restrict the term ornament or ornamentation to the hypermorphosis in the skull of vertebrates, which are analogous to large structures in other groups. The term sculpturing will be used to describe the texture on the bone that does not necessarily produce a hypermorphosis. Using these narrow definitions, in a chameleon the large casque would be considered bone ornamentation, whereas the bumpy texture on the surface of the cranial bones would be considered bone sculpturing (Figure 1).

Vertebrate skull development, emphasis on reptiles

Both terms, ornamentation and sculpturing, are used in conjunction with the descriptor, dermal. This association assumes that both structures are developed and limited to the roofing bones, or the dermatocranium. As seen in Figure 2, the vertebrate skull is formed by three major units (Hall, 2005; Kardong, 2012): the splanchnocranium or visceral cranium (composed of cartilage and endochondral bone), the chondrocranium (composed of cartilage and/or endochondral bone), and the dermatocranium (composed of intramembranous bone, also known as dermal or membrane bone). The lizard skull is

formed by two kinds of bone, intramembranous and endochondral bone (Romer, 1956; Hall, 2005). Intramembranous bone forms the exocranium, which overlies endochondral elements or endocranial bones (Rieppel, 1993; Trueb, 1993). As this study is not restricted to bones of dermal origin, but to all the bones comprising the cranial structure, a more generalized term, cranial bone sculpturing, will be used.

Sculpturing across taxa

Cranial bone sculpturing has been well documented in basal tetrapods (Bystrow, 1935; Coldiron 1974; Shooch, 2002; Witzmann, 2009; Witzmann and Soler-Gijon, 2010; Witzmann et al, 2010; Morkovin, 2015). A correlation between their physiology and the cranial bone sculpturing has been well hypothesized, specifically by the presence of the rete vasculosum (Bystrow, 1935). The rete vasculosum was proposed to assist in cutaneous respiration, specifically in the carbon exchange on land to avoid excessive carbon dioxide in the bloodstream or hypercapnia (Bystrow, 1947; Witzmann et al, 2010; Janis et al., 2012).

Although the functional purpose of cranial bone sculpturing is still debated and appears to be taxon specific, cranial bone sculpturing has evolved multiple times, being observed and defined in several taxa (Trueb, 1993; Jared et al., 2015; Clarac et al., 2016; de Buffrenil et al., 2016; Protzel et al., 2017). Additional functions for cranial bone sculpturing include: mechanical reinforcement of the bone (Coldiron, 1974; Evans, 2008; Rhinehart and Lucas, 2013), assisting in thermoregulation (e.g. the osteoderms in alligators, Seidel, 1979; Clarac et al., 2015), increase in surface area to allow for an increase in integument (Cosgriff and Zawiskie, 1979; Schoch, 2001), or strengthening the

attachment of the skin to the surface of bone or coosification of the skin (Romer, 1947; Trueb, 1993; Witzmann, 2009; Witzmann et al., 2010, Dias and Richter, 2002).

There are reports where the cranial bone sculpturing assists a specialized morphological structure. For some hylid frogs, such as *Corythomantis greeningi* and *Aparasphenodon brunoi*, the cranial bone sculpturing helps with gland excretions, assisting in the injection of a toxin to a potential predator during predation attempts (Jared et al, 2015). Ceratopsian dinosaurs have highly vascularized, grooved nasal complexes, rostral complexes, that supported the keratinized rhamphotheca surmounting these bones (Horner and Goodwin, 2008). In chameleons, cranial bone sculpturing, coupled with an epidermal structure, is plays a role in the accentuating UV light coloration (Protzel et al., 2017). Overall the functionality of this feature has been overlooked and understudied, especially in consideration of reptiles.

Sculpturing across Squamata

Cranial bone sculpturing has been applied in a phylogenetic context for Squamata on multiple occasions. Camp (1923) was one of the earliest phylogenetic studies that considers this trait. He described both the "embossed tuberculate osteoderms" in *Heloderma* and the "dermal cranial ossifications" that occurred in iguanians (cf. *Amblyrhynchus* and *Phyrnosoma mcallii)* and rarely in gekkotans. To identify qualitatively this character, Estes et al. (1988; character 129), defined it as dermal rugosities, or impressions left in the dermal bone from the cephalic scales. The character was coded in consideration of three character states: (0) absent, (1) present but not vermiculate, or (2) present and vermiculate. This character was found to be uninformative at this level of a phylogenetic analysis, as it varied too much within the basal taxa.

Conrad (2008) coded four characters regarding dermal sculpturing: (0, irregular; 1, pitted; 2, bumps/hornlets) and characters 8, 9 and 10 regarding the location of the observed sculpturing (maxilla, prefrontal, frontal/parietal), and character 7 regarding the type of bone sculpturing observed. Conrad's character definition differs from Estes et al. (1988) in how the character was coded as well as the character states varying. Conrad's (2008, 2017) characters did not consider the lack of sculpturing (i.e. smooth) as a character state, therefore, when bone sculpturing was not observed, he scored this trait as inapplicable (-). In the further development of the character, incorporating both location and type of cranial sculpturing occurring, this character was listed as possible synapomorphies for groups, primarily based on the location of the occurrence of cranial sculpture: maxilla (Teiidae, Anguimorpha, Cordyloidea, and Priscagamidae†), prefrontal (clade Opluridae + Tropidurinae + *Liolaemus*+ *Leiocephalus*, and clade Crotaphytidae + Iguanidae + Polychrotiformes + Hoplocercidae + Chameleontiformes) and frontal/parietal (Autarchoglossa). In this analysis, gekkotans were marked as this character being inapplicable (-) for character 7 and smooth for characters 8 through 10, creating a possible bias in the evaluation of this character. Though geckos bearing described cranial bone sculpturing were listed as being reviewed in the study, the cranial bone sculpturing was overlooked by Conrad (2008), (e.g. *Phyllurus* and *Pachydactylus*). Though the sculpturing was recorded accurately for *Saltuarius* in a later study, due to the limited number of individuals sampled, a true representation of the sculpturing types within gekkotans was not accurately represented (2017).

Gauthier et al. (2012) included character 572, dermal skull bone ornamentation. Cranial bone sculpturing was scored in this single character and with four states: (0)

smooth, (1) lightly rugose about the frontoparietal suture, (2) present over dorsum, and (3) present on jugal-postorbital bar. This varies from the previous analyses as this study accounts for the lack of cranial bone sculpturing and attempts to incorporate location and presence in one character. This analysis does not account for the other varying types of cranial bone sculpturing previously mentioned, only accounting for the extreme, rugose, cranial bone sculpturing (Gauthier et al., 2012). Gauthier et al. (2012) found that the cranial bone sculpturing was occurring on three different areas of the skull: dorsal regions of the skull (Hoplocercinae, and Autarchoglossa), around the frontoparietal suture (Varanidae) and on the jugal post-orbital bar (Priscagaminae and Xenosauridae). All gekkotans within this analysis, with the exception of the extreme rugosities of *Saltuarius cornutus,* were scored as being smooth (Gauthier et al., 2012).

Sculpturing of Gekkota

Gekkota is a species-species rich group, currently estimated to include over 1,700 species (Bauer, 2013; Uetz et al., 2017), and highly appropriate for the study of evolutionary patterns. Gekkota is currently divided into seven families (Uetz et al., 2017): Carphodactylidae (7 genera), Eublepharidae (6 genera), Gekkonidae (61 genera), Diplodactylidae (25 genera), Sphaerodactylidae (12 genera), Pygopodidae (**7** genera), and Phyllodactylidae (10 genera). Geckos have been regarded as having smooth bones, or showing no bone sculpturing (Williston, 1925; Conrad, 2008; Evans, 2008; Gauthier et al., 2012). Cranial bone sculpturing has been described in the dermatocranium of geckos as isolated observations of individual descriptions: *Phyllurus*, *Carphodactylus*, *Nephrurus* (Bauer, 1990 and Stephenson, 1960), *Pachydactylus (*Bauer and Lamb, 2005 and Evans, 2008), *Quedenfeldtia,* and *Homonota* (Daza et al., 2012), and in fossil groups

(*Rhodanogekko vireti* and *Cadurcogekko verus*; Daza et al., 2014; Bolet et al., 2015). In both Conrad (2008) and Gauthier et al. (2012), the use of the character cranial bone sculpturing was flawed in its coding (Simões et al., 2016). To date only one systematic review of cranial bone sculpturing within has been produced (Glynne et al., 2015).

Objectives

A revision of the bone sculpturing observed in gekkotans is necessary at this point. Using previously defined categories (Janis et al., 2012; de Buffrenil et al., 2015), I will review in detail the surface of each bone that comprises the skull in geckos. I will then investigate the distribution of this feature in gekkotans by optimizing the presence and type of bone sculpturing on a gekkotan genus level molecular phylogeny (Gamble et al., 2015). I will also explore the relationship between bone sculpturing and body size in both interspecific and intraspecific contexts.

CHAPTER II

Cranial sculpturing in a phylogenetic context

Objectives and predictions

The presence of cranial bone sculpturing has been documented in individual gekkotan species (Stephenson, 1960; Bauer, 1990), however it needs to be evaluated in a phylogenetic context including a large taxon sample. The main objective of this study was to explore the distribution of cranial bone sculpturing within Gekkota. This raised the following questions: 1) how variable is cranial bone sculpturing among gekkotan taxa, 2) is cranial bone sculpturing homogeneous in the various bones within the skull, and 3) is the occurrence of cranial bone sculpturing linked to phylogeny. Given these questions, I hypothesized that the presence of cranial bone sculpturing is linked to phylogeny within Gekkota.

Methods

Characters and character state definitions. To evaluate cranial bone sculpturing within geckos, a bone by bone inspection of one or more species from each gekkotan genus was completed. A total of 26 skull bones were analyzed in each skull, including the premaxilla, maxillae, nasals, prefrontals, lacrimals, frontal, parafrontal bones, parietals, postorbitofrontals, quadrates, squamosals, supratemporals, jugals, vomers, palatines, pterygoids, ectopterygoids, epipterygoids, dentaries, coronoids, splenials, surangulars, otostapes, supratemporals, compound bone, basicranium (the last two bones were treated as a single unit), and osteoderms when present (Figures 3 and 4).

Character scores were assigned under the hypothesis that the qualitative similarities of the cranial bone sculpturing described in previous morphological studies were comparable to what was observed within gekkotans. The following definitions were used for each state: granular (i.e., rugose, or pustulose), vermicular (i.e., grooved), as well as pitted (Bystrow, 1935; Coldiron, 1974; de Buffrenil et al., 2015). Characters were scored using multi-state characters: (0) bone smooth, not having sculpturing, (1) bone grooved or vermicular, (2) bone pitted or pit and ridge, and (3) bone rugose or granular (Figure 5). Non-universal elements for the Gekkota, such as the lacrimal, parafrontal bones, supratemporal, and osteoderms, were coded as inapplicable (-) when they were absent from the skull. When osteoderms were present they were scored as being (0) smooth or (1) sculptured, because, the sculpturing observed did not clearly fit into the categories defined for this study. If a representative skull was missing from the data set or if the characters could not be observed, the character scores were coded as unknown (?). For this study, smooth or unsculptured bones were defined as having a continuous surface texture of the bone. Grooved or vermicular bones sculpturing were defined by the presence of shallow and interconnected grooves in the surface of the bone. Pitted or pit and ridge bone sculpturing was defined as a repetitive pattern of rounded pits surrounded by a network of crests in surface of the bone. Rugose or granular bone sculpturing was defined as there being distinct projections stemming from the surface of the bone. A complete list of the characters and characters states scored is included in Appendices A and B.

List of specimens. I used the gekkotan phylogenetic based on molecular data (Gamble et al., 2015). This publication is the most updated Gekkotan molecular tree,

incorporating 5 nuclear protein-coding genes (RAG1, RAG2, C-MOS, ACM4, and PDC) and one mitochondrial fragment (ND2 and associated tRNAs). Cranial bone sculpturing was observed in specimen trying to match the taxon sampling in Gamble et al. (2015). For the 148 genera used in Gamble et al.'s 2015 study, 134 skeletally mature adults were represented in this study on the genus level, and 95 matching on the species level. Only five genera were not represented in this study (Viz., *Uvidicolus*, *Paniegekko*, *Tukutuku*, *Hesperoedura*, and *Altiphylax*), therefore they were left as missing data (?).

Visualization. Cranial bone sculpturing was determined using skeletonized specimens, digital photographs of skeletonized specimens from museum collections, and high-resolution X-ray computed tomography (HRCT), both from Drs. Aaron M. Bauer and Juan D. Daza's digital collection as well as from Digimorph (digimorph.org). Most of the specimens were scanned at The University of Texas High-Resolution X-ray CT facility (UTCT) and the American Museum of Natural History (AMNH). Three dimensional renderings were obtained with Avizo lite v. 9.4.0 (Thermo Fisher Scientific Inc., Waltham, MA, USA, 2017). Each skull model was rendered using the "volume rendering" option, allowing for an accurate 3D skull to be viewed. The skulls were virtually sliced using the program function "orthoslice", to allow for observation of the deeper bones within the skull. Since material density threshold in volume rendering option can affect the surface appearance in HRCT models, the threshold values were calibrated ensuring that the values used matched bone appearance in computed tomography images and/or the skeletonized specimens. These threshold values were recorded to ensure replication if needed (Figure 6). Digital images, specimen from digimorph.org, and skeletonized materials were used to score individuals if they were

not. if they were not represented with a CT scan. Skull characters were scored using the best available pictures. If the bone was not visible, it was treated as unknown data (?). If it is a known bone that is identified in the skull of that individual, it will be treated as inapplicable data (-). Direct observations were done in skeletonized specimens from the Bell museum of Natural History using a Leica MZ6 dissecting microscope. As disarticulation of these specimen preparations would be necessary for the observation of the inner bones (e.g., the palatine, vomer, pterygoid, etc.), not all bones within the skeletonized skull were suitable for getting information about sculpturing. For this reason, along with the ease and accuracy of rendering and observation, this study favored the use of CT scans when available. For each specimen used the identification number and preparation will be noted below.

Analyses. To determine the prevalence of cranial bone sculpturing across Gekkota, the unordered characters were mapped using the molecular phylogeny of Gamble et al. (2015). Tree file with taxon names was downloaded from the dryad repository (file: *Diurnality_6gene.part1.Yule*, https://datadryad.org//resource/doi:10.5061/dryad.97b50, Gamble et al., 2015). The file was opened in Mesquite 3.40, and the morphological characters and scores were added to the matrix editor in that file. The updated tree file with morphological data were exported to Winclada for parsimony optimizations. Winclada's interface is advantageous because allows simultaneous visualization of all characters in the tree.

Character mapping of the 26 morphological traits was done using different criteria (Parsimony [fast, slow and unambiguous optimization] and likelihood methods). Parsimony methods were completed using the fast, slow and unambiguous optimizations

in Winclada v. 1.0000, (i.e., Nixon, 1999-2002). Likelihood methods were completed using Mesquite 3.40. The character states were simplified to represent if cranial bone sculpturing was absent (0) or present (1) for the likelihood analysis. This was to accommodate for the polymorphic states that were found in select individuals (e.g. *Blaesodactylus antongilensis* UMMZ 192320).

Results

General. Cranial bone sculpturing of any of the categories listed above was found present in 22 genera examined in this study (*Orraya, Phyllurus, Saltuarius, Underwoodisaurus, Carphodactylus, Goniurosaurus, Hemitheyconyx, Holodatylus, Queldenfeldtia, Euleptes, Thecadactylus, Phyllopezus, Pseudothecadactylus, Haemodracon, Gehyra, Hemidactylus turcicus, Uroplatus, Matotoa, Paredura, Blaesodactylus, Homopholis*, and *Chondrodactylus*). Cranial bone sculpturing confirmed the presence of sculpturing types (grooves, pits, and rugosities) listed in literature. The cranial bone sculpturing was found exclusively in dermal bones and was more frequently on the dorsal surface of the snout, with the exception of *Chondrodactylus bibronii*. Cranial bone sculpturing was also observed on the osteoderms of 5 genera examined (*Rhyncoedura ornata*, *Tarentola mauritanica*, *Gekko gecko, Geckolepis maculata* and *Microgecko persicus*); however, outside of *Geckolepis maculata* the sculpturing identified did not fit the categories defined for the study (Figure 7). *Rhyncoedura ornata* and *Microgecko persicus* had osteoderms that were too small to properly analyze with the CT scan available and may be what are considered "beam hardening" artifacts (when the edge of the specimen looks bright as a result of the scanning process). *Geckolepis maculata*'s osteoderms were distinctly smooth, whereas *Tarentola mauritanica* has a

combination of grooved and pitting. *Gekko gecko* was unique in that it appeared to have a singular pit central to the osteoderm with the osteoderm experienced a form of hyperossification or being rugose.

Parsimony. The lack of dermal bone sculpturing, or presence of smooth dermal bones was the most prevalent condition among gekkotans. Using parsimony (Acctran and Deltran optimizations), the ancestral condition for the Gekkota is having a skull with smooth maxilla and prefrontal bones. Pygopodidae was the single family where members all had smooth bones (Figures 6, 9, and 12). There are other clades within the remaining families that show prevalence of smooth bones, including the new world sphaerodactylid geckos, some members of Phyllodactylidae (*Gymnodactylus*, *Phyllopezus*, *Garthia*, *Homonota*, and *Phyllodactylus*), and many clades within Gekkonidae (e.g., the Indopacific gecko group, *Nactus*, *Dixonius*, *Heteronotia*, *Luperosaurus*, *Lepidodactylus*, *Pseudogecko*, *Gekko*, *Ptychozoon*).

Most families were predominately smooth and didn't had many members where cranial bone sculpturing was observed. Diplodactylidae had predominately smooth bones with the exception of two individuals, *Rhynchoedura* and *Pseudothecadactylus* (Figures 8, 11, and 14). The genus *Rhynchoedura* has osteoderms that had a sculpturing texture. The genus *Pseudothecadactylus* changed from the ancestral state with the maxilla and prefrontal bones bearing rugose sculpturing. The nasal and frontal bones were also rugose for this taxon, while the parietal bones were grooved. Phyllodactylidae also had predominately smooth bones with the exception of three genera, *Tarentola, Haemodracon* and *Thecadactylus* (Figures 9, 12, and 15). *Tarentola mauritanica* has osteoderms that had a sculpturing texture. The genera *Haemodracon* and *Thecadactylus*

both retained the ancestral state of smooth maxilla and prefrontal bones. However, they both have grooved sculpturing on the frontal and prefrontals. While the new world sphaerodactyls remained smooth, the Old World *Quedenfeldtia*, *Euleptes*, and *Teratoscincus roborowskii* all had grooved cranial bone sculpturing occurring on the frontal bone (Figures 9, 12, and 15). For *Quedenfeltia* and *Teratoscincus* there was additional grooving on the parietals. *Teratoscincus* is the only member of the Sphaerodactylidae that diverged from the ancestral condition and developed grooved prefrontals.

For Eublepharidae and Gekkonidae, though they could also be considered predominately smooth, the ancestral states varied according to the optimizations. Under an unambiguous optimization the ancestral state for Eublepharidae remained smooth with only *Goniurosaurus* having grooved sculpturing occurring on the nasal, prefrontal and postorbitofrontal bones. Under a fast optimization (ACCTRAN), the ancestral state was a grooved frontal and parietal for the clade consisting of *Goniurosaurus, Eublepharis, Holodactylus,* and *Hemitheconyx*. *Goniurosaurus* has additional grooved sculpturing occurring on the nasal, prefrontal and postorbitofrontal bones. *Eublepharis* under this optimization, had a reversal to the ancestral state of bearing smooth frontal and parietal bones. Under slow optimization (DELTRAN), the ancestral state for the clade consisting of *Hemitheconyx* and *Holodactylus* was to have grooved frontal and parietal bones. *Goniurosaurus* then appears to have a convergence in these characters, as well as additional grooved sculpturing occupying the maxilla, nasal, and postorbitofrontal bones. For Gekkonidae the majority of the cranial bone sculpturing that occurred did not vary across the different optimizations (*Gekko, Microgecko, Gehyra, Hemidactylus,*

Uroplatus, Matoatoa, Homopholis and *Blaesodactylus*; Figures 10, 13, and 16). *Gekko gecko* and *Microgecko* had osteoderms that possessed sculpturing that was uncategorized in this study. *Gehyra vorax* and *Hemidactylus turcicus* had grooved sculpturing that occupied the premaxilla, maxilla, nasal, prefrontal, frontal, parietal and postorbitofrontal bones. *Uroplatus* had grooved sculpturing occurring on the frontal and parietal bones. *Matoatoa* was unique in that it was one of two members of the Gekkonidae that has rugose sculpturing along the premaxilla, nasal, maxilla and prefrontal bones. The clade comprised of *Homopholis* and *Blaesodactylus* shared an ancestral state of grooved sculpturing occupying the maxilla, nasal, prefrontal, frontal, parietal and postorbitofrontal bones. When variation did occur in the optimizations, it occurred in two genera, *Paroedura* and *Chondrodactylus* (Figures 10, 13, and 16). In the fast optimization, *Paroedura stumpffi* and *Paroedura picta* have an ancestral state of grooved nasal, prefrontal, frontal, parietal and postorbitofrontal bones. *Paroedura stumpffi* diverged from the ancestral state to have rugose nasal, prefrontal, frontal, parietal and postorbtitofrontal bones; whereas *Paroedura picta* only additionally had the nasal bones grooved.

Though the presence of sculpturing was not consistently found within gekkotans, when cranial bone sculpturing was present, it was predominantly found within members of the Carphodactylidae (Figure 8, 11, and 14). Though the characters varied between the three optimizations, rugose bone sculpturing of the frontal bones was found to be the ancestral condition for the members of the Carphodactylidae. For the unambiguous and slow optimizations, the ancestral condition for the family also included rugose parietal bones. Under fast optimization, the ancestral condition for Carphodactylidae, with the

exclusion of *Orraya*, included rugose sculpturing on the nasal and prefrontal bones. *Phyllurus* and *Saltuarius* had the ancestral condition of rugosities occurring on the maxilla and postorbitofrontal bnones. The clade containing *Uvidicolus sphyrurus*, *Nephrurus levis*, and *Underwoodisaurus milii*, had an ancestral condition that included a reversal to smooth maxilla, nasal, prefrontal and frontal bones. *Underwoodisaurus* diverged to the have grooved sculpturing that occupies the nasal, prefrontal, frontal, and parietal bones. For the unambiguous and slow optimizations, *Phyllurus* and *Salturarius* had an ancestral character of rugose postorbitofrontals. For the slow optimization, the ancestral characters for this clade also included rugose nasal, prefrontal, and parietal bones.

Likelihood. Changing character states to absent (0) or present (1) did not have any effect in the optimized ancestral condition of smooth cranial bones for gekkotans. Cranial bones that are unique to few taxa, including osteoderms, parafrontals, lacrimals, and supratemporals, were not included in this analysis. Lacking any cranial sculpturing was the ancestral condition for each bone across gekkotans (Figures 17-27), which is consistent with the synapomorphies of Gekkota previously identified (Gauthier et al., 2012). There were multiple cranial bones that were observed to be smooth, across all taxa and included: squamosal(s), jugal(s), vomer(s), palatine(s), pterygoid(s), ectopterygoid(s), dentary(s), surangular(s), compound bone(s), otostape(s), epipterygoid(s) and the braincase (Figure 25). Though the overall ancestral condition for gekkotans is smooth, the presence of cranial bone sculpturing was the ancestral condition for Carphodactylidae for the frontal and parietal bones (Figure 21 and 22). Cranial sculpturing is a defining feature of the Carphodactylidae, and occurs convergently in one

genus within Diplodactylidae (*Pseudothecadactylus*) and four within Gekkonidae (*Matoatoa, Paroedura, Chondrodactylus, and Blaesodactylus*). Other clades might be defined as presenting the plesiomorphic condition (smooth) in all members (e.g., Pygopodidae, Sphaerodactylinae), while pitted is an autapomorphy for *Chondrodactylus bibronii.*

Discussion

This study contributed to the identification of cranial features that serve to diagnose some gekkotan clades based on cranial bone sculpturing. Though the cranial bones in gekkotans are predominately smooth, cranial bone sculpturing is present in bones of at least 22 gekkotans. The cranial bone sculpturing found is also consistent with the previous described bone sculpturing patterns in the various taxa of other studies (Bystrow, 1935; Coldiron, 1974; Conrad, 2008; de Buffrenil et al., 2015; Gauthier et al, 2012; Conrad, 2017). As the consistency lies in the categorical descriptions shared and refined between authors, homology cannot be established with certainty. Even within the categories, the variation of the cranial bone sculpturing observed appeared to be unique to the species examined (e.g. the rugosities of *Phyllurus platurus* compared to the rugosities of *Saltuarius salebrosus* or *Matoatoa, Figure 28*). Future analyses may concentrate in expanding these observations with larger sample size and filling the gaps in from the missing genera (i.e., *Uvidicolus*, *Paniegekko*, *Tukutuku*, *Hesperoedura*, and *Altiphylax*).

Within Gekkota, the cranial bone sculpture showed intrageneric variation. In the genus *Hemidactylus*, one species had smooth cranial bones (*H. frenatus*), while the other species bore grooved (*H. turcicus*). In the genus *Chondrodactylus,* one species had grooved cranial bones (*C. angulifer*) while the other species bore pitted bones (*C.*

bibronii). In the genus *Paroedura,* one species had grooved cranial bones (*P. picta*) while the other bore rugose bones (*P. stumpffi*). Finally, the genus *Blaesodactylus* also had a species bearing grooved cranial bones (*Blaesodactylus boivini*) while the other bore grooved and pitted sculpturing (*Blaesodactylus antongilensis*). In some species, there were some autapomorphic cranial bone sculpturing. These include the extreme projections of *Saltuarius salebrosus* and *Phyllurus*, the distinct pitting of *Chondrodactylus bibronii*, the combined grooving and pitting of *Blaesodactylus antongilensis*, and the extreme grooving in *Hemidatylus turcicus*. Finally, *Rhynchoedura ornata*, *Microgekko persicus, Gekolepis maculata. Tarentola mauritanica,* and *Gekko gecko* had unique sculpturing occurring in their osteoderms.

When cranial bone sculpturing was present, it was not homogenous across the skull but was limited to certain bones. There was consistency in that of the 22 taxa with cranial bone sculpturing, the sculpturing was occurring on the outer side of the bones of the dermatocranium. There were also some bones that were more frequently sculptured, such as the frontal bone, which was sculptured for all 22 taxa (Figure 6). This led to an interesting pattern of the cranial bone sculpturing distribution: 1) frontal + the muzzle unit, 2) frontal + the parietal table, and 3) muzzle unit + frontal, + parietal table, across the entirety of the outer superior surface of the skull, even extending to the outer edge of the quadrate bone in some forms. When occurring across the entirety of the skull, as seen in *Chondrodactylus bibronii,* the suture lines become harder to differentiate, and indicating that these bones outgrowth might be serving to reinforce the skull (Evans, 2008; Figure 29). Despite the cranial bone sculpturing occurring across the outer superior surface of the skull, the inner surface of bones of the skull and the jaw bones remained

smooth. There was only one instance, *Chondrodactylus bibronii*, in which cranial bone sculpturing occurring on the dentary(s), surangular(s) and quadrate(s). Future research can test how an increase in cranial bone sculpturing can affect the distribution of stress across the skull, this can likely be tested by means of Finite Element Analyses (Moreno et al., 2008; Curtis et al, 2013).

Overall, the ancestral condition for gekkotans would be to have smooth cranial bones. Carphodactylidae departed from this condition and developed extensive cranial bone sculpturing earlier in their evolution. It would be important to also consider the fossil record in future studies. There are multiple gekkotan fossils that have been identified as bearing cranial bone sculpturing (e.g., *Rhodanogekko vireti, Cadurcogekko piveteaui;* Daza et al., 2014). Incorporation of fossil taxa may lead to a shift in the proposed ancestral state, but it also may lead to a better understanding of gekkotan evolutionary history. Showing that there is at least one Diplodactylid that has cranial bone sculpturing (*Pseudothecadactylus*), the argument for placing *Cadurcogekko* may be better supported. Thus, supporting the idea posited by Daza et al. (2014) that pygopodoideans range may have extended beyond Australasia. However, care must be taken in scoring of the fossils as some fossils look to be heavily sculptured but may have had the thin laminar bone missing due to fossil degradation (i.e. *Laonogekko lefevrei*, Daza et al., 2014). This study also found that special care must be taken to ensure proper rendering of the cranial bones. If rendered improperly, bones could look to be heavily sculptured, when the ‘sculpture’ being observed is the possible cancellous bone beneath a thin layer of laminar bone (Figure 30). This was verified by confirming the presence of the cranial sculpturing using the stacks of images used to create the 3D rendering (Figure

5). The uniqueness of gekkotan bones being primarily smooth is of importance to note, as well as the variation of cranial bone sculpturing that is being seen within gekkotan lineages.

CHAPTER III

Variation of size sculpturing

Objectives and predictions

Described cranial bone sculpturing in the literature is frequently mentioned for large geckos (*Nephurus*, Stephenson, 1960; *Chondrodactylus* and *Phyllurus*, Bauer, 1990). Given this observation, these questions arise: 1) does cranial bone sculpturing is influenced by body size among the Gekkota?, and 2) does cranial bone sculpturing varies along the ontogeny?. **I hypothesize that cranial bone sculpturing is influenced by body size, and this will be reflected within a species across a post-hatchling developmental series.**

Methods

Interspecific variation.

List of specimens. To increase the taxonomic sampling and to improve the resolution of variation across size, many specimens prepared under different methods were inspected. This includes CT scans and Drs. Aaron M. Bauer and Juan D. Daza's digital images of skeletonized and clear and stained individuals. Each specimen used is recorded in Appendix E with the preparation identified.

Measurements. As many specimens are limited to cranial data, only the skull length will be considered in this study. The skull length (the tip of the snout to the occipital condyle, or the distance from the anterior-most part of the premaxilla to the occipital condyle) was taken as outlined in Daza et al. (2008) for the comparison of body sizes (Appendix E).

Data acquisition. Specimen measurements were obtained from as many CT scans as available from both Drs. Aaron M. Bauer and Juan D. Daza's collection using Avizo lite v 9.0.0. Each image stack was opened including the appropriate voxel sizes outlined in the contents file. The volume rendering was created as outlined in Chapter 2, with the measurements being acquired in a dorsal view using the "3D measurement" tool. To utilize the specimen in the digital library, dorsal view images of the skull with a visible scale were used for measurements using ImageJ (Schneider et al., 2012). Images included both skeletonized and clear and stained specimen.

Analysis. As seen in the previous chapter, the most frequently sculptured bone is the frontal bone. In consideration of this, the score for the frontal bone was used as the indicator to represent the cranial bone sculpturing score for the skull. Standard measurement analyses were then completed using the score for the frontal bone conjunction with the head measurements.

Intraspecific variation.

List of specimens. To determine the development of cranial bone sculpturing in the post-hatchling developmental series of highly, sculptured species, one species representing each of the two extreme bone sculpturing types was used (pitted: *Chondrodactylus bibronii*, and rugose: *Saltuarius salebrosus*). These species were selected based on the results from personal observations from the previous section as well as being one of the few sculptured genera with juveniles in the collections. Using the measurements provided by the staff at the California Academy of Science (CAS), a series of three specimens including a post-hatchling juvenile, young adult, and skeletally mature

adult were used to assess the development of cranial bone sculpturing in a developmental series. Sexual dimorphism was not considered for this study.

Data acquisition. Upon receiving the six loaned specimens, the animals were scanned at University of Texas CT lab, and the data rendered using Avizo lite v.9.0.0 (Thermo Fisher Scientific Inc., Waltham, MA, USA, 2017). Using the data generated from the first hypothesis, each skull and the top two bones that most frequently bear bone sculpturing were segmented and rendered to be used in the analysis (frontal and parietal). The frontal and both parietals were segmented individually. Though segmented individually, as the parietals are fused for *Chondrodactylus*, the two were considered as a single unit for both specimen in this analysis. The surface area and the surface volumes were recorded and compared among the two post-hatchling developmental series. The segmentation was completed using the "magic wand" tool to select the desired area. After the entire bone was segmented, to ensure proper rendering, each label file was "smoothed," using the "smooth" function in Avizo. The label files were then rendered to ensure the completeness and saved accordingly. Each of the label files were used to generate a surface file (.surf) using the tool, "generate surface." The surface file was then used to create a surface area volume calculation using the tool, "surface area volume." This calculation produced the surface area (mm^2) for the skull, the frontal and the parietal bones.

Data analysis. To account for the increase in skull length that accompanies any ontogenetic development, the logarithm of the combined surface area (parietals+ frontals) was regressed against the logarithm of the skull length. Logarithm transformation was

used for all the linear regressions. The measurements for each were recorded and analyzed as seen in Figures 41 and 42.

Results

Interspecific variation. To visualize skull length across families, size was plotted against their cranial bone sculpturing score. Lack of sculpturing or smooth skull bones was found in specimens from small to large size (ranging about 5 mm to 55 mm; Figure 31). The same was observed for the species showing the grooved skull sculpturing, although the range variation in size was slightly narrow (ranging about 8mm to 45mm; Figure 31). Though there was only one record of pitting occurring within the data collected, *Chondrodactylus bibronii,* the skull length still falls within the range of the skull lengths below it in the grooved category. The rugose scores were even more limited in range than the grooved individuals (ranging about 18mm to 38mm; Figure 31), suggesting that the individual must have a large head for this cranial bone sculpturing to be developed. There was a single rugose individual, *Matoatoa brevieps,* who fell outside of this range and having a miniaturized skull of 8.32 mm. Overall, this supports that there is a relationship between the size of the individual and the cranial bone sculpturing. To better analyze the data points collected, an independent graph was considered for each family.

The family Pygopodidae showed lack of sculpturing across a range of various skull sizes (ranging from 7 mm to 30 mm; Figure 32). Carphodactylidae was represented by medium to large size members and encompassed three of the cranial sculpturing categories: smooth skulls, ranging from 20 mm to 27 mm; grooved skulls, ranging from 23 mm to 26 mm, and rugose skulls, ranging from 24 mm to 36 mm (Figure 33). The

skulls with the rugose cranial sculpturing were the larger skulls of this family (i.e., *Phyllurus, Saltuarius, Carphodatylus,* and *Orraya*). The family Diplodactylidae was represented by a variation of skull sizes and encompassed three of the cranial bone sculpturing categories: smooth skulls, ranging from 8 mm to 38 mm; grooved skulls, ranging from 14 mm to 34 mm, and rugose skulls, ranging from 19 mm to 27 mm (Figure 34). The grooved members of this family have a higher variation of skull sizes, where the rugose members are again of a larger skull size (*Naultinus grayii* and *Pseudothecadactylus australis*; Figure 34). The family Eublepharidae showed smooth sculpturing (ranging from 14 –37mm; Figure 35) and grooved sculpturing (ranging from 18–30 mm; Figure 35). Sphaerodactylidae members showed both smooth (ranging from 4–27 mm; Figure 36) and grooved (ranging from 9–12 mm; Figure 36) cranial sculpturing occurring across the various skull sizes. The members of Phyllodactylidae also showed both smooth (varying from 7–24 mm; Figure 37) and grooved (varying from 14 –27 mm; Figure 37) across the various skull sizes. Finally, the members of Gekkonidae represented at least one of the cranial sculpturing types: smooth (ranging from 5–49 mm), grooved (ranging from 8 –55 mm), pitted (23 mm), and rugose (ranging from 7–18mm). The one pitted individual, *Chondrodactylus bibronii*, was on the larger side of skull length (23 mm). Uniquely, the rugose category is not limited to the larger skull sizes in this family but a smaller and average sized skull length (*Matotoa breviceps* and *Paroedura stumpffi;* Figure 38).

Intraspecific variation. Though the intraspecific variation of the location of the sculpturing varied between the two series analyzed, both series showed a positive allometric increase as the developmental trajectory increased (Figures 39 and 40). In

looking at the pitted series (Figures 39 and 41), the parietals comprised 8.73% of the total surface area of the skull and 15.40% of the total volume of the skull at the juvenile post-hatchling stage. For the younger adult, the percent of the skull that's occupied by the parietal for the surface area increased to 9.87%, and volume increasing as well to compromise 17.90% of the skull at this stage. For the skeletally mature adult in the series, the percentage of the skull's total surface area that is occupied by the parietals is 8.74% and the parietals make up 27.74% of skull's total surface volume. In the juvenile of the pitted series, the frontal bone took up 5.63% of the total surface area while comprising 18.25% of the total volume of the skull. For the young adult, the frontal bone comprised 5.80% of the total surface area of the skull and 14.80% of the total volume. Finally, the frontal bone comprised 5.60% of the surface area and 19.07% of the total volume of the skull in the skeletally mature adult.

Chondrodactylus bibronii with a 15.12 mm skull length already has well developed grooves that cover the premaxilla, nasal, maxilla, prefrontal, frontal, parietal, and surangular bones (Figure 41). The quadrate in this individual begins to develop a textured surface, not quite grooved, along the dorsal side of the medial column and the cephalic condyle. At this stage the sutures throughout the skull are still relatively unfused and appear to be more kinetic compared to the later stages. The young adult, skull length of 22.09 mm, varied greatly within the 7 mm difference of developmental progress. The bones increased in area and have transformed shapes greatly, (e.g., a broadening in the quadrates, an increase in the width between the quadrates, the postorbitofrontals broadening). The cranial sculpturing has changed from being grooved to being pitted. Though there are still elongated pits towards the outer edges of the bones (e.g. the

parietals and the postorbitofrontals), the frontal, nasal, premaxilla, maxilla, and prefrontal are extremely pitted. The quadrate does not bear any signs of texturing at this stage but has an increased presence of grooving on the surangular, of which is now expanding and present on the dentary. The skeletally mature adult, 26.22 mm in skull length, is the most extreme in sculpturing, with the pits appearing to be sunken deeper into ridges between them. The pitting on this individual covers the entirety of the dorsal portion of the skull, extending along the lateral edges of the dentary, surangular and quadrate.

In the rugose series (Figures 40 and 42), the parietals comprised 6.55% of the total surface area of the skull and 10.58% of the total volume of the skull at the juvenile post-hatchling stage. In the young adult, the parietals increased to contain 7.17% of the total surface area of the skull and 9.76% of the total volume of the skull. The percentage of the skeletally mature skull's total surface area that is occupied by the parietals is 8.55%, with the parietals comprising 19.51% of skull's total surface volume. In the juvenile, the frontal bone took up 5.68% of the total surface area while comprising 15.46% of the total volume of the skull. The frontal bone comprised 5.77% of the total surface area of the skull and 12.12% of the total volume of the skull in the young adult stage. Finally, the frontal bone comprised 5.59% of the surface area and 19.56% of the total volume of the skull in the skeletally mature adult.

Saltuarius salebrosus starting at a skull size of 19.87 mm has little to no cranial bone sculpturing present aside from the postorbitofrontals and the seven individual nodules (3 arising from each parietal surrounding the depression and one the posterior end of the frontal bone). At a 10 mm increase to a skull length of 29.88 mm, the cranial bone sculpturing drastically changes. There are multiple distinct rugosities projecting

from the parietals and frontal, with smaller rugosities on the prefrontal and nasal bones. There are rugosities in the same location of the frontal and parietal bones in the young adult that were observed where the nodules were in the juvenile. The postorbitofrontals also have rugosities developing as they continue to ossify, extending around the orbit. The rugosities continue down the frontal bone around the orbit, to the prefrontal. There is no cranial sculpturing occurring on the jawline. In the older adult, a 7.8 mm increase in skull length, allows for an extreme difference in cranial sculpturing. The entire dorsal surface (nasal, maxilla, prefrontal, frontal, and parietal bones) all have extensive rugosities occupying the entirety of the dorsal side of the bone. The rugosity placement of those seven nodules observed in the first two individuals are even further hyperossified in the third individual. In this adult there is also a sculptured texture that can be observed on the outside of the quadrate, comparable to the placement of the sculpturing found on *Chondrodactylus bibronii*'s quadrate.

Discussion

The interspecific analysis supports that cranial bone sculpturing is not limited to the largest members of each family but can be see varying across a wide range of skull sizes (e.g., *Matoatoa breviceps*). In consideration of this, almost no miniaturized taxa bear cranial bone sculpturing within Gekkota (with the aforementioned exception). However, there are known miniaturized squamates that do have this character (e.g., *Brookesia* and *Rhampholeon*).

In consideration of the intraspecific variation the post-hatchling series supports the continued ossification of the cranial bone sculpturing after birth. With both series

having a positive trend of allometric growth, cranial bone sculpturing is increasing the surface area over time.

Cranial bone sculpturing can originate following two alternative transformations (ordered): 1) from smooth to rugose, and 2) from smooth, to grooved, to pitted (J.D.D., personal comm.).

FIGURES

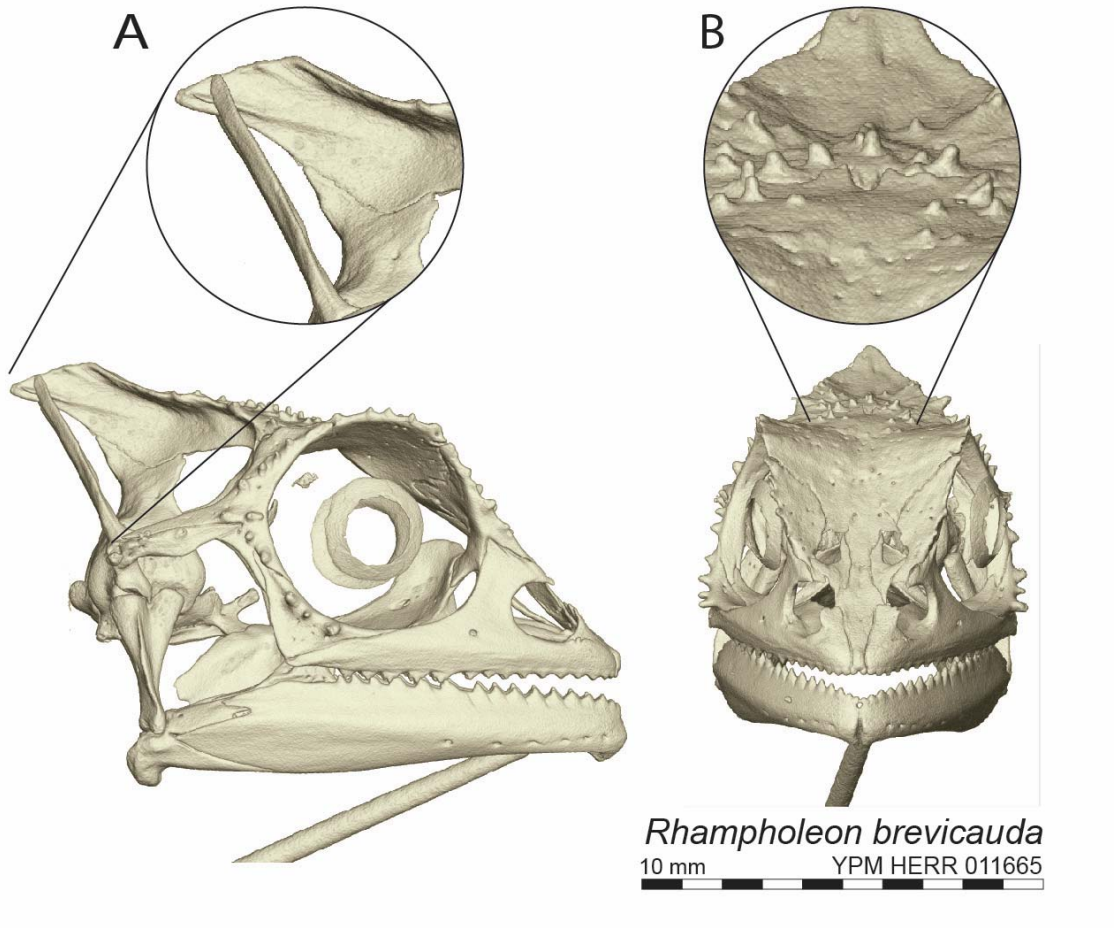

Figure 1. Differentiation of ornament and sculpture: dorsal and lateral views of the ornamentation (A) and cranial sculpturing (B).

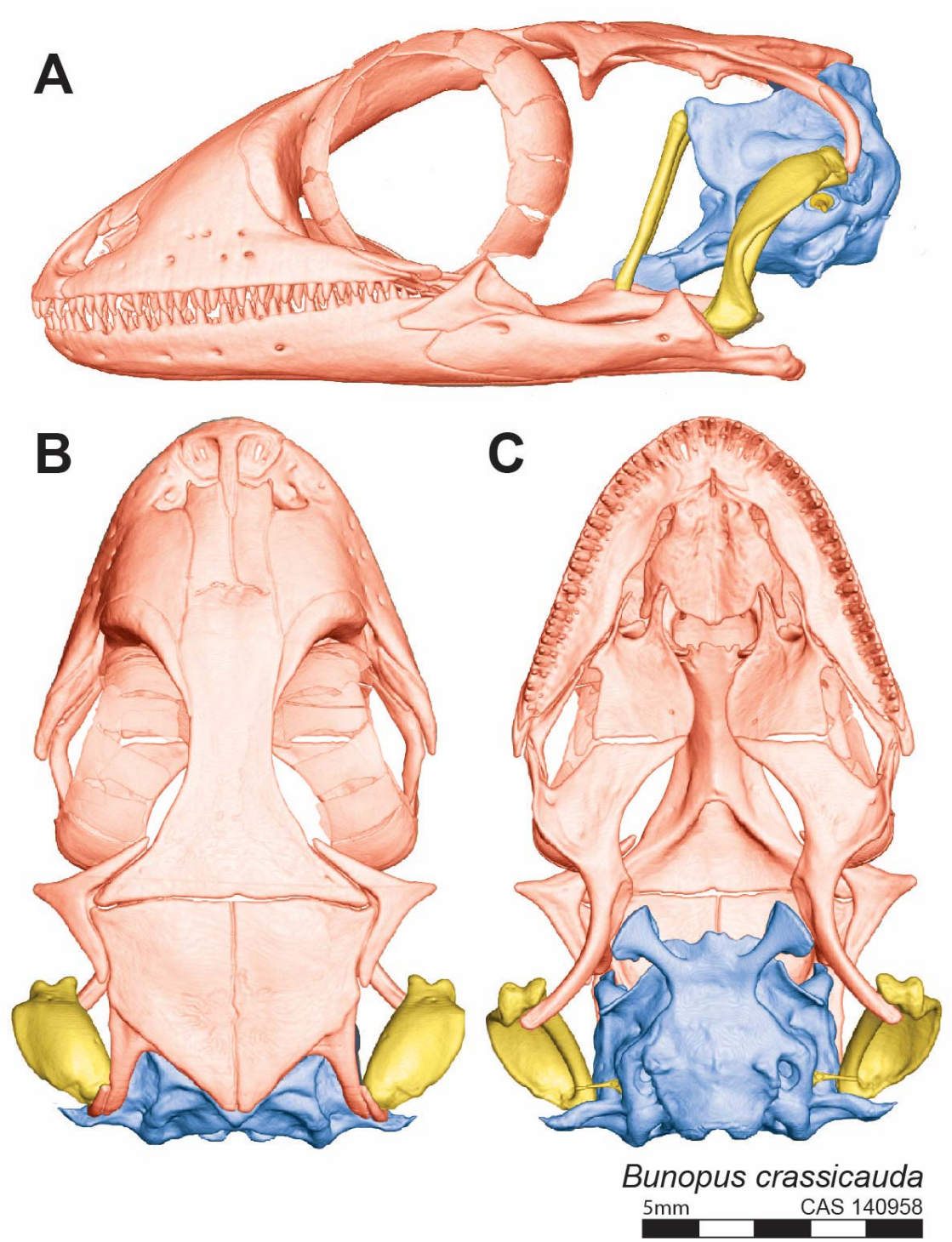

Figure 2. Three major units of the reptile skull: dorsal (A), ventral (B), and lateral (C) views showing the splanchnocranium (yellow), chondrocranium (blue), and the dermatocranium (red).

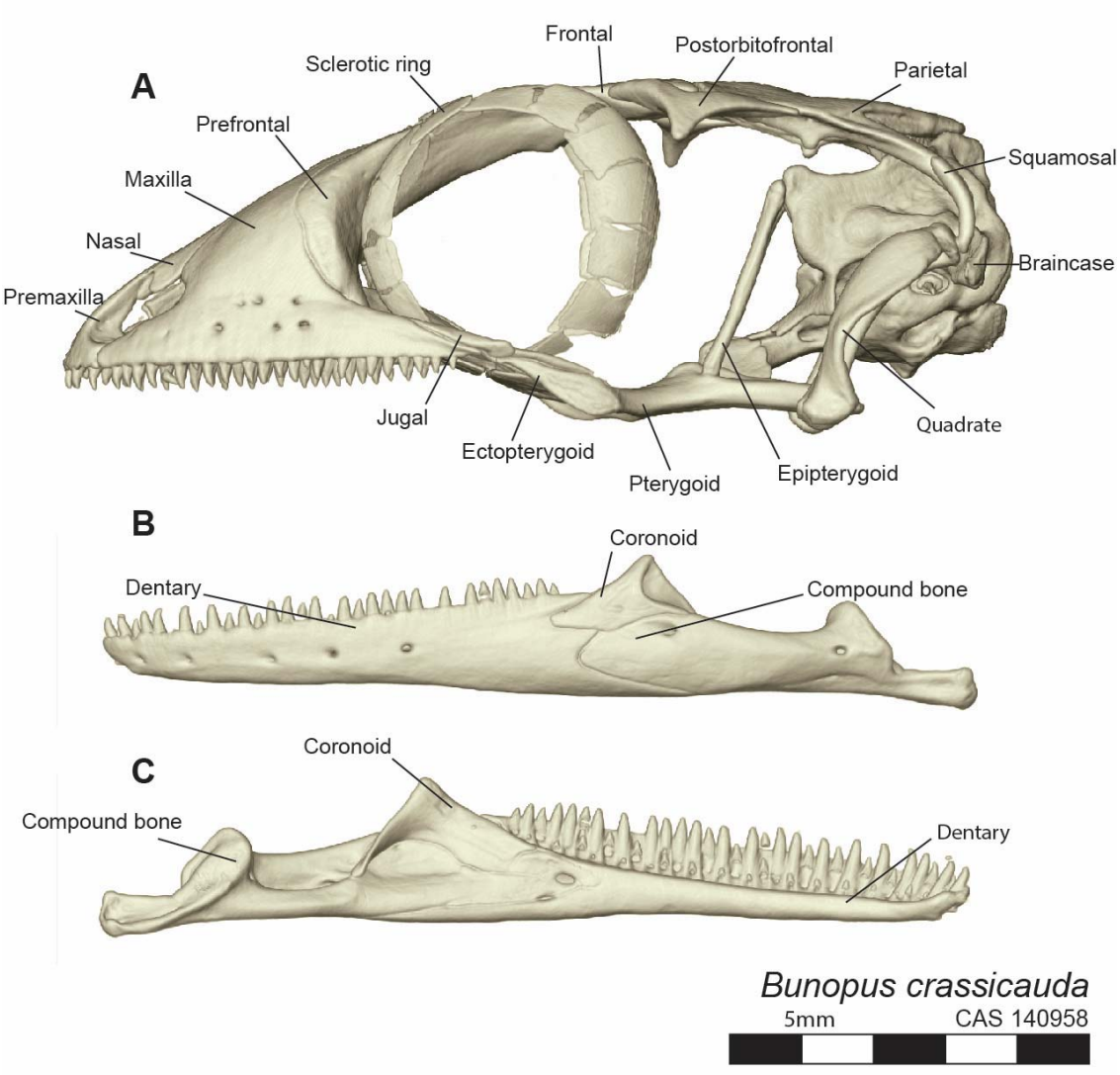

Figure 3. Labeled gecko skull: left lateral (A) view of the labeled skull, with lateral (B) and medial (C) views of the labeled jaw in a gecko.

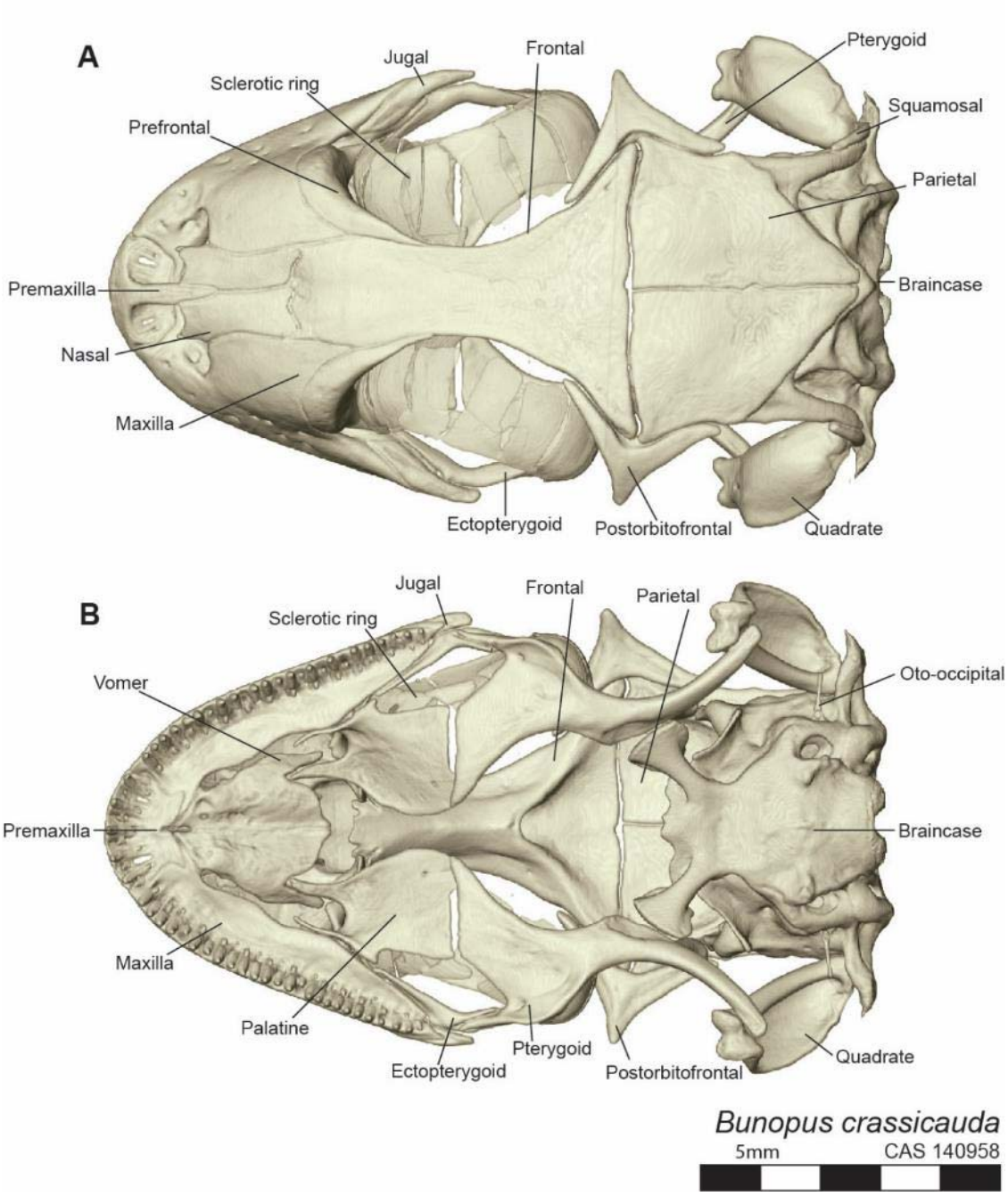

Figure 4. Labeled gecko skull (continued): dorsal (A) and ventral (B) views of the labeled skull of a gecko.

Character State and description	Dorsal	Lateral	C.T. Image
0: Smooth No change in texture Smooth, flat compact bone	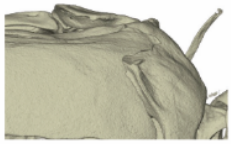	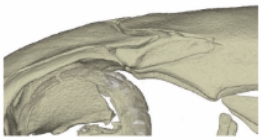	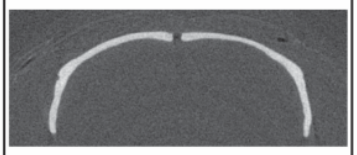
1: Grooved Textured in appearance bearing interconnected, often shallow grooves	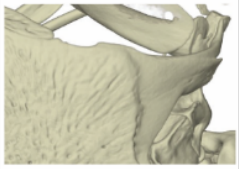		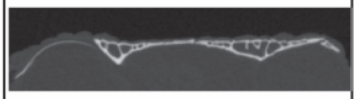
2: Pitted Textured in appearance, rounded pits surrounded by a network of crests	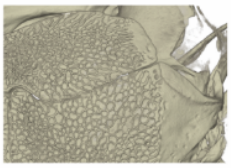	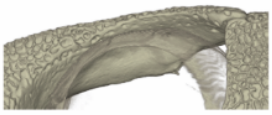	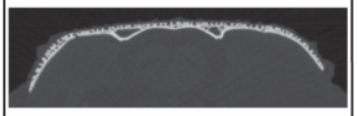
3: Rugose Textured in appearance, projections stemming from the surface of the skull	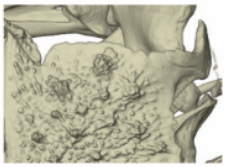	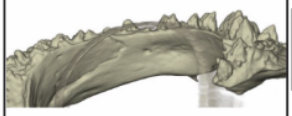	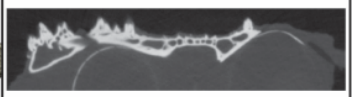

Figure 5. Bone sculpturing examples. Each state is illustrated with a dorsal and lateral view of the parietal region of the a gekkotan skull and a cross-section from the stack of computed tomography images.

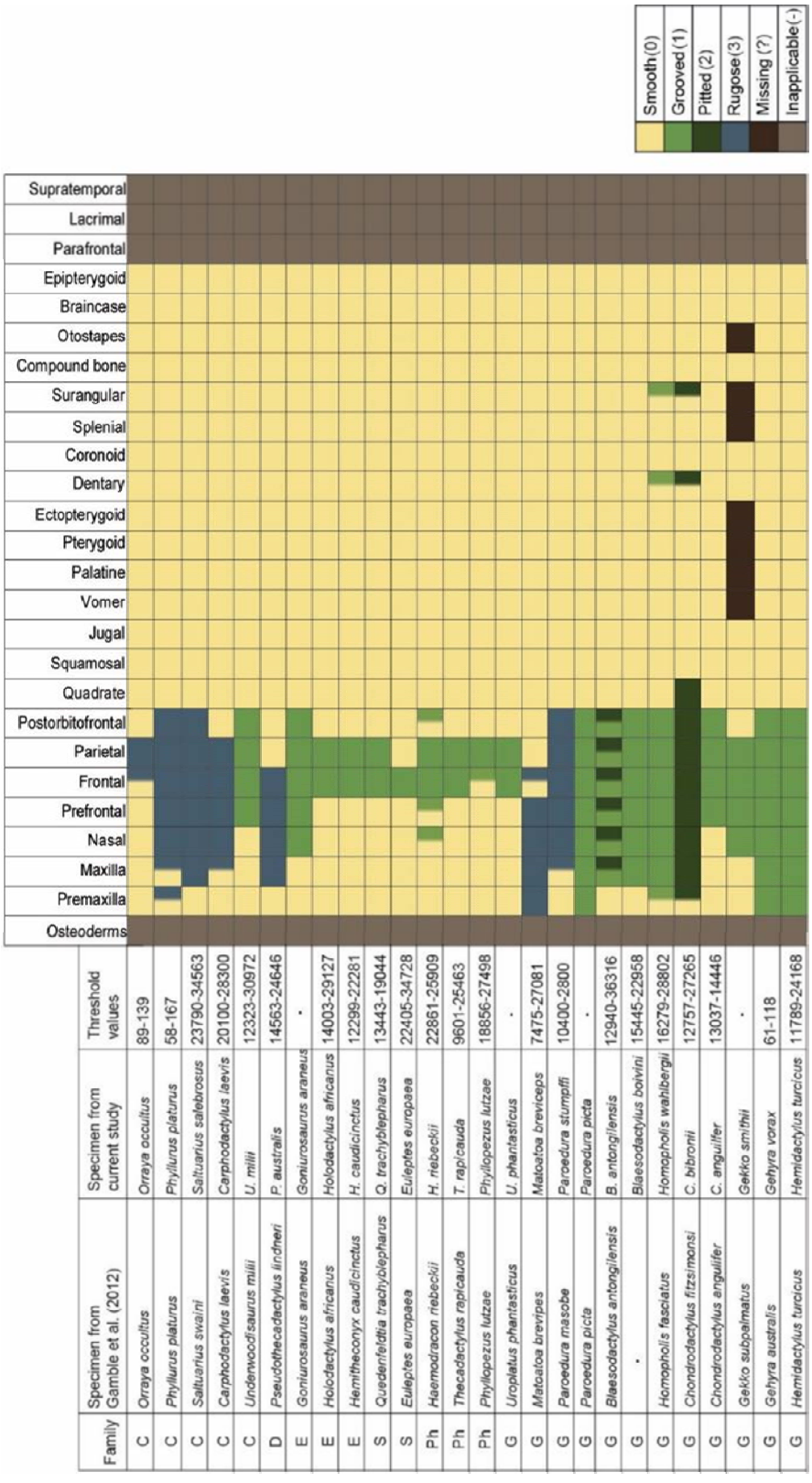

Family	Specimen from Gamble et al. (2012)	Specimen from current study	Threshold values
C	*Orraya occultus*	*Orraya occultus*	89-139
C	*Phyllurus platurus*	*Phyllurus platurus*	58-167
C	*Saltuarius swaini*	*Saltuarius salebrosus*	23790-34563
C	*Carphodactylus laevis*	*Carphodactylus laevis*	20100-28300
C	*Underwoodisaurus milii*	*U. milii*	12323-30972
D	*Pseudothecadactylus lindneri*	*P. australis*	14563-24646
E	*Goniurosaurus araneus*	*Goniurosaurus araneus*	-
E	*Holodactylus africanus*	*Holodactylus africanus*	14003-29127
E	*Hemitheconyx caudicinctus*	*H. caudicinctus*	12299-22281
S	*Quedenfeldtia trachyblepharus*	*Q. trachyblepharus*	13443-19044
S	*Euleptes europaea*	*Euleptes europaea*	22405-34728
Ph	*Haemodracon riebeckii*	*H. riebeckii*	22861-25909
Ph	*Thecadactylus rapicauda*	*T. rapicauda*	9601-25463
Ph	*Phyllopezus lutzae*	*Phyllopezus lutzae*	18856-27498
G	*Uroplatus phantasticus*	*U. phantasticus*	-
G	*Matoatoa brevipes*	*Matoatoa brevipes*	7475-27081
G	*Parcedura masobe*	*Parcedura stumpffi*	10400-2800
G	*Parcedura picta*	*Parcedura picta*	-
G	*Blaesodactylus antongilensis*	*B. antongilensis*	12940-36316
G	-	*Blaesodactylus boivini*	15445-22958
G	*Homopholis fasciatus*	*Homopholis wahlbergii*	16279-28802
G	*Chondrodactylus fitzsimonsi*	*C. bibronii*	12757-27265
G	*Chondrodactylus angulifer*	*C. angulifer*	13037-14446
G	*Gekko subpalmatus*	*Gekko smithii*	-
G	*Gehyra australis*	*Gehyra vorax*	61-118
G	*Hemidactylus turcicus*	*Hemidactylus turcicus*	11789-24168

Figure 6. Bone-by-bone frequency of cranial sculpting for sculptured taxa. Taxa used by Gamble et al. (2015) compared to this study, as well as thresholds identified.

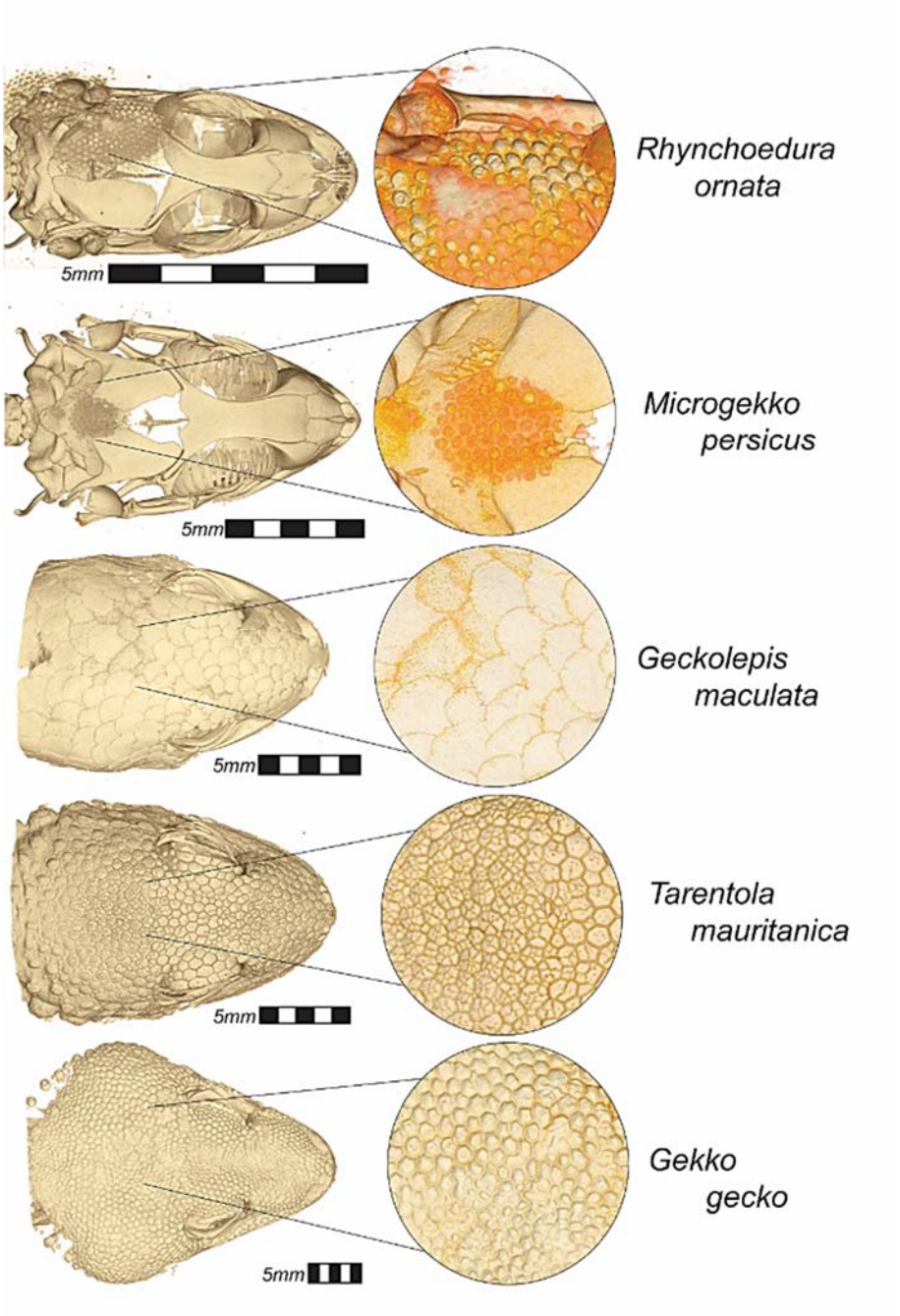

Figure 7. Osteoderms observed in Gekkota. Cranial sculpturing variation observed on the osteoderms in *Geckolepis, Tarentola,* and *Gekko,* with putative osteoderms observed on *Rhynchoedura* and *Microgekko.*

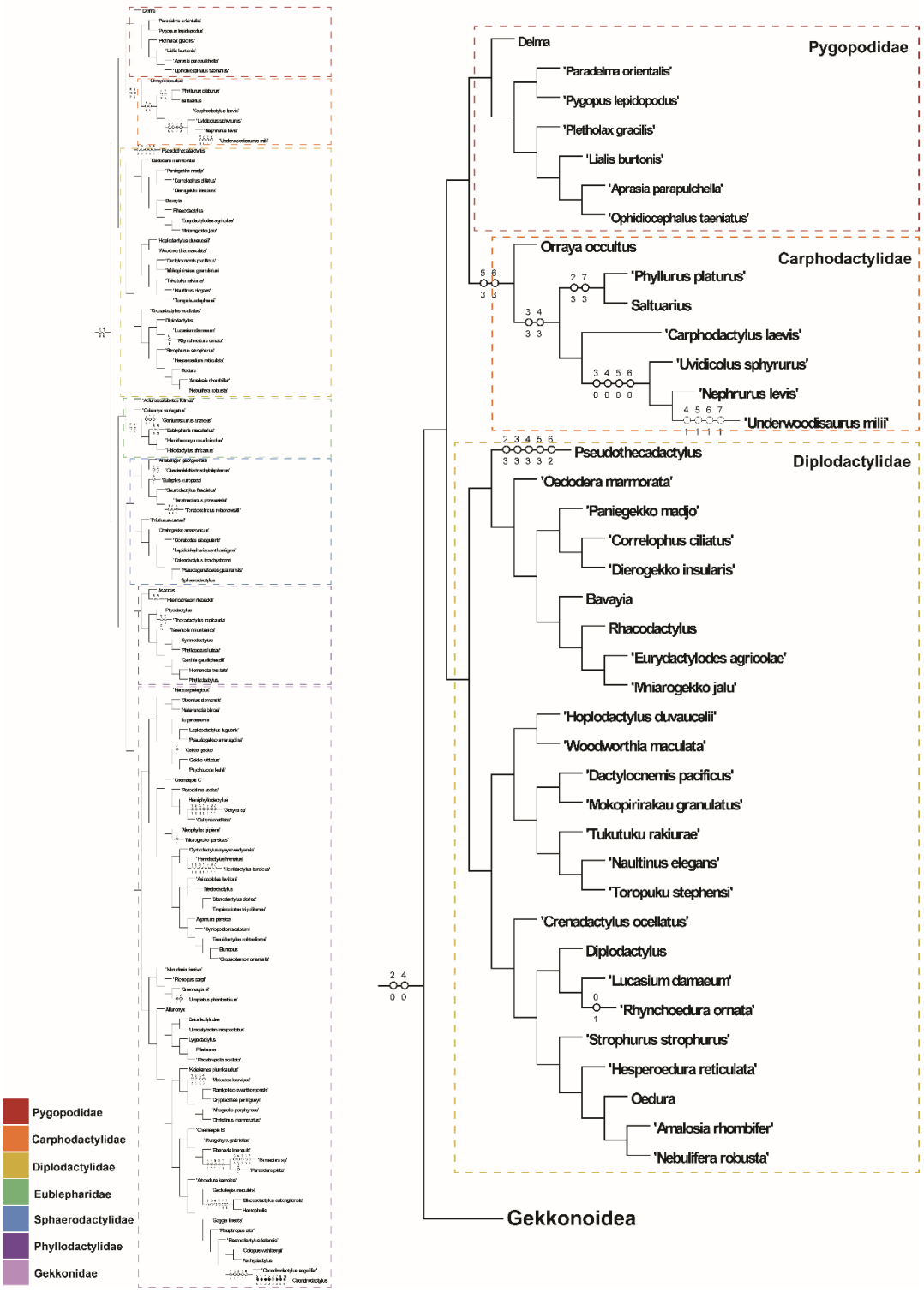

Figure 8. Parsimony character optimization results for Pygopodoidea using the fast function (ACCTRAN). Tree topology is based on multigene phylogenetic analysis (Gamble et al., 2012). White circles indicate homoplasy, solid black circles synapomorphic characters, and color coded by family.

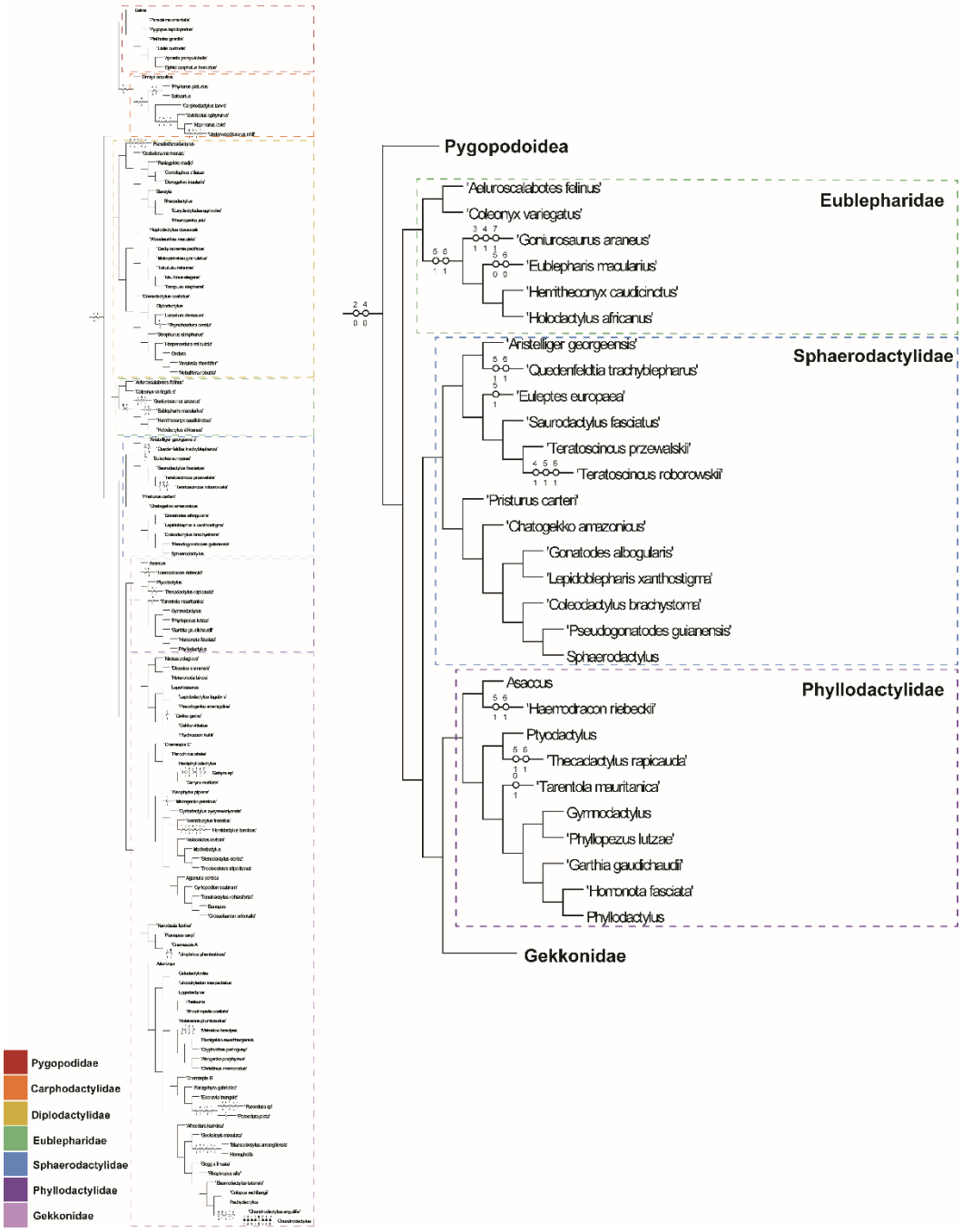

Figure 9. Parsimony character optimization results for Eublepharidae, Sphaerodactylidae, and Phyllodactylidae using the fast function (ACCTRAN). Tree topology is based on multigene phylogenetic analysis (Gamble et al., 2012). White circles indicate homoplasy, solid black circles synapomorphic characters, and color coded by family.

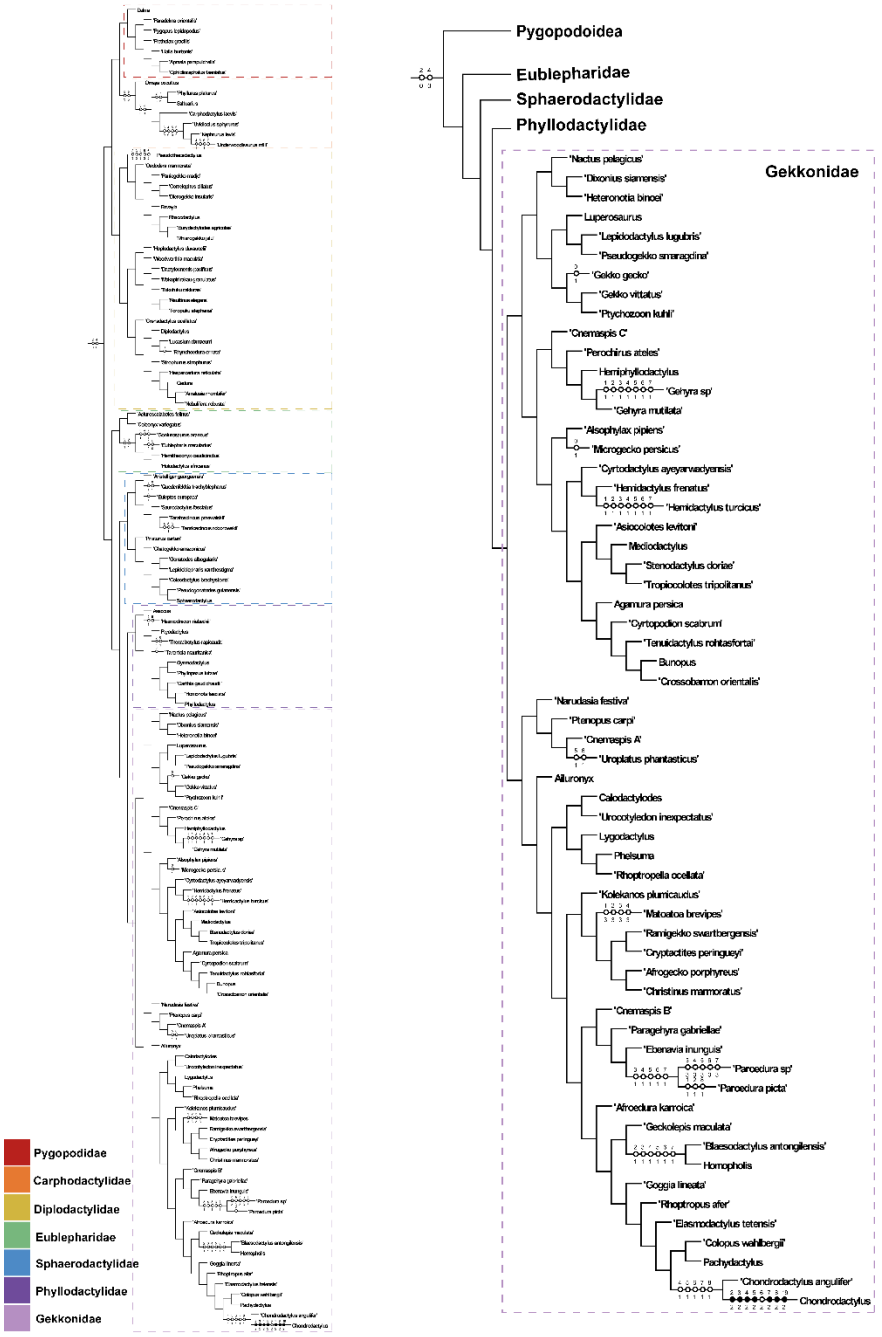

Figure 10. Parsimony character optimization results for Gekkonidae using the fast function (ACCTRAN). Tree topology is based on multigene phylogenetic analysis (Gamble et al., 2012). White circles indicate homoplasy, solid black circles synapomorphic characters, and color coded by family.

Figure 11. Parsimony character optimization results for Pygopodoidea using the slow function (DELTRAN). Tree topology is based on multigene phylogenetic analysis (Gamble et al., 2012). White circles indicate homoplasy, solid black circles synapomorphic characters, and color coded by family.

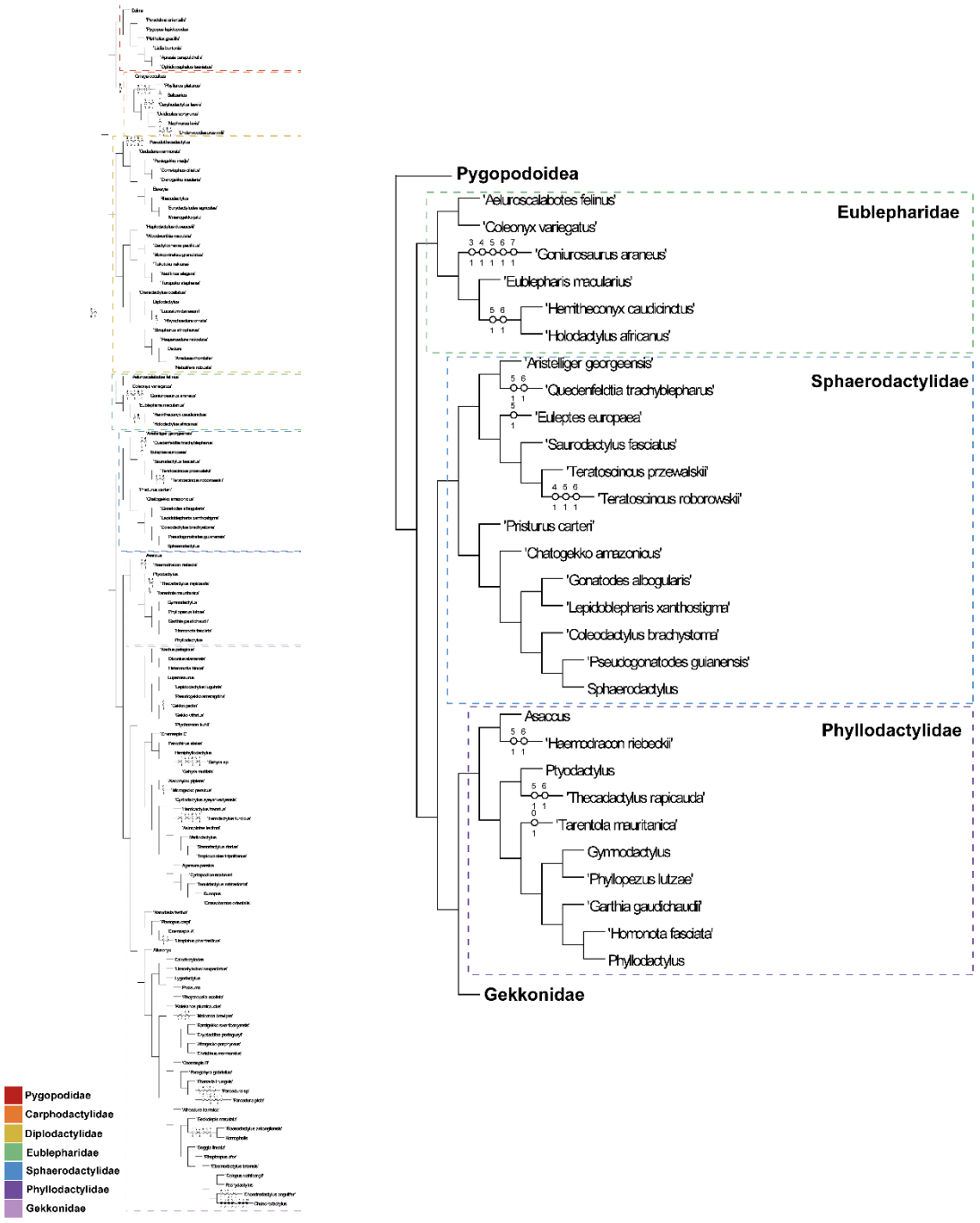

Figure 12. Parsimony character optimization results for Eublepharidae, Sphaerodactylidae, and Phyllodactylidae using the slow function (DELTRAN). Tree topology is based on multigene phylogenetic analysis (Gamble et al., 2012). White circles indicate homoplasy, solid black circles synapomorphic characters, and color coded by family.

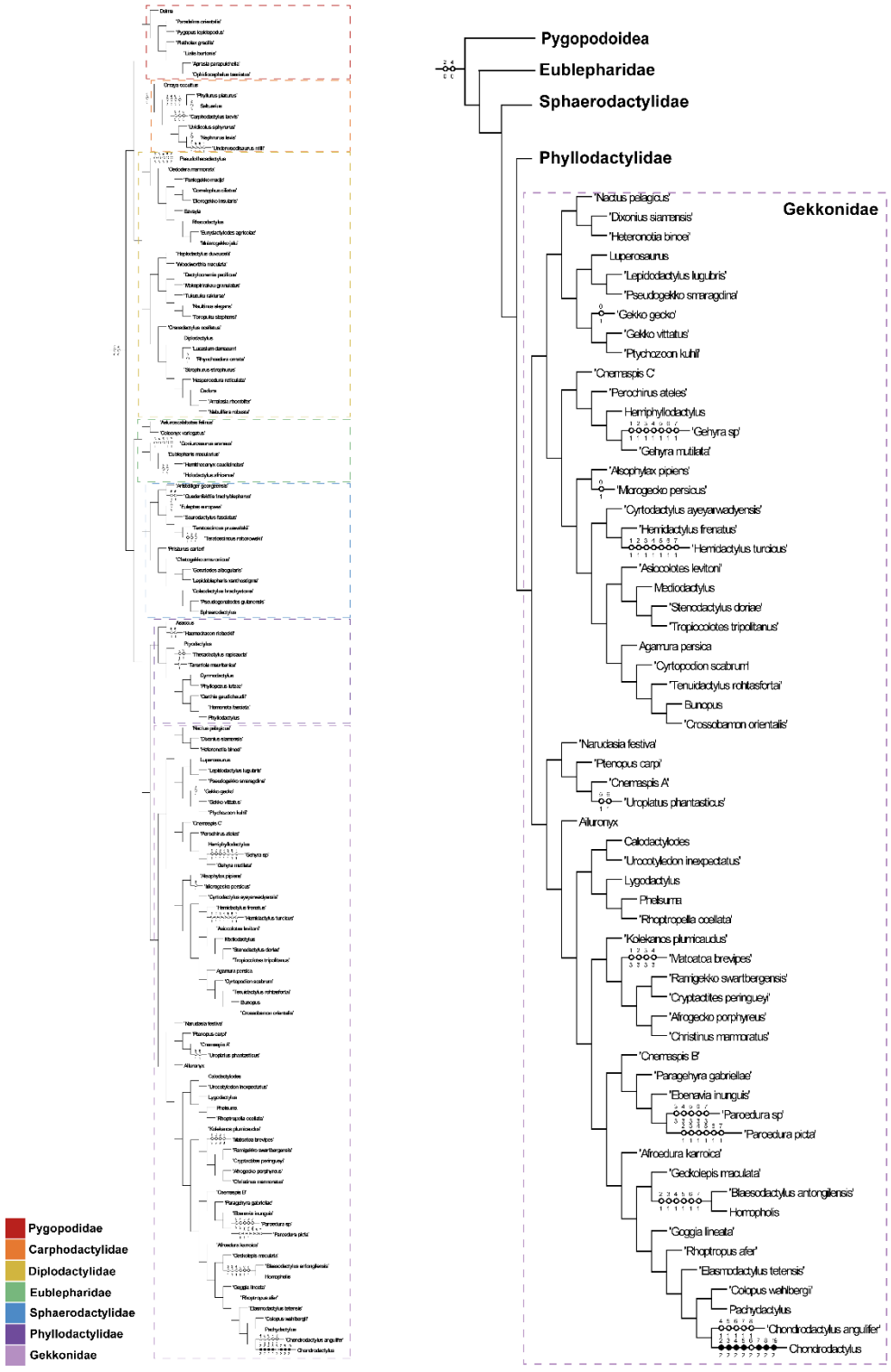

Figure 13. Parsimony character optimization results for Gekkonidae using the slow function (DELTRAN). Tree topology is based on multigene phylogenetic analysis (Gamble et al., 2012). White circles indicate homoplasy, solid black circles synapomorphic characters, and color coded by family.

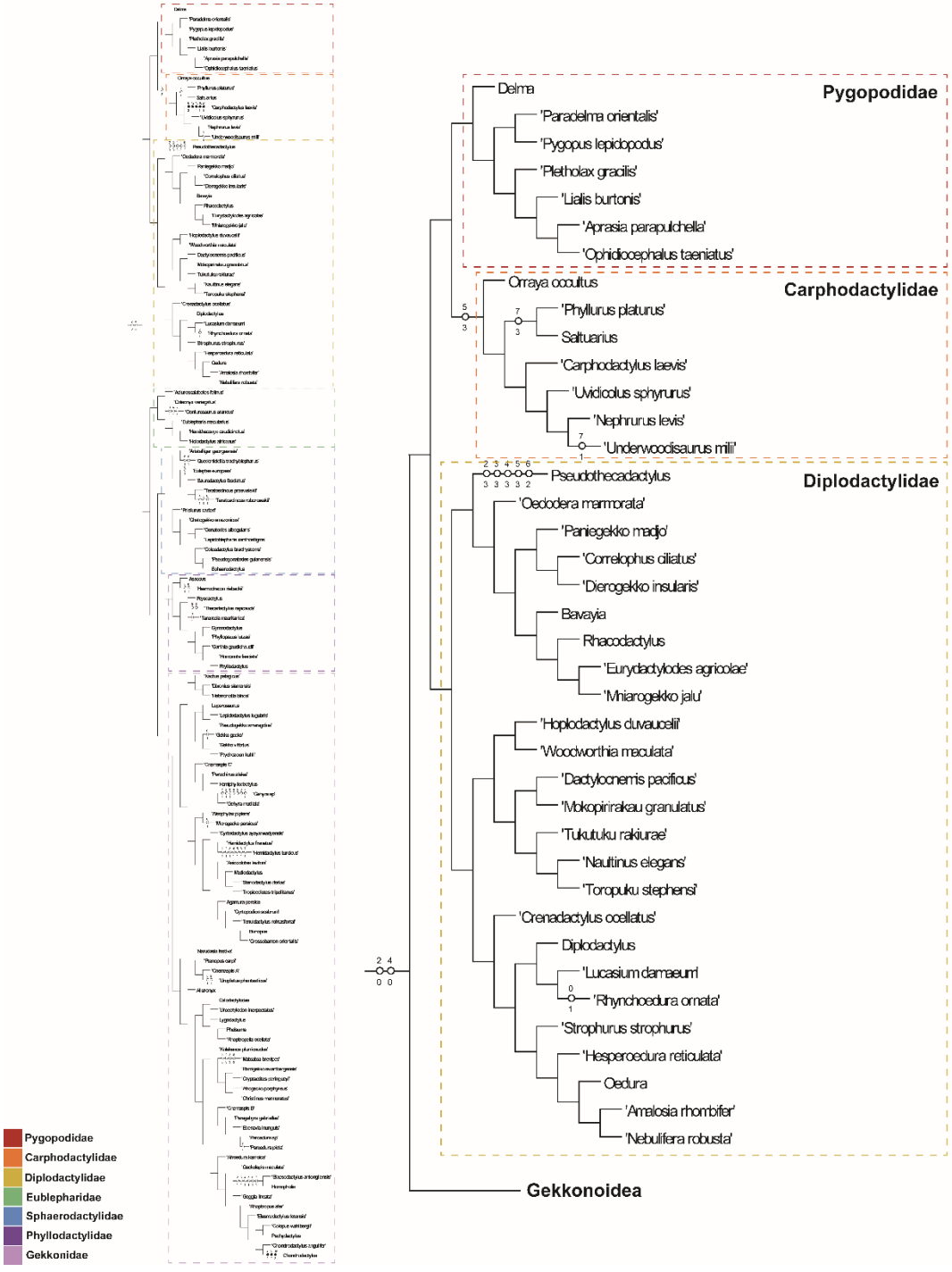

Figure 14. Parsimony character optimization results for Pygopodoidea using the unambiguous function (UNAMBIG). Tree topology is based on multigene phylogenetic analysis (Gamble et al., 2012). White circles indicate homoplasy, solid black circles synapomorphic characters, and color coded by family.

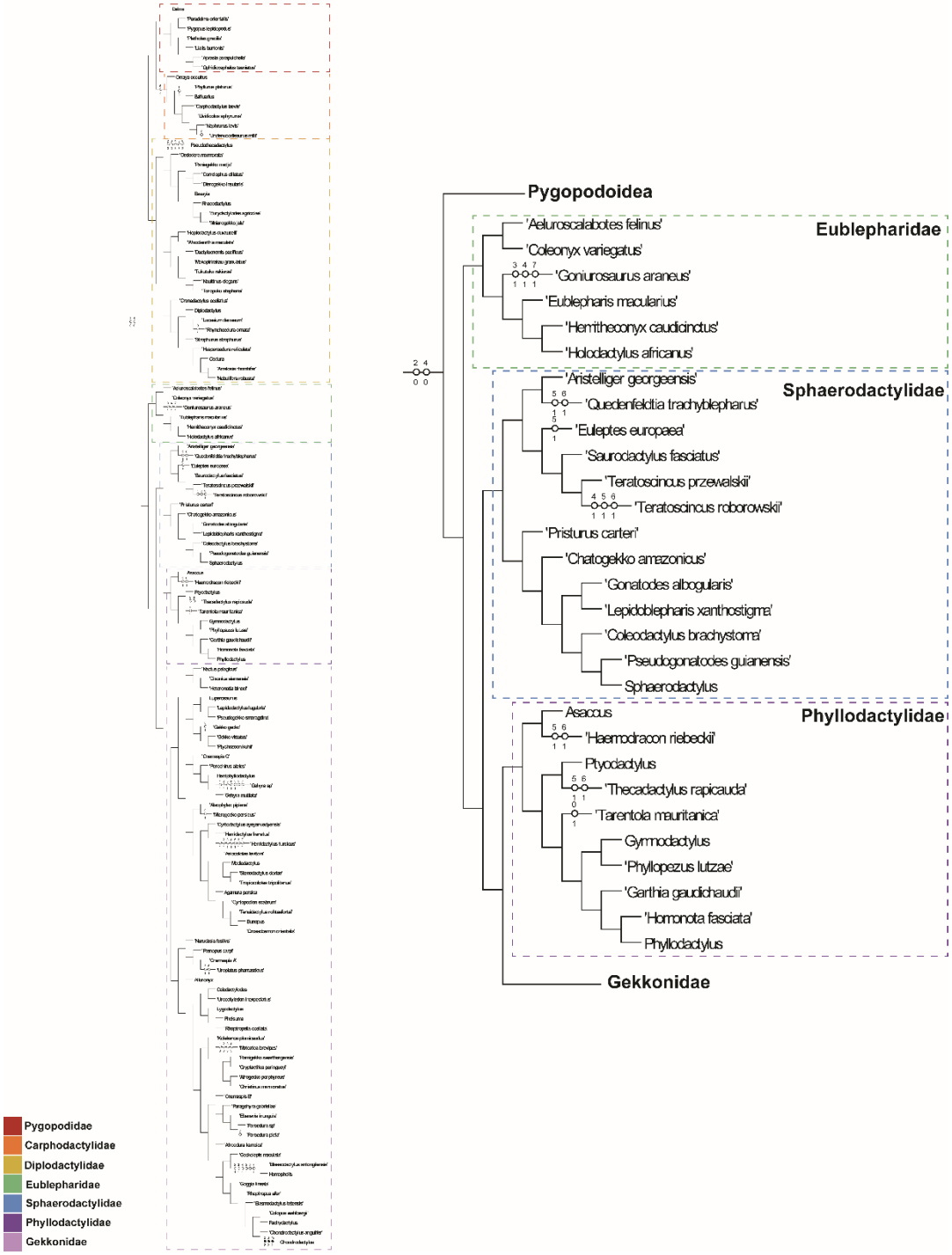

Figure 15. Parsimony character optimization results for Eublepharidae, Sphaerodactylidae, Phyllodactylidae using the unambiguous function (UNAMBIG). Tree topology is based on multigene phylogenetic analysis (Gamble et al., 2012). White circles indicate homoplasy, solid black circles synapomorphic characters, and color coded by family.

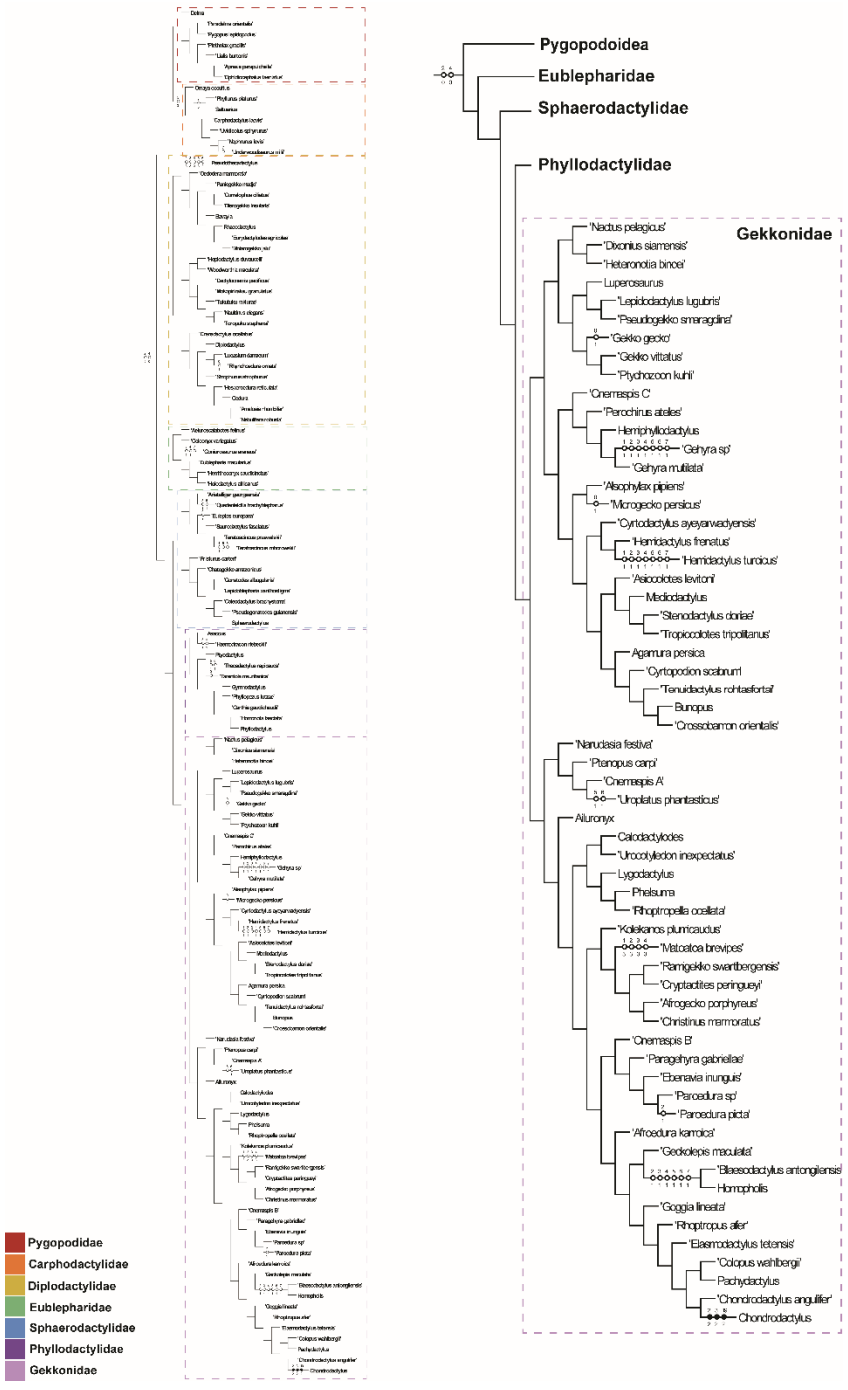

Figure 16. Parsimony character optimization results for Gekkonidae using the unambiguous function (UNAMBIG). Tree topology based on multigene phylogenetic analysis (Gamble et al., 2012). White circles indicate homoplasy, solid black circles synapomorphic characters, and color coded by family.

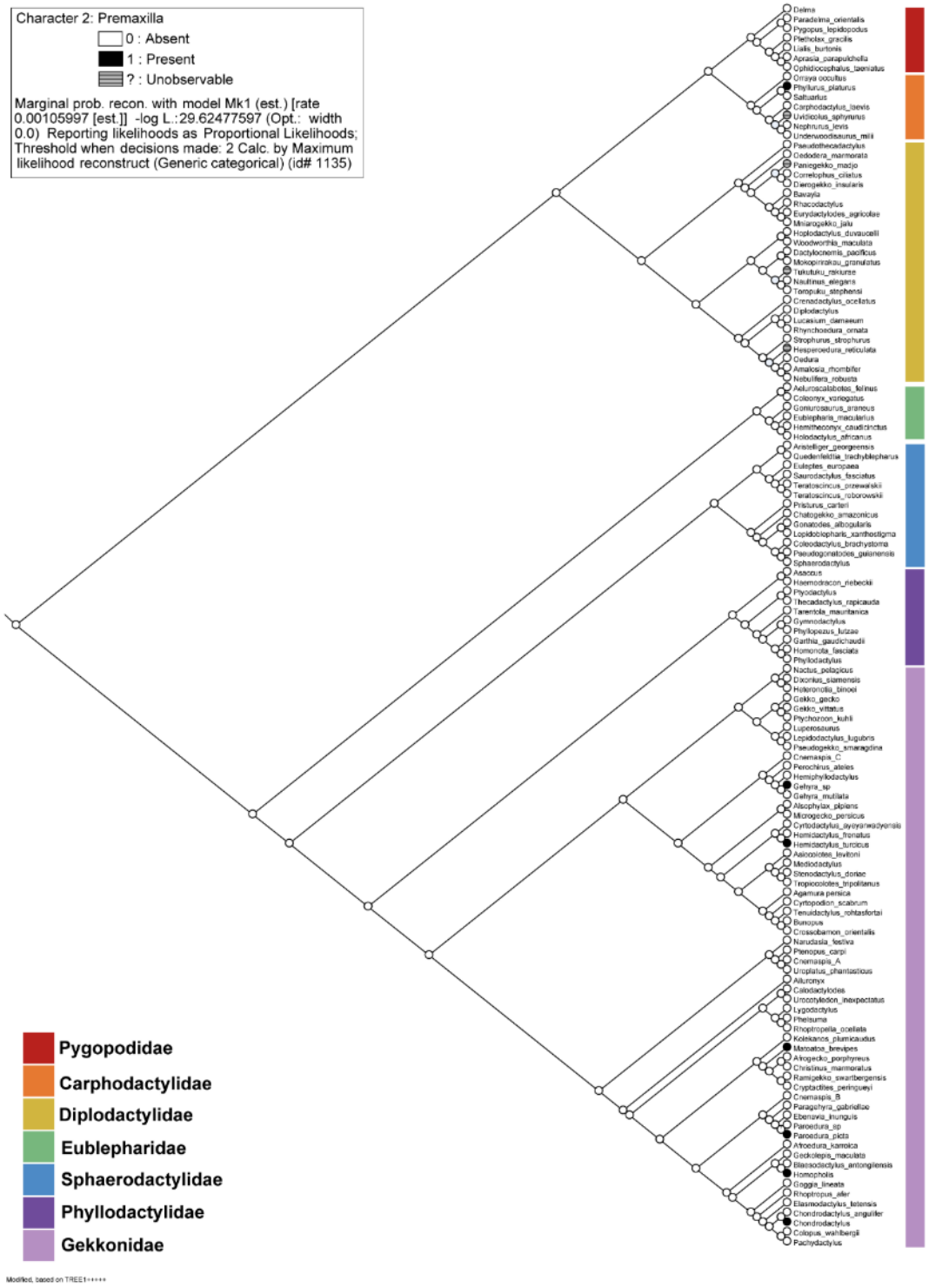

Figure 17. Likelihood character optimization results for the premaxilla. Results of character optimization using likelihood methods. Each family is grouped together by colored box.

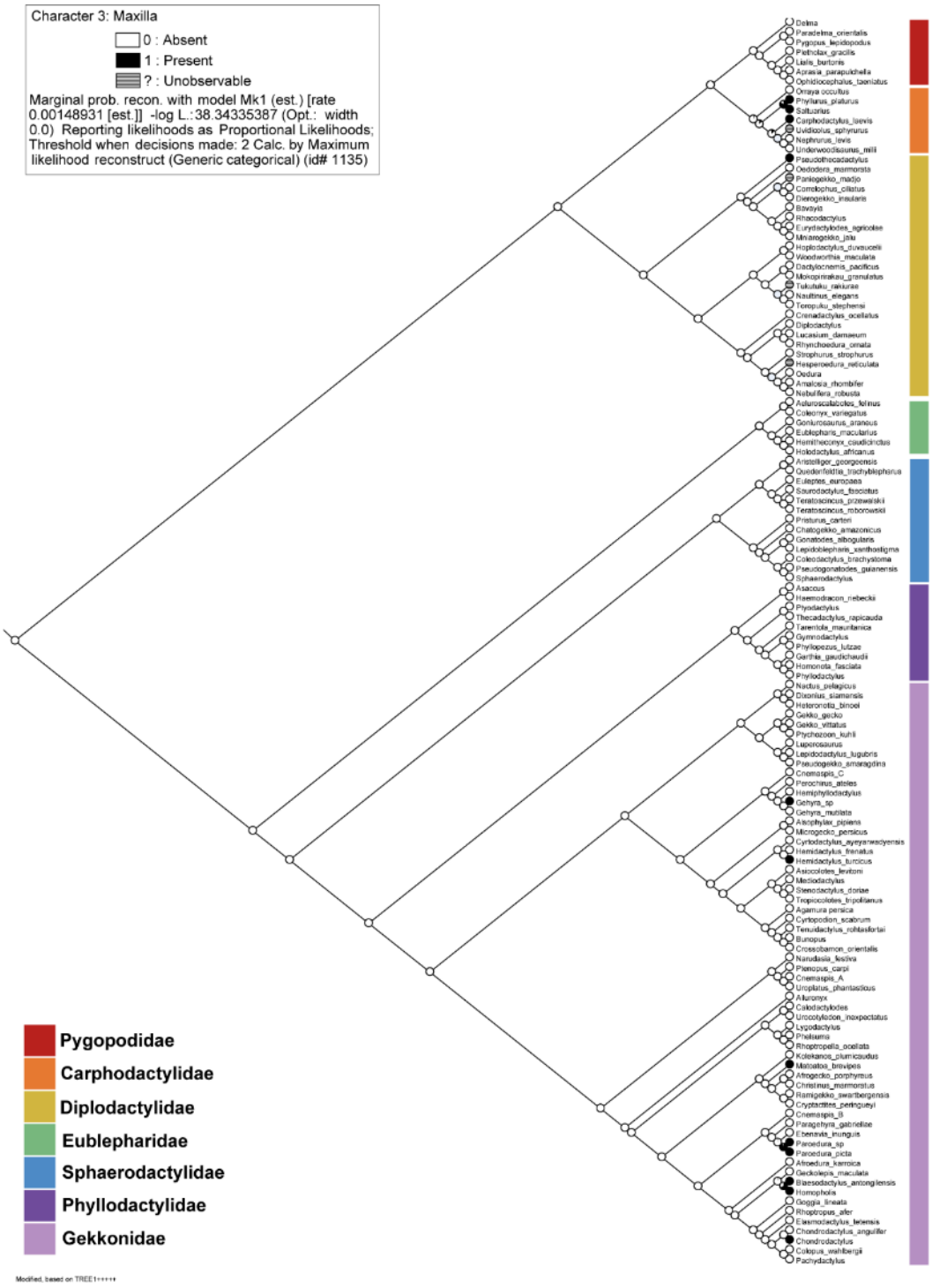

Figure 18. Likelihood character optimization results for the maxilla(s). Results of character optimization using likelihood methods. Each family is grouped together by colored box.

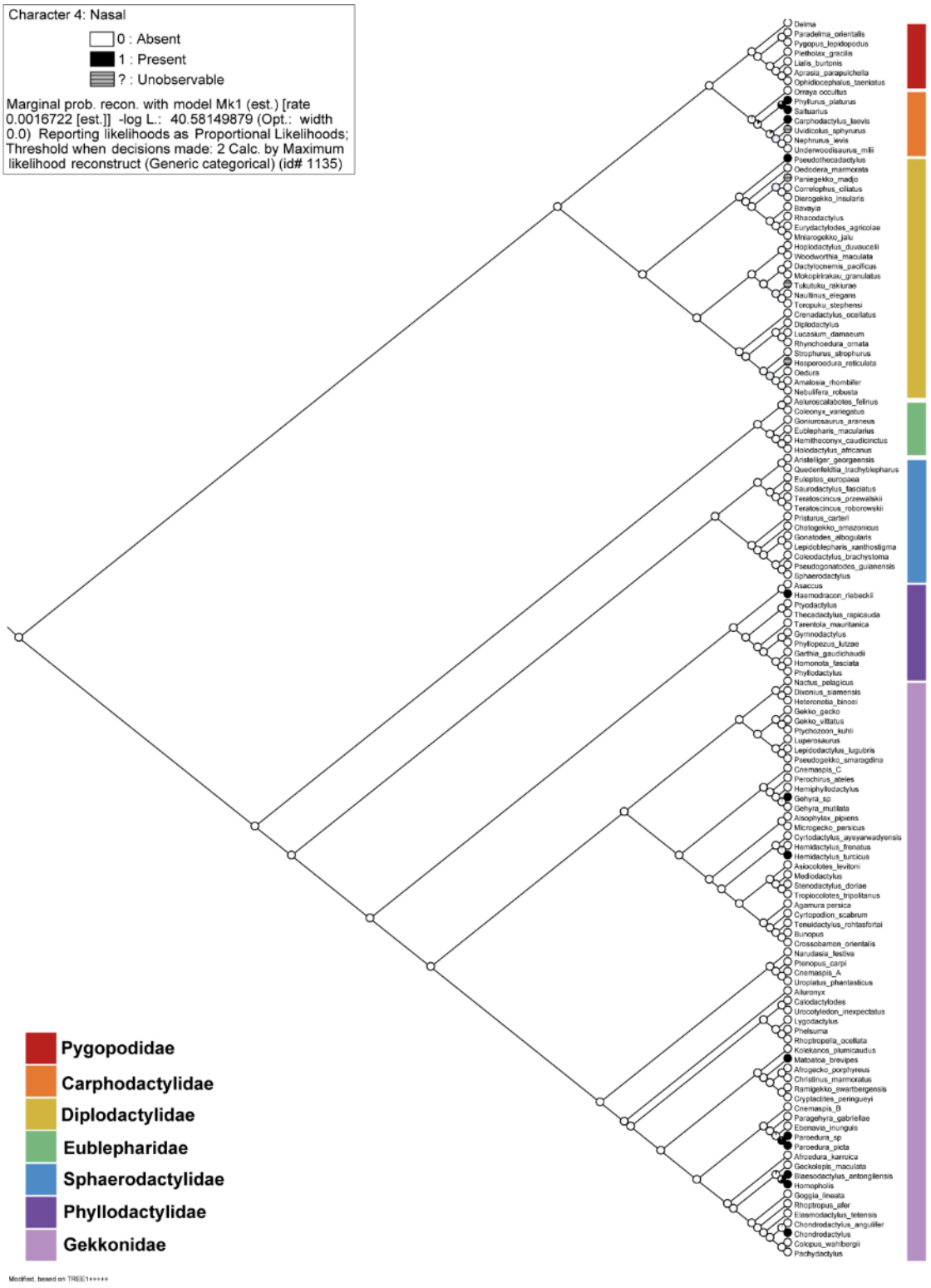

Figure 19. Likelihood character optimization results for the nasal(s). Results of character optimization using likelihood methods. Each family is grouped together by colored box.

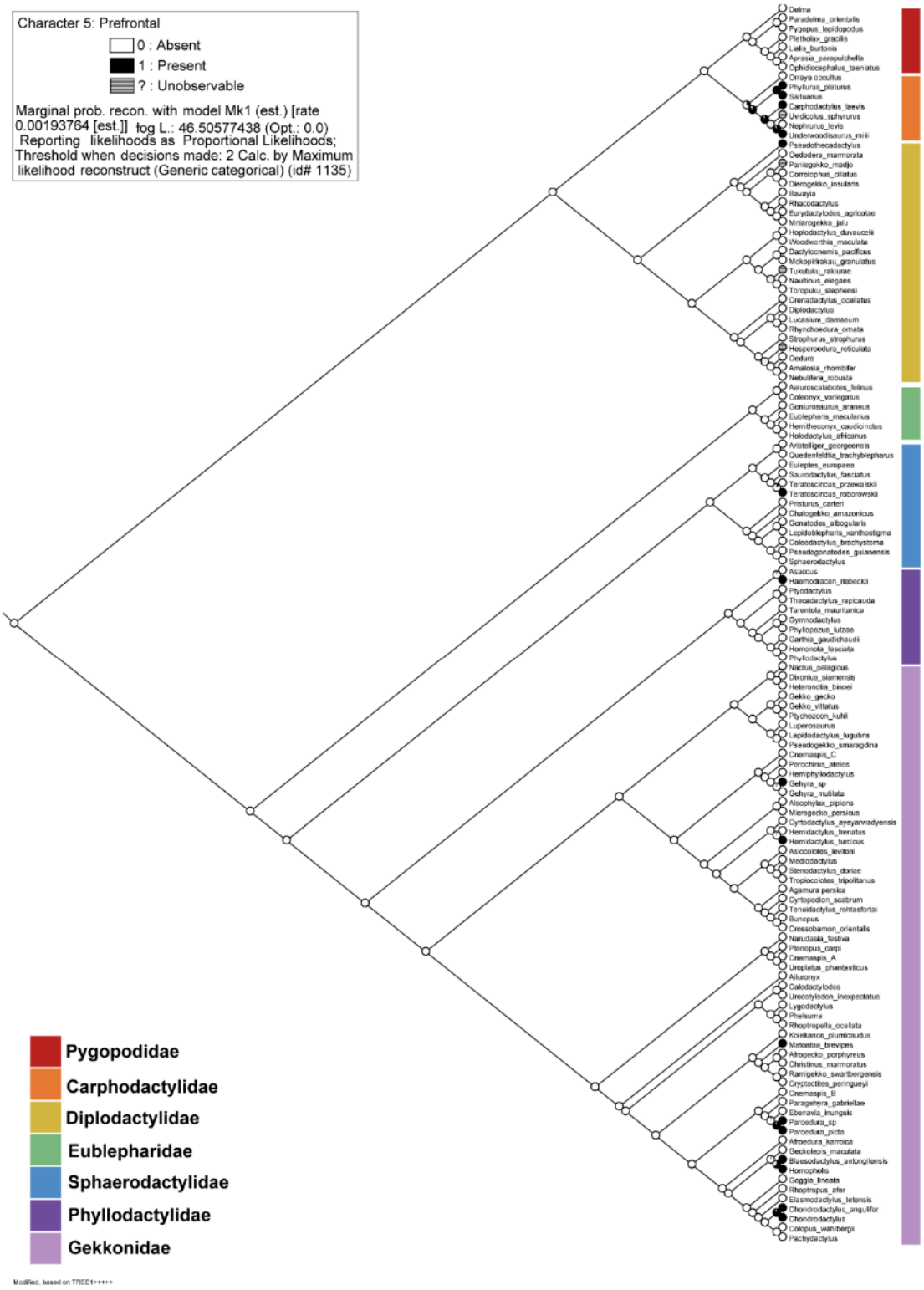

Figure 20. Likelihood character optimization results for the prefrontal(s). Results of character optimization using likelihood methods. Each family is grouped together by colored box.

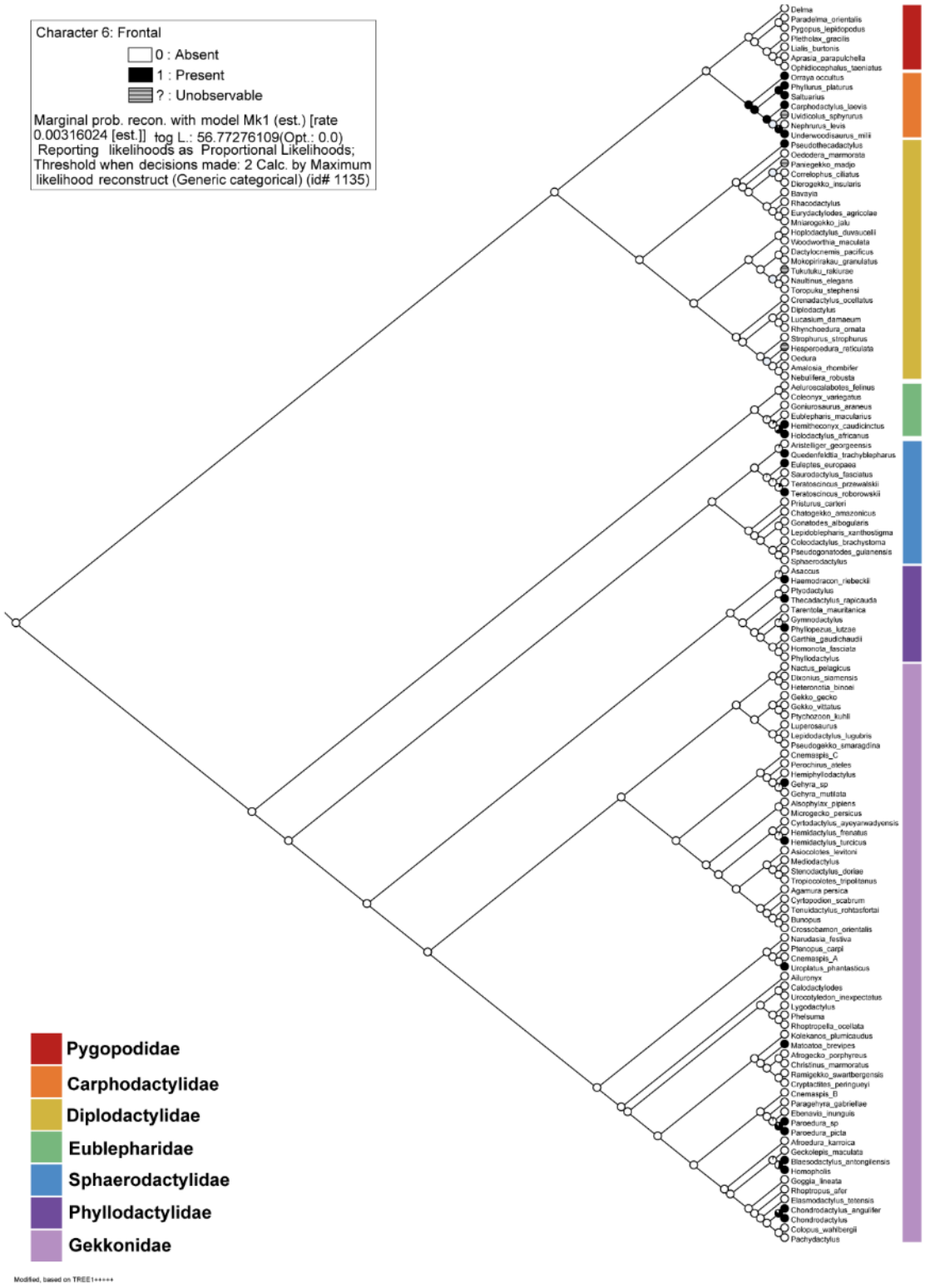

Figure 21. Likelihood character optimization results for the frontal. Results of character optimization using likelihood methods. Each family is grouped together by colored box.

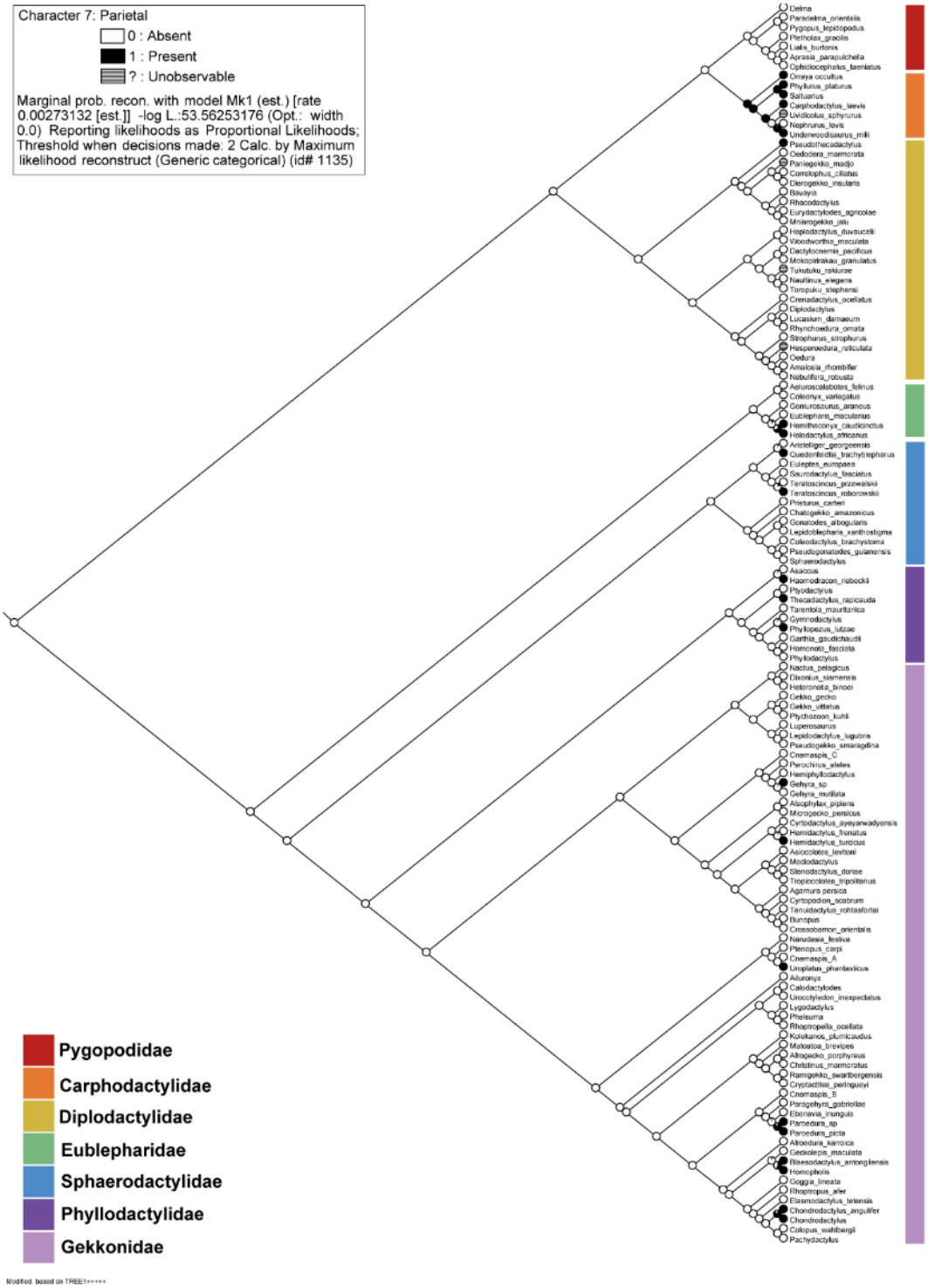

Figure 22. Likelihood character optimization results for the parietal(s). Results of character optimization using likelihood methods. Each family is grouped together by colored box.

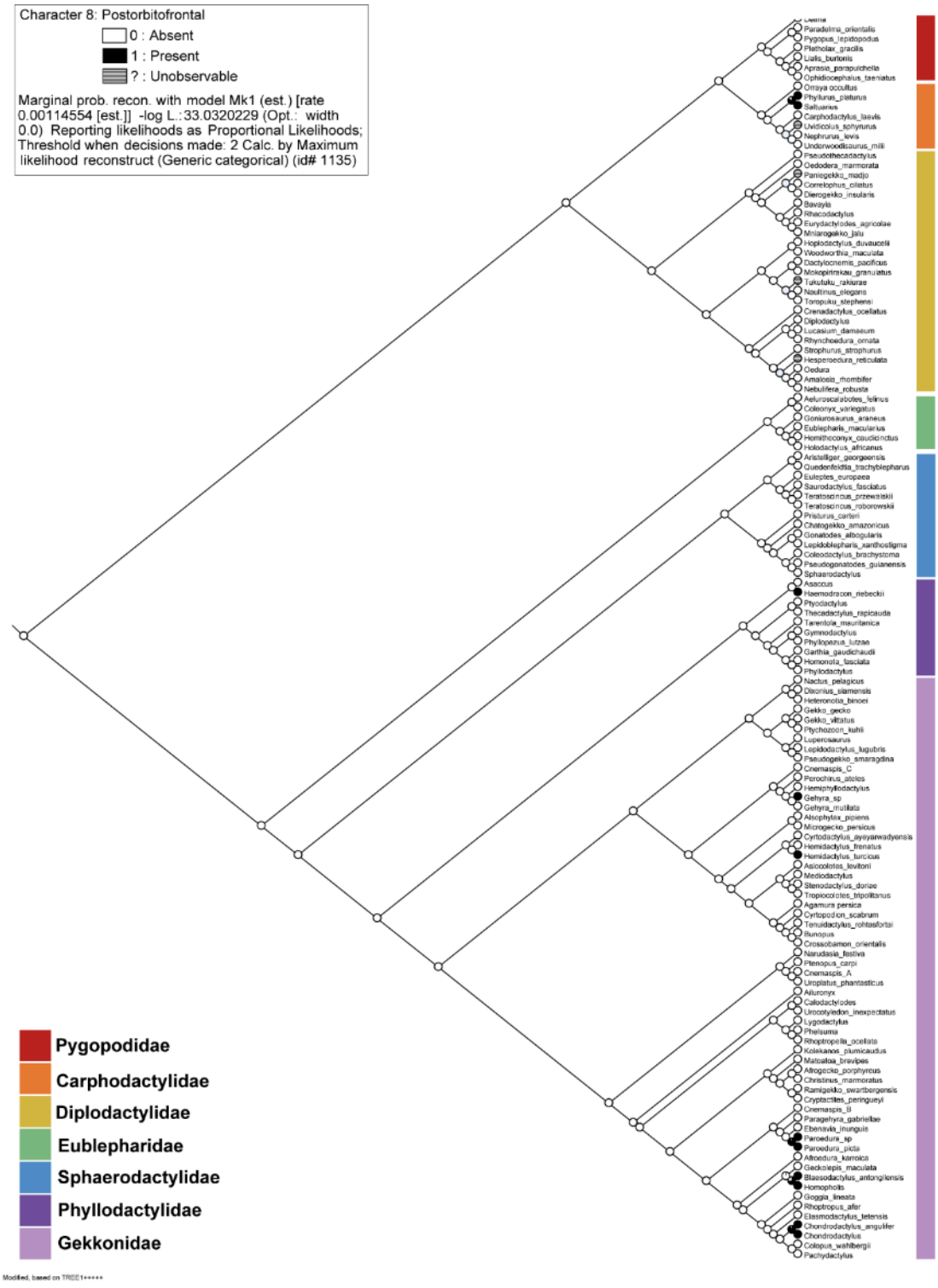

Figure 23. Likelihood character optimization results for the postorbitofrontals. Results of character optimization using likelihood methods. Each family is grouped together by colored box.

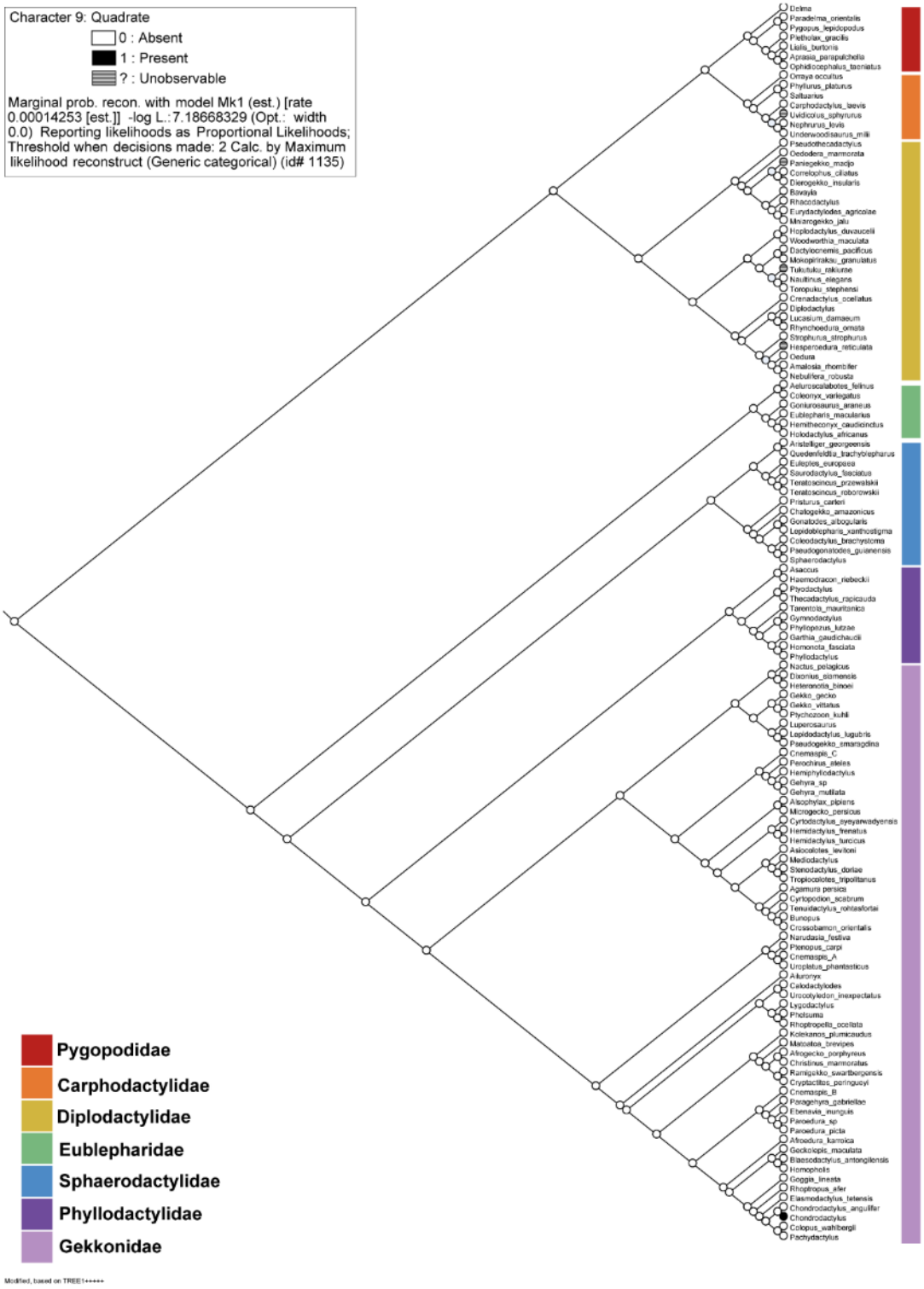

Figure 24. Likelihood character optimization results for the quadrates. Results of character optimization using likelihood methods. Each family is grouped together by colored box.

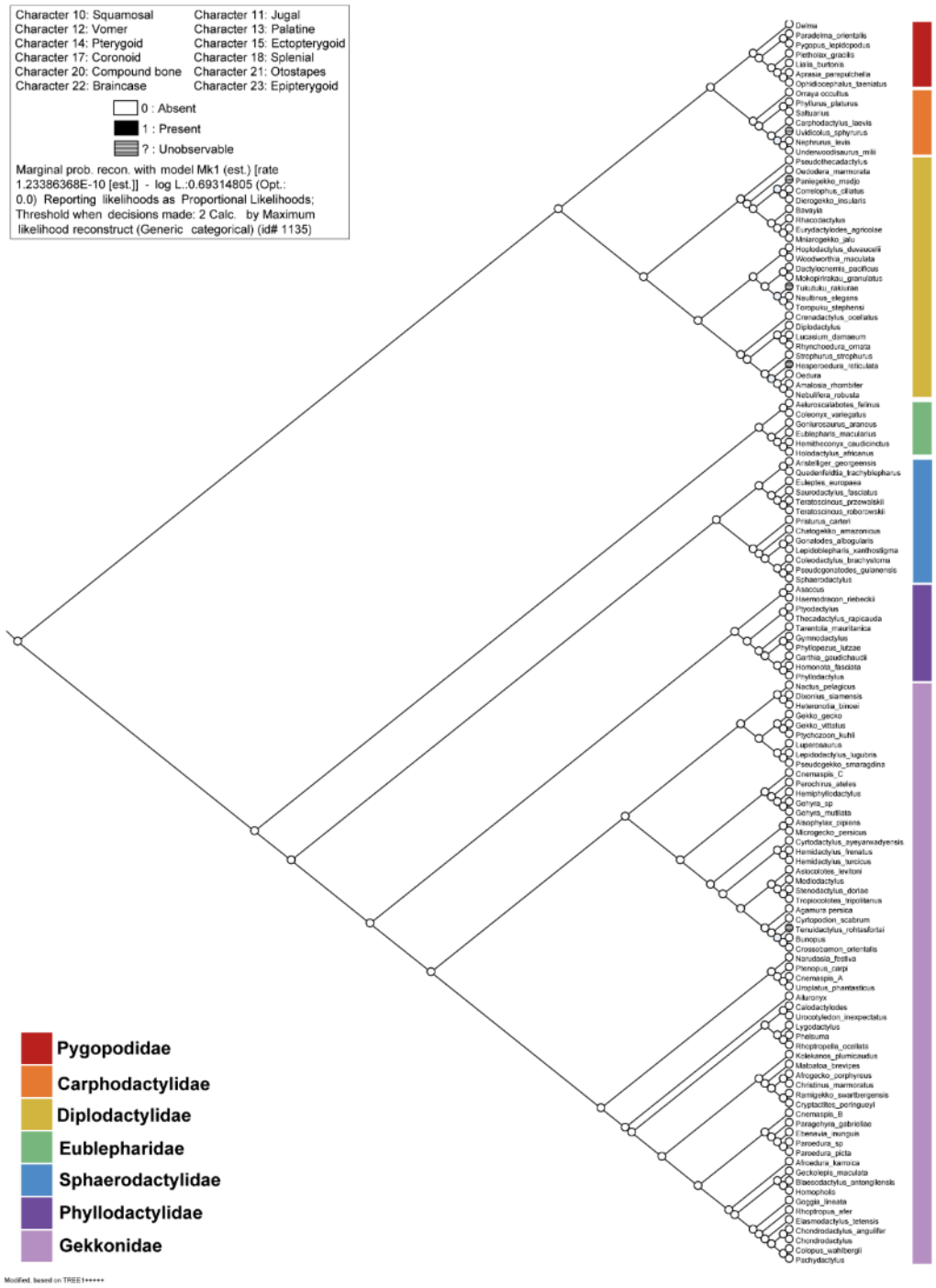

Figure 25. Likelihood character optimization results for the smooth bones. Results of character optimization were the same for the following: squamosal(s), jugal(s), vomer(s), palatine(s), pterygoid(s), ectopterygoid(s), coronoid(s). splenial(s), compound bone(s), otostape(s), epiptyergoid(s), and the braincase. Each family is grouped together by colored box.

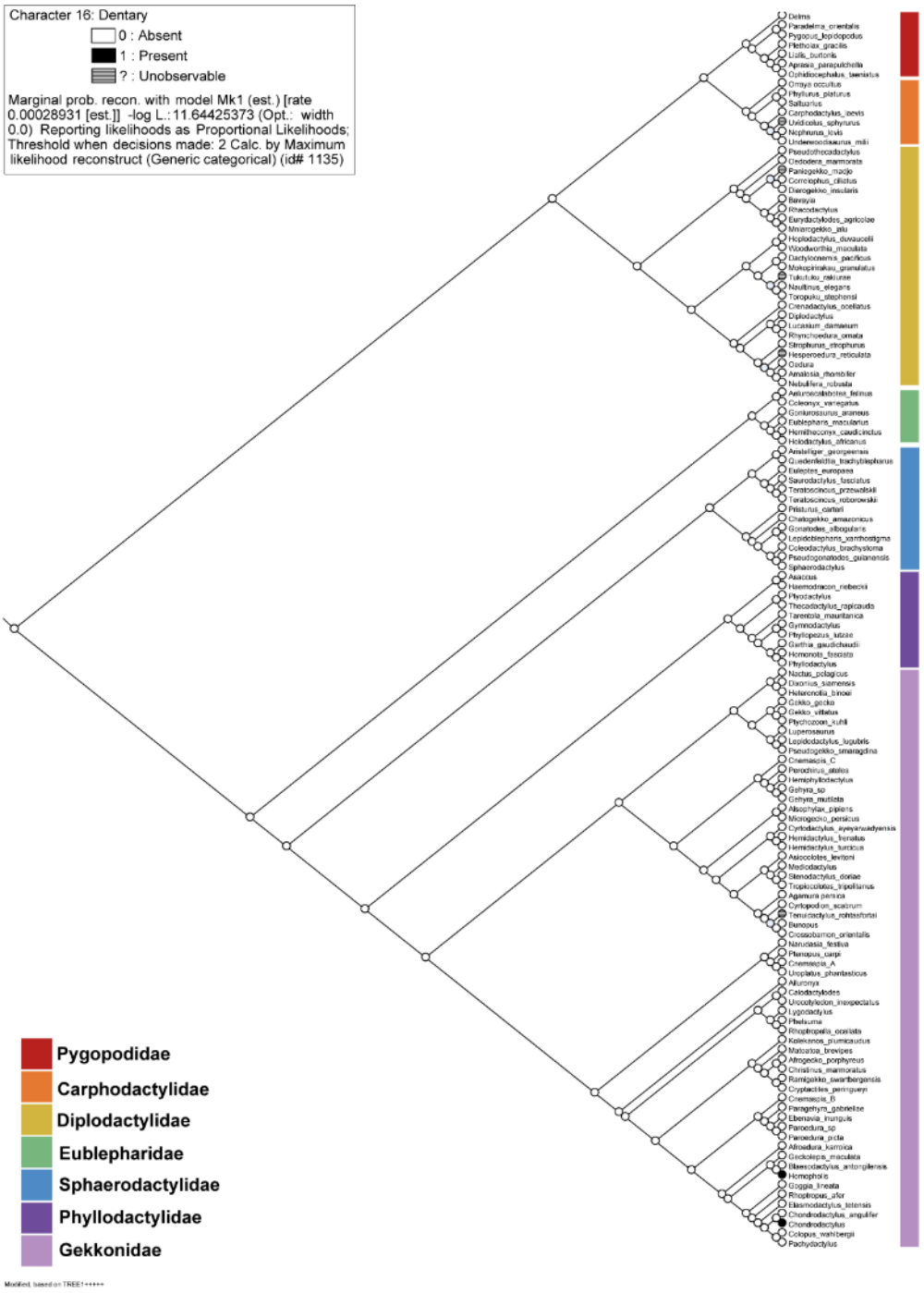

Figure 26. Likelihood character optimization results for the dentary(s). Results of character optimization using likelihood methods. Each family is grouped by colored box.

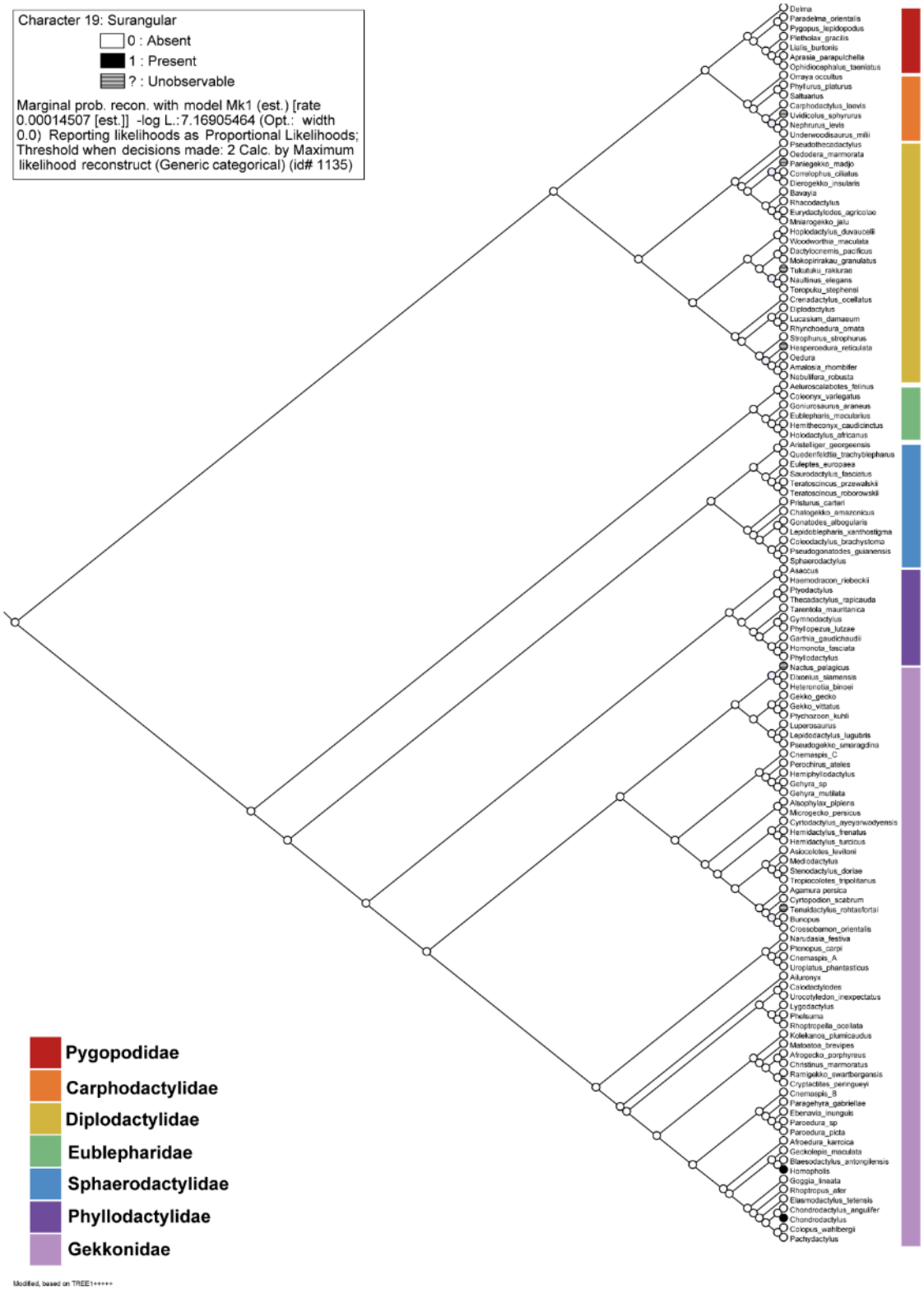

Figure 27. Likelihood character optimization results for the surangular(s). Results of character optimization using likelihood methods. Each family is grouped together by colored box.

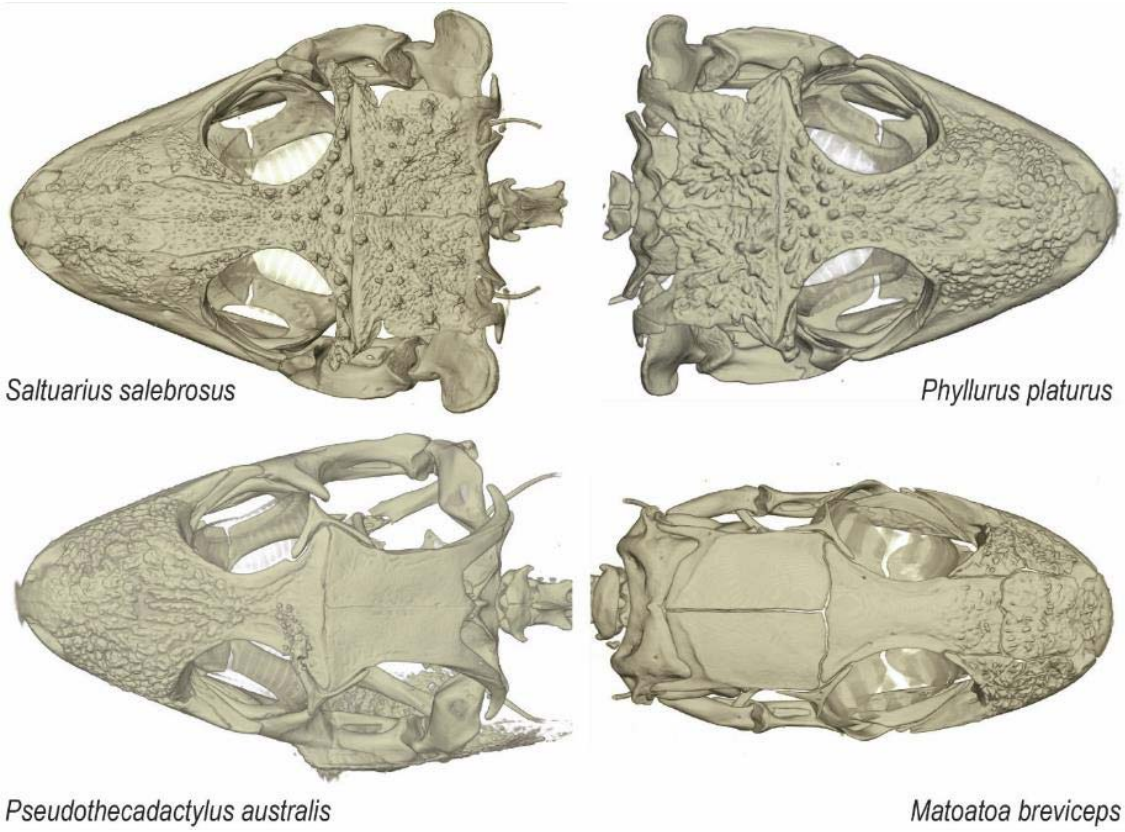

Figure 28. Examples of rugose variation.

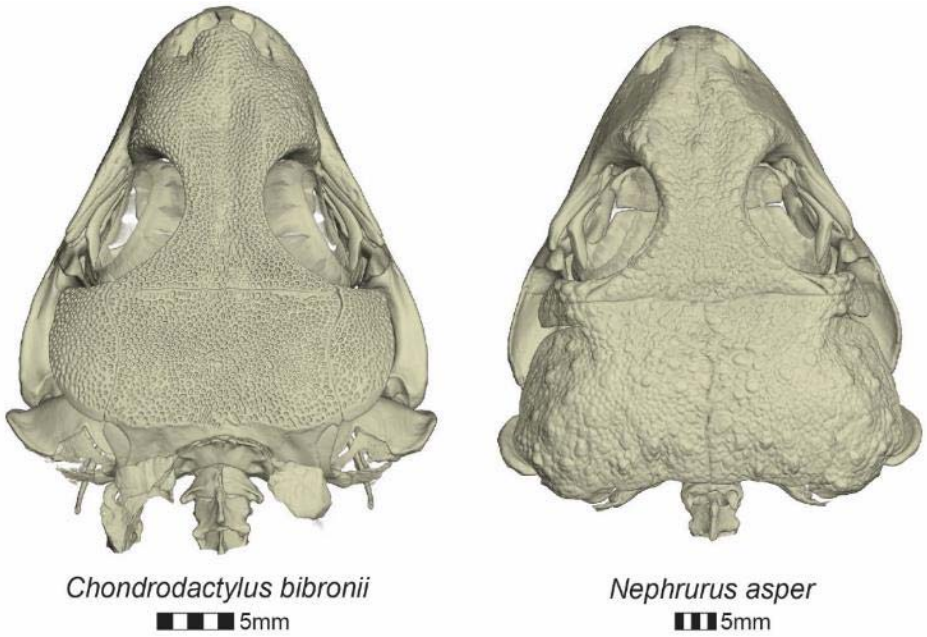

Figure 29. Extensive cranial bone sculpturing as seen on *Chondrodactylus bibronii* (left) and *Nephrurus asper* (right).

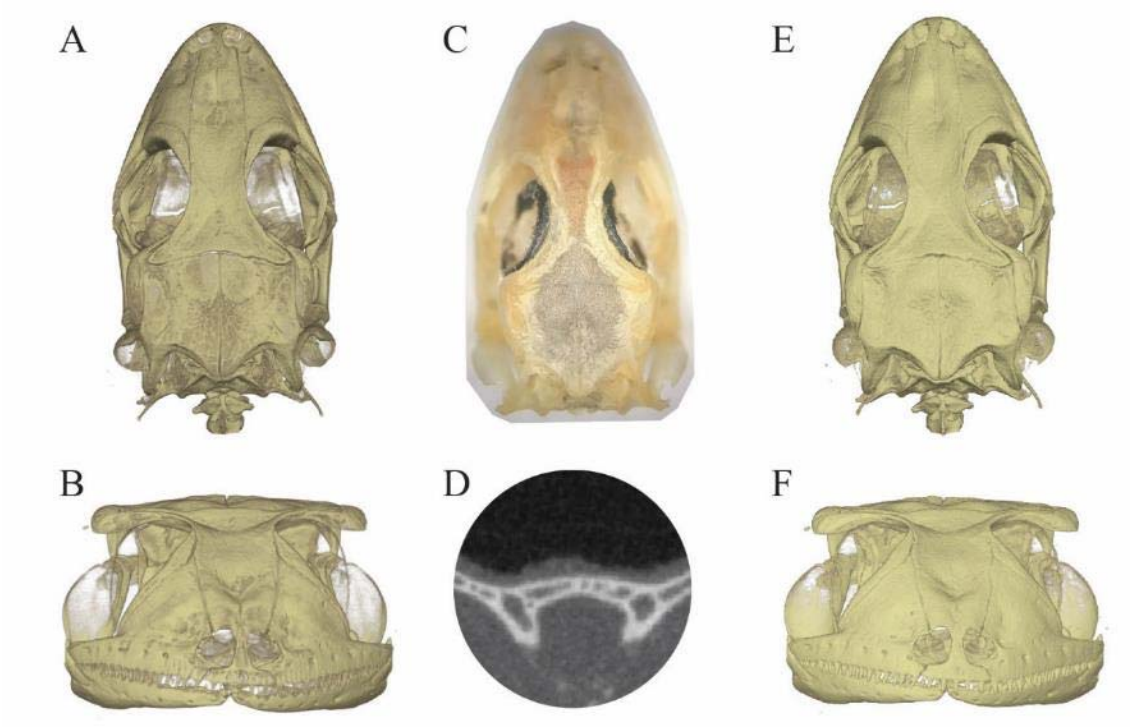

Figure 10. Threshold rendering verification in: *Hemidactylus frenatus* (CAS 215743) shown in dorsal (A, C, and E), rostral (B and F), and a coronal cut through the frontal (D). Skeletonized skull showing the grooved-like appearance (C). Skull shown digitally rendered with incorrect threshold limits (23790 – 45336, A and B). Skull digitally rendered with correct threshold limits (26483 – 35012, E and F) reflecting the computed tomography image (D).

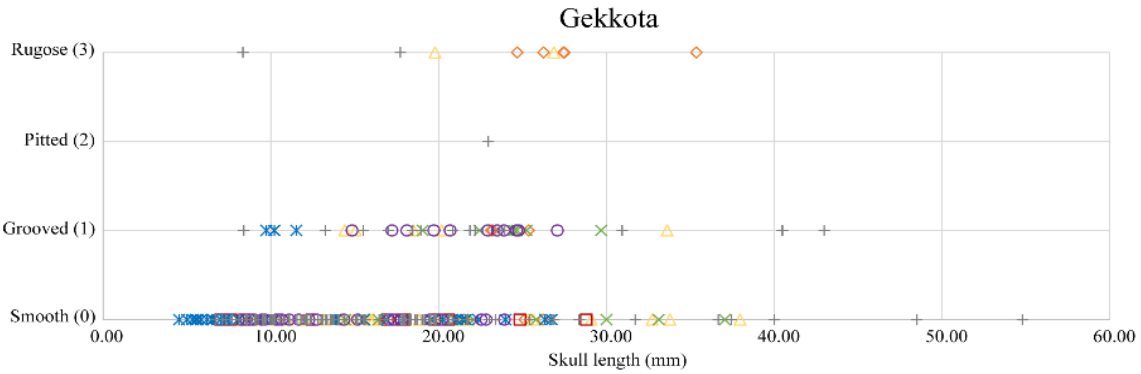

Figure 31. Cranial sculpturing and size variation in (Gekkota): cranial bone sculpturing in relation to skull length.

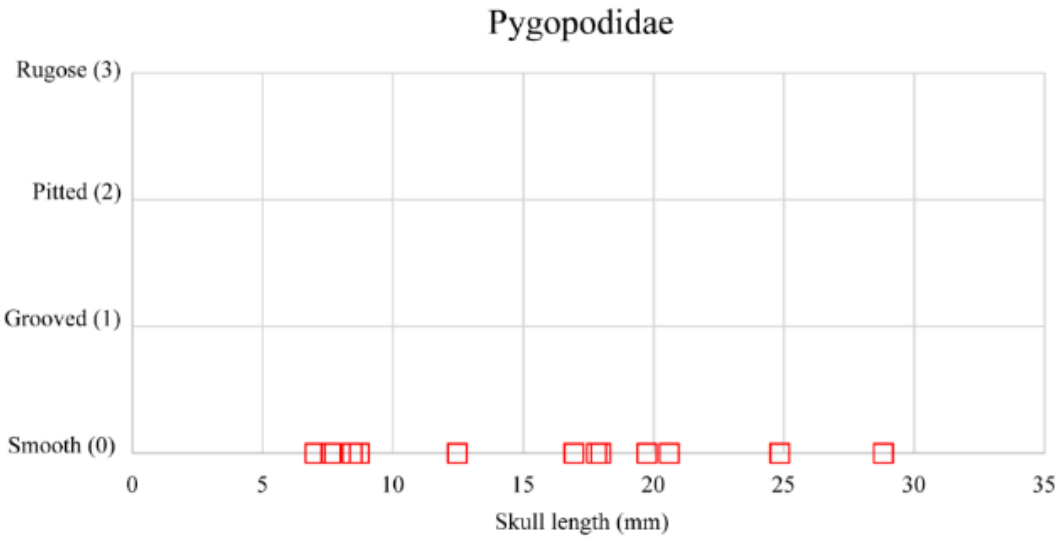

Figure 32. Cranial sculpturing and size variation in the Pygopodidae.

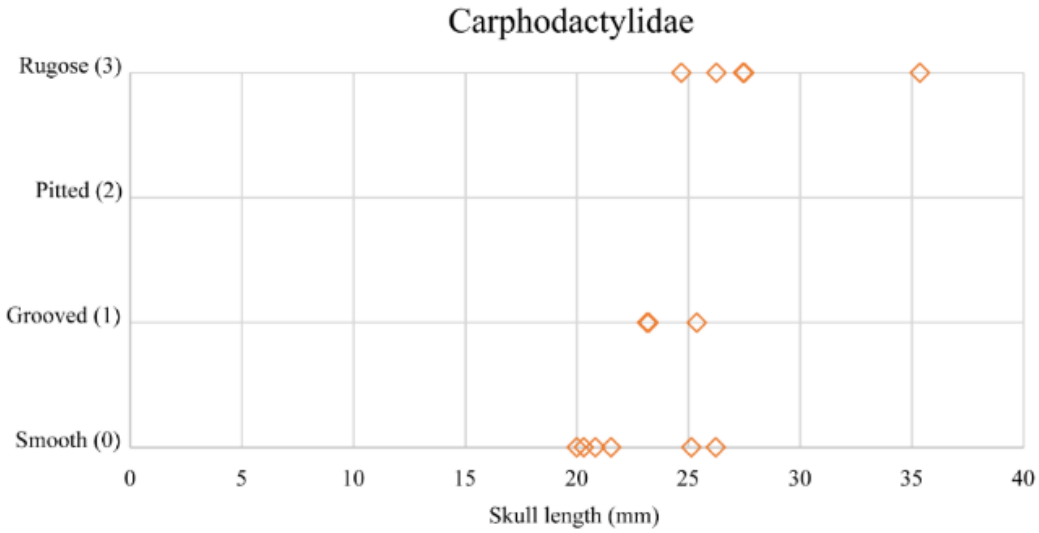

Figure 33. Cranial sculpturing and size variation in the Carphodactylidae.

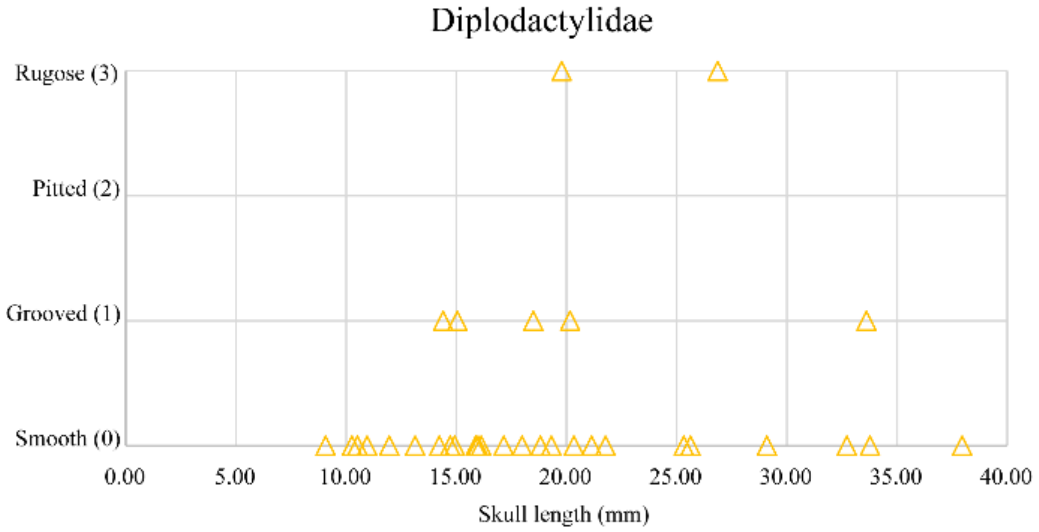

Figure 34. Cranial sculpturing and size variation in the Diplodactylidae.

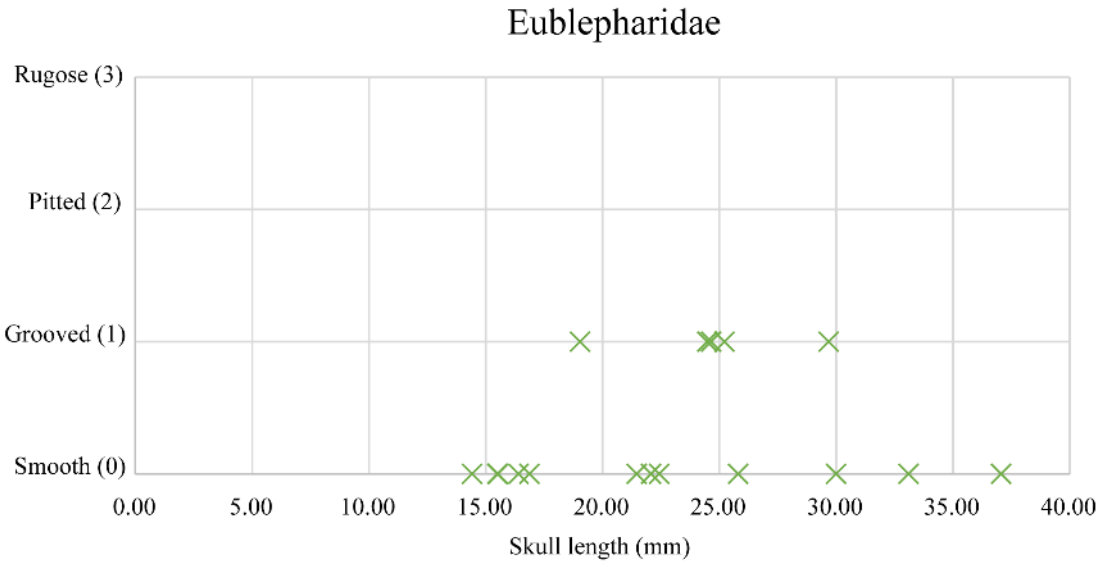

Figure 35. Cranial sculpturing and size variation Eublepharidae.

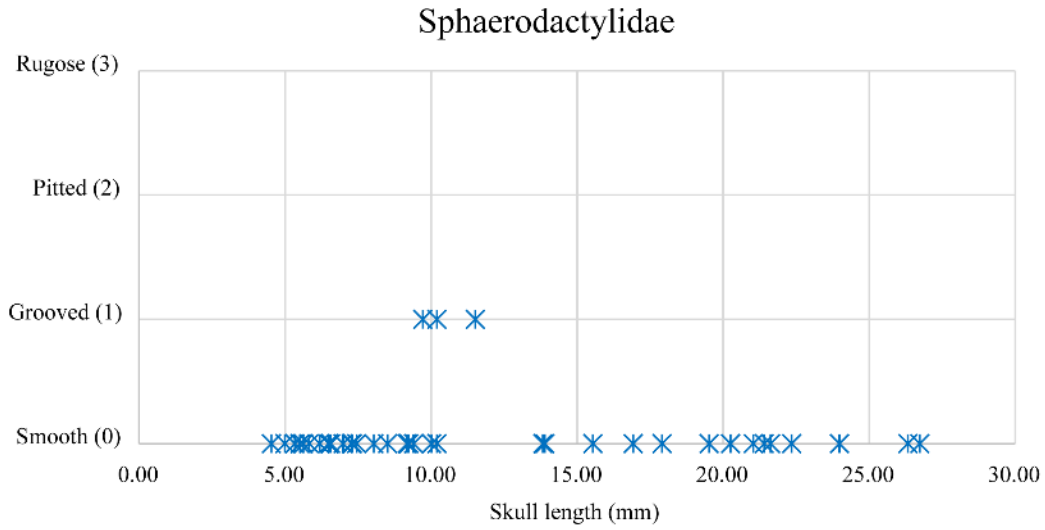

Figure 36. Cranial sculpturing and size variation in the Sphaerodactylidae.

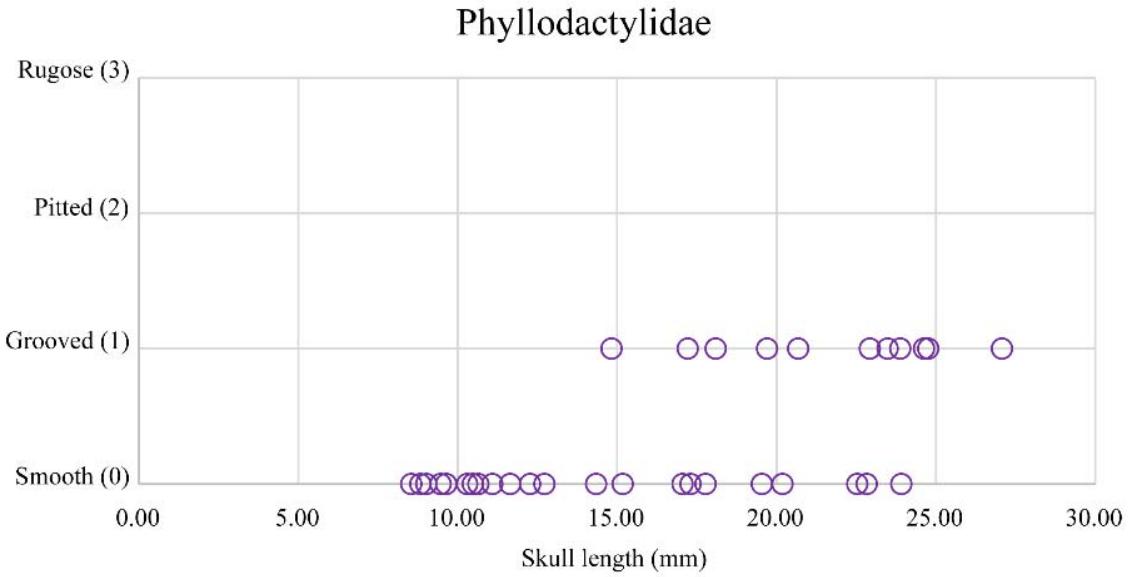

Figure 37. Cranial sculpturing and size variation in the Phyllodactylidae.

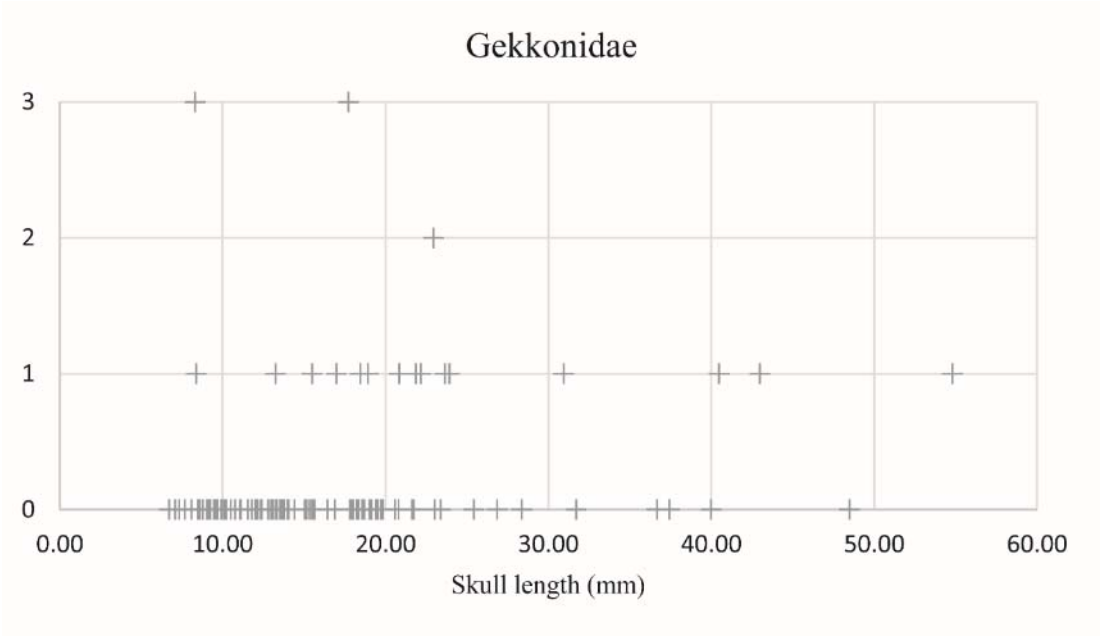

Figure 38. Cranial sculpturing and size variation in the Gekkonidae.

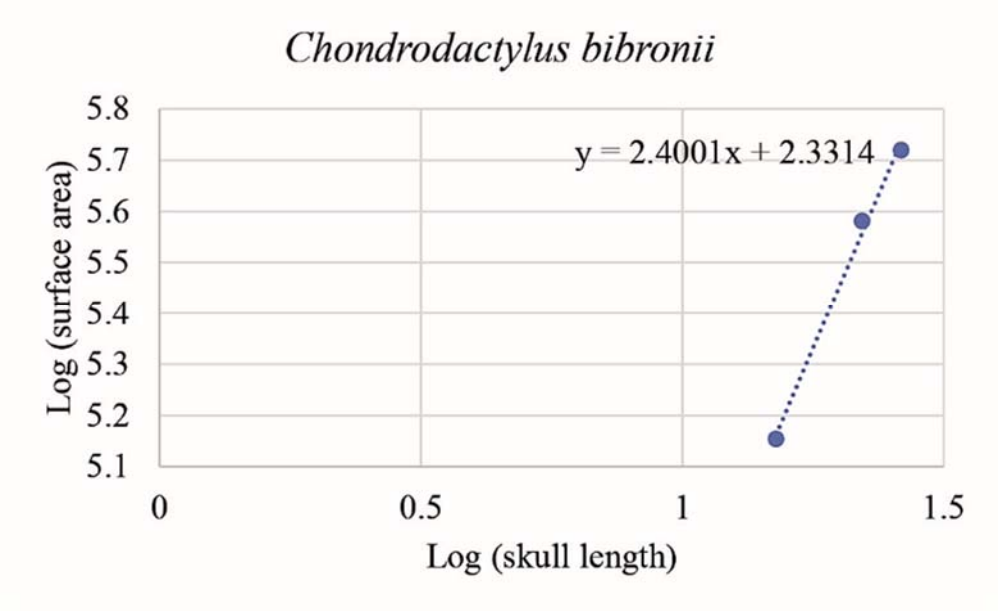

Figure 39. Post-hatchling developmental series (Pitted). Positive allometric grow rate of surface area over the skull length.

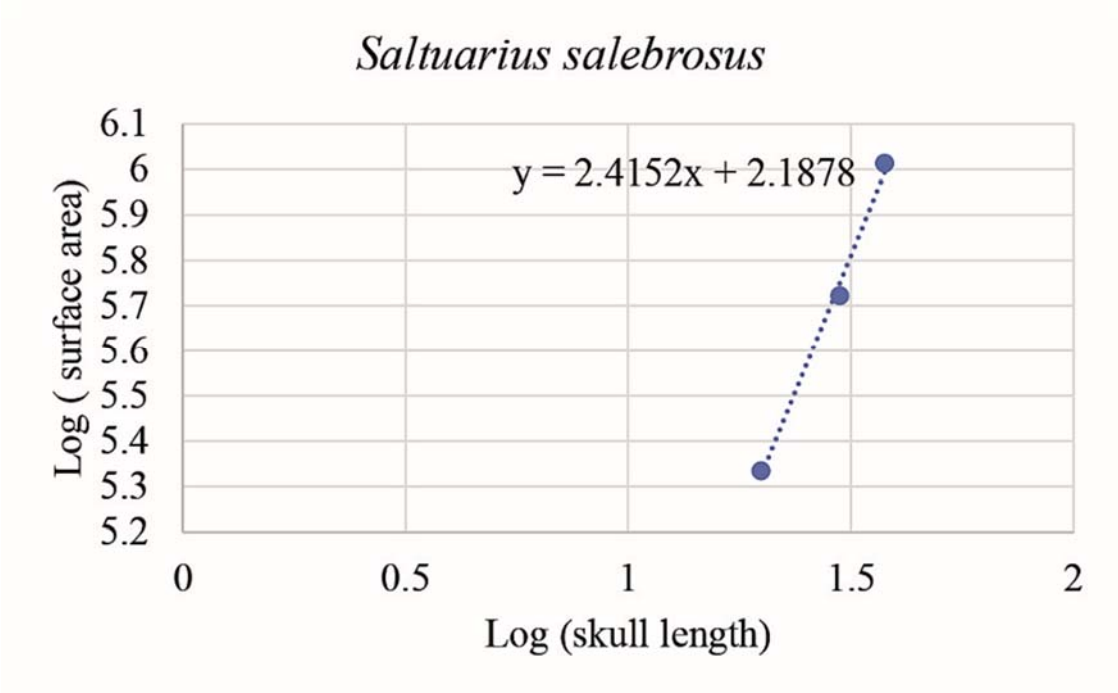

Figure 40. Post-hatchling developmental series (Rugose). Positive allometric grow rate of surface area over the skull length.

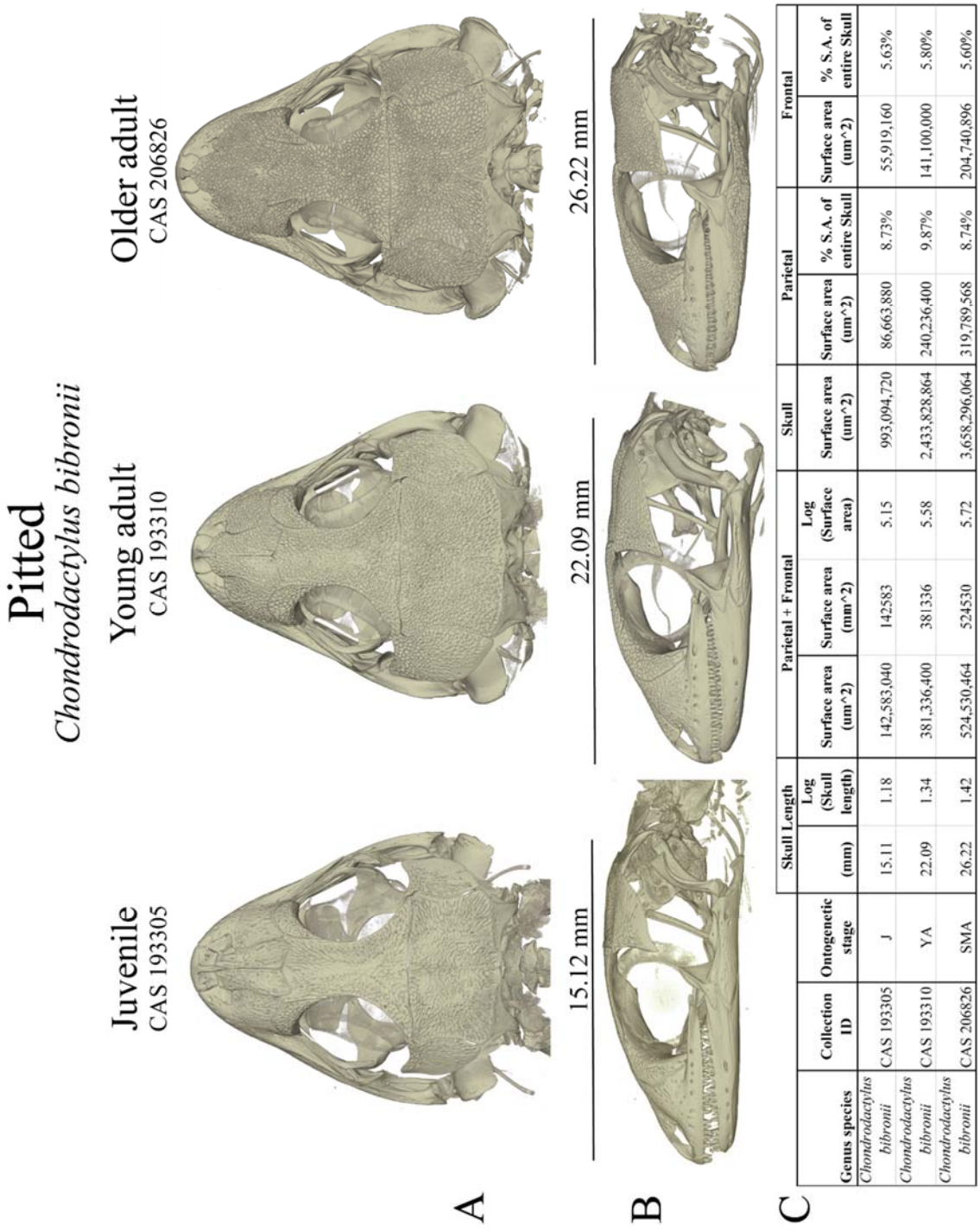

C

Genus species	Collection ID	Ontogenetic stage	Skull Length		Parietal + Frontal			Skull	Parietal		Frontal	
			(mm)	Log (Skull length)	Surface area (um^2)	Surface area (mm^2)	Log (Surface area)	Surface area (um^2)	Surface area (um^2)	% S.A. of entire Skull	Surface area (um^2)	% S.A. of entire Skull
Chondrodactylus bibronii	CAS 193305	J	15.11	1.18	142,583,040	142583	5.15	993,094,720	86,663,880	8.73%	55,919,160	5.63%
Chondrodactylus bibronii	CAS 193310	YA	22.09	1.34	381,336,400	381336	5.58	2,433,828,864	240,236,400	9.87%	141,100,000	5.80%
Chondrodactylus bibronii	CAS 206826	SMA	26.22	1.42	524,530,464	524530	5.72	3,658,296,064	319,789,568	8.74%	204,740,896	5.60%

Figure 41. Post-hatchling developmental series depicting the pitted character in: dorsal (A) and lateral (B) views of *Chondrodatylus bibronii*, with accompanying data (C).

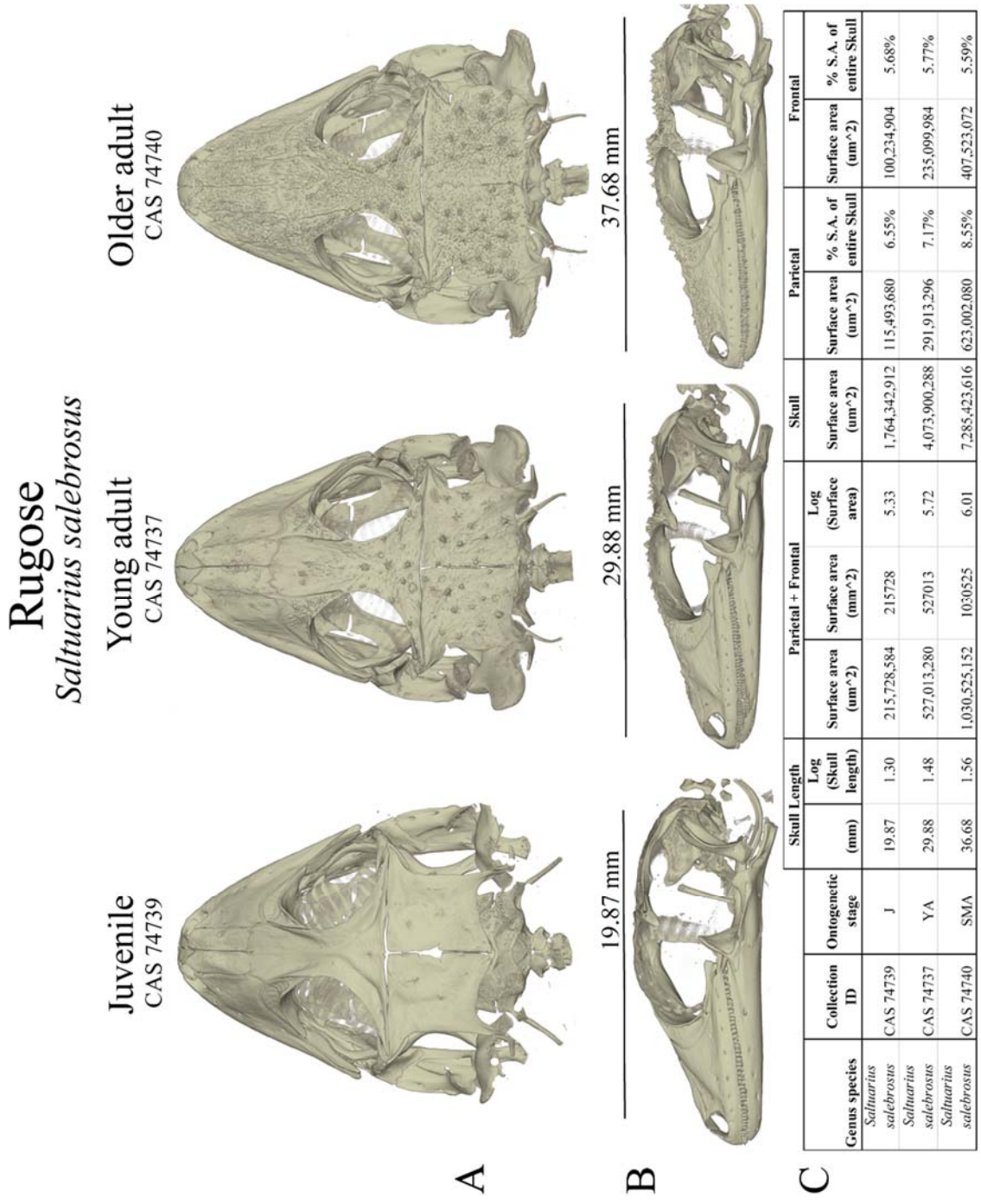

Genus species	Collection ID	Ontogenetic stage	Skull Length (mm)	Log (Skull length)	Parietal + Frontal Surface area (um^2)	Parietal + Frontal Surface area (mm^2)	Log (Surface area)	Skull Surface area (um^2)	Parietal Surface area (um^2)	Parietal % S.A. of entire Skull	Frontal Surface area (um^2)	Frontal % S.A. of entire Skull
Saltuarius salebrosus	CAS 74739	J	19.87	1.30	215,728,584	215728	5.33	1,764,342,912	115,493,680	6.55%	100,234,904	5.68%
Saltuarius salebrosus	CAS 74737	YA	29.88	1.48	527,013,280	527013	5.72	4,073,900,288	291,913,296	7.17%	235,099,984	5.77%
Saltuarius salebrosus	CAS 74740	SMA	36.68	1.56	1,030,525,152	1030525	6.01	7,285,423,616	623,002,080	8.55%	407,523,072	5.59%

Figure 42. Post-hatchling developmental series depicting the rugose character in: dorsal (A) and lateral (B) views of *Saltuarius salebrosus*, with accompanying data (C).

REFERENCES

Bauer, A.M. (1990). Phylogenetic systematics and biogeography of the Carphodactylini (Reptilia: Gekkonidae), Bonner Zoologische Monographien, 30:1–220

Bauer, A.M. (2013). Geckos—The Animal Answer Guide. Baltimore: The Johns Hopkins University Press, 1–192. Print.

Bauer, A. M., & Lamb, T. (2005). Phylogenetic relationships of southern African geckos in the *Pachydactylus* group (Squamata: Gekkonidae). Journal of the Herpetological Association of Africa, 54:105–129.

Boulenger, G.A. Catalogue of the lizards in the British Museum (Natural History). 2nd ed. Volume 1. Geckonidae, Eublepharidae, Uroplatidae, Pygopodidae, Agamidae. London: British Museum (Natural History), 1885-1887.

Bolet, A., Daza, J. D., Augé, M., & Bauer, A. M. (2015). New genus and species names for the Eocene lizard Cadurcogekko rugosus Augé, 2005. *Zootaxa*, *3985*(2), 265–274.

Bystrow, A.P. (1935). Morphologische Untersuchungen der Deckknochen des Schädels der Stegocephalen. 1. Mitteilung. Schädel der Stegocephalen. Acta Zoologica (Stockholm), 16:65–141.

Bystrow, A.P. (1947). Hydrophilous and zenophilous labyrinthodonts. Acta Zoologica (Stockholm), 28:137–164.

Camp, C.L. 1923. Classification of the lizards. Bulletin of the American Museum of Natural History, 48:289–481.

Clarac, F., Souter, T., Cornette, R., Cubo, J., & de Buffrénil, V. (2015). A quantitative assessment of bone area increase due to ornamentation in the Crocodylia. Journal of Morphology, 276:1183–1192.

Clarac, F., Souter, T., Cubo, J., de Buffrénil, V., Brochu, C., & Cornette, R. (2016). Does skull morphology constrain bone ornamentation? A morphometric analysis in the Crocodylia. Journal of Anatomy, 229:292–301.

Coldiron, R.W. (1974). Possible functions of ornament in the labyrinthodont amphibians. Occasional papers of the Museum of Natural History, University of Kansas, 33:1–19.

Conrad, J. L. (2008). Phylogeny and systematics of Squamata (Reptilia) based on morphology. Bulletin American Museum of Natural History, 310:1–182.

Conrad, J. L. (2017). A new lizard (Squamata) was the last meal of *Compsognathus* (Theropoda: Dinosauria) and is a holotype in a holotype. Zoological Journal of the Linnean Society, 20: 1-51.

Cosgriff, J. W., & Zawiskie, J. M. (1979). A new species of the Rhytidosteidae from the *Lystrosaurus* Zone and a review of the Rhytidostoidea. Palaeontologia Africana, 22:1–27.

Daza, J. D., Abdala, V., Thomas, R., & Bauer, A. M. (2008). Skull anatomy of the miniaturized gecko *Sphaerodactylus roosevelti* (Squamata: Gekkota). Journal of Morphology, 269(11), 1340–1364.

Daza, J. D., Aurich, J., & Bauer, A. M. (2012). Anatomy of an enigma: An osteological investigation of the Namibian festive gecko (*Narudasia festiva*: Gekkonidae: Gekkota). Acta Zoologica, 93:465–486.

Daza, J. D., & Bauer, A. M. (2010). The circumorbital bones of the Gekkota (Reptilia: Squamata). Anatomical Record, 293: 402–413.

Daza, J. D., Bauer, A. M., & Snively, E. D. (2014). On the fossil record of the Gekkota. *Anatomical Record*, *297*(3), 433–462.

de Buffrenil, V. (1982). Morphogenesis of bone ornamentation in extant and extinct crocodilians. Zoomorphology, 1982:155–166.

de Buffrénil, V., Clarac, F., Canoville, A., & Laurin, M. (2016). Comparative data on the differentiation and growth of bone ornamentation in gnathostomes (Chordata: Vertebrata). Journal of Morphology, 277:634–670.

Dias, E. V. & Richter, M. (2002). On the squamation of *Australerpeton cosgriffi* Barberna, a temnospondyl amphibian from the Upper Permian of Brazil, Annals of the Brazilian Academy of Science, 74: 477–490.

Estes, R., De Queiroz, K., & Gauthier, J. A. "Phylogenetic relationships within Squamata." Phylogenetic Relationships of the Lizard Families. Essays Commemorating Charles L. Camp. Ed. R. Estes & G. Pregill. Stanford: Stanford University Press, 1988. 119–281.

Evans, S. E. (2008). The skull of lizards and tuatara. In Gans, C., Gaunt, A. S., & Adler, K. (Eds): Biology of the Reptilia, Vol 20, Morphology H: The skull of Lepidosauria. 1–347.

Gamble, T., Greenbaum, E., Jackman, T. R., & Bauer, A. M. (2015). Into the light: diurnality has evolved multiple times in geckos. Biological Journal of the Linnean Society, 115:896–910.

Gauthier, J. A., Kearney, M., Maisano, J. A., Rieppel, O., & Behlke, A. D. B. (2012). Assembling the squamate tree of life: Perspectives from the phenotype and the fossil Record. Bulletin of the Peabody Museum of Natural History, 53:3–308.

Glynne, E., Daza, J.D., Bauer, A.M. Gekkota skulls: taking the rough with the smooth. Society for the Study of Amphibians and Reptiles, Annual Meeting at the University of Kansas. Lawrence, Kansas, USA. July 30 – August 2, 2015. Poster Presentation. 18.

Griffing, A. H., Daza, J. D., DeBoer, J. C., & Bauer, A. M. (2017). Developmental osteology of the parafrontal bones of the Sphaerodactylidae. The Anatomical Record. 301:581-606.

Hall, B.K. (2005). Bones and cartilage: developmental skeletal biology. Academic Press, New York, 792 pp.

Horner, J. R., & Goodwin, M. B. (2008). Ontogeny of cranial epi-ossifications in *Triceratops*. Journal of Vertebrate Paleontology, 28:134–144.

Janis, C. M., Devlin, K., Warren, D. E., & Witzmann, F. (2012). Dermal bone in early tetrapods: a palaeophysiological hypothesis of adaptation for terrestrial acidosis. Proceedings of the Royal Society B: Biological Sciences, 279:3035–3040.

Jared, C., Mailho-Fontana, P.L., Antoniazzi, M. M., Menders, V.A., Barbaro, K. C., Rodrigues, M. T., & Brodie Jr., E. D. (2015). Venomous frogs use heads as weapons. Current Biology, 25:2166–2170.

Kardong, K. (2012). Vertebrates: Comparative anatomy, function, evolution, 6th ed. McGraw-Hill, New York.

Maddison, W. P. & D.R. Maddison. (2018). Mesquite: a modular system for evolutionary analysis. Version 3.40 http://www.mesquiteproject.org

Morkovin, B. I. (2015). On the development of surface ornamentation of skull bones in the ontogeny of Early Triassic benthosuchids (Amphibia, Temnospondyli). Paleontological Journal, 49:57–69.

Nixon, K. C. 1999-2002. WinClada ver. 1.0000 Published by the author, Ithaca, NY, USA.

Protzel, D., Heß, M., Scherz, M. D., Schwager, M., Padje, A. V. & Flaw, F. (2018). Widespread bone-based fluorescence in chameleons. Scientific Reports, 8:698

Rinehart, L. F., & Lucas, S. G. (2013). The functional morphology of dermal bone ornamentation in temnospondyl amphibians. The Triassic System. New Mexico Museum of Natural History and Science, 61: 524–532.

Romer, A. S. (1947). Review of the Labyrinthodontia. Bulletin of the Museum of Comparative Zoology, 99:368

Romer, A. S. (1956). Osteology of the Reptiles. University of Chicago Press, Chicago.

Rieppel, O. (1984). The structure of the skull and jaw adductor musculature in the Gekkota, with comments on the phylogenetic relationships of the Xantusiidae (Reptilia: Lacertilia). Zoological Journal of the Linnean Society, 82: 291–318.

Rieppel, O. "Patterns of diversity in the reptilian skull." *The Skull. Volume 2. Patterns of Structural and Systematic Diversity.* Ed. J. Hanken & B. K. Hall. The University of Chicago Press, Chicago. 1993. 344–390.

Schoch, R. R. (2001). Can metamorphosis be recognized in Paleozoic amphibians? Neues Jahrbuch für Geologie und Paläontologie, 220:335–367.

Schoch, R. R. (2002). The evolution of metamorphosis in temnospondyls. Lethaia, 35: 309–327.

Seidel, M.R. (1979). The osteoderms of the American alligator and their functional significance. Herpetologica, 35:375–380.

Simões, T. R., Caldwell, M. W., Palci, A., & Nydam, R. L. (2016). Giant taxon-character matrices: Quality of character constructions remains critical regardless of size. *Cladistics*, 1-22, published online.

Trueb, L. "Patterns of cranial diversification among the Lissamphibia." *The Skull. Volume 2. Patterns of Structural and Systematic Diversity.* Ed. J. Hanken & B. K. Hall. Chicago: The University of Chicago Press, 1993. 255–343.

Uetz, P., Freed, P. & Jirí Hošek (eds.), The Reptile Database, http://www.reptile-database.org.

Williston, S.W. (1925). The osteology of the reptiles. Cambridge: Harvard.Print.

Witzman, F. (2009). Comparative histology of sculptured dermal bones in basal tetrapods, and the implications for the soft tissue dermis. Palaeodiversity, 2:233–270.

Witzmann F., & Soler-Gijon R. (2010). The bone histology of osteoderms in temnospondyl amphibians and in the chroniosuchian *Bystrowiella*. Acta Zoologica (Stockholm), 91:96–114.

Witzmann, F., Scholz, H., MüLler, J., & Kardjilov, N. (2010). Sculpture and vascularization of dermal bones, and the implications for the physiology of basal tetrapods. Zoological Journal of the Linnean Society, 160:302–340.

APPENDIX A: Characters and Character States (Parsimony)

The following is a list of the characters and character states used in the analysis. All characters below were unordered.

Character 0. Osteoderms:

(0) bone smooth, not ornamented (1) bone sculptured

Character 1 –25 correspond to each individual bone and were scored in the same way (see below). Bones were examined in this order: Ch-1, Premaxilla; Ch-2, Maxilla; Ch-3, Nasal; Ch-4, Prefrontal; Ch-5, Frontal; Ch-6, Parietal; Ch-7, Postorbitofrontal; Ch-8, Quadrate; Ch-9, Squamosal; Ch-10, Jugal; Ch-11, Vomer; Ch-12, Palatine; Ch-13, Pterygoid; Ch-14, Ectopterygoid; Ch-15, Dentary; Ch-16, Coronoid; Ch-17, Splenial; Ch-18, Surangular; Ch-19,Compoud; Ch-20, Otostapes; Ch-21, Braincase; Ch-22, Epipterygoid; Ch-23, Parafrontal; Ch-24, Lacrimal; Ch-25, Supratemporals.

Character states:

(0) bone smooth, not ornamented

(1) bone sculptured

(2) bone pitted or pit and ridge

(3) bone rugose or granular

(?) Character not represented in the study.

(-) Character unknown or not observed in the study.

APPENDIX B: Characters and Character States (Likelihood)

The following is a list of the characters and character states used in the likelihood analysis. Characters were considered as unordered for this analysis.

Characters:

Character 1. Osteoderms:

Character 2. Premaxilla:

Character 3. Maxilla:

Character 4. Nasal:

Character 5. Prefrontal:

Character 6. Frontal:

Character 7. Parietal:

Character 8. Postorbitofrontal:

Character 9. Quadrate:

Character 10. Squamosal:

Character 11. Jugal:

Character 12. Vomer:

Character 13. Palatine:

Character 14. Pterygoid:

Character 15. Ectopterygoid:

Character 16. Dentary:

Character 17. Coronoid:

Character 18. Splenial:

Character 19. Surangular:

Character 20. Compound bone:

Character 21. Otostapes:

Character 22. Braincase:

Character 23. Epipterygoid:

Character 24. Parafrontal:

Character 25. Lacrimal:

Character 26. Supratemorporal:

Character states:

(0) bone smooth, not ornamented.

(1) bone sculptured.

(?) Not represented in the study.

(-) Unknown or not observed in the study.

APPENDIX C: Specimens examined for character optimization

Codes for Institutional Collections: AMB, Aaron M. Bauer, personal collection, Villanova, PN, USA; AMNH, American Museum of Natural History, New York, NY, USA; AMR, Australian Museum, Darlinghurst, NSW, AUS; BMNH, The Natural History Museum, London, ENG**;** CAS, California Academy of Sciences, San Francisco, CA, USA; CMNH, Cleveland Museum of Natural History, Cleveland, OH, USA**;** FMNH, The Field Museum of Natural History, Chicago, IL, USA; JFBM, Bell Museum of University of Minnesota, St Paul, MN, USA; MCZ, The Museum of Comparative Zoology, Cambridge, MA, USA; MTR, Miguel T. Rodrigues, personal collection, São Paulo, SP, BRA**;** QMJ, Queensland Museum, South Brisbane, QLD, AUS; SAM, South Australian Museum, Adelaide, SA, AUS **;** SHSVMH-H, The Sam Houston State Vertebrate Museum, Herpetology Collection, Huntsville, TX, USA; TNHC, Texas Natural History Collection, University of Texas, Austin, TX, USA; UMMZ, University of Michigan Museum of Zoology, Ann Arbor, MI, USA; USNM, National Museum of Natural History, Smithsonian Institution, Washington D.C., USA; WAM, Western Australian Museum, Northbridge, WA, AUS; YPM, Peabody Museum of Natural History, Yale University, New Haven, CT, USA.

Preparation type is indicated according to the following key: C&S = cleared and stained, DI = digital images of specimens, Sk = dry skeleton, and CT = high-resolution X-ray computed tomography.

List of specimens examined (including collection number; preparation): *Aeluroscalabotes felinus* (FMNH 166958; CT); *Afroedura karroica* (CAS 198274;CT); *Afrogecko porphyreus* (CAS 175312; CT); *Agamura persica* (CAS 140562; CT); *Ailuronyx seychellensis* (CAS 167459; CT); *Alsophylax pipiens* (CAS 143679; CT); *Altiphylax levitoni* (121037A; CT); *Amalosia rhombifer* (CAS 100919; CT); *Apraisia parapulchella (*WAM 62884; CT); *Aristelliger goergeensis* (CAS 176485; CT); *Asaccus elisae* (CAS 218137; CT); *Bavayia robusta* (AMB 7335; CT); *Blaesodactylus antongilensis* (UMMZ 192320; CT); *Blaesodactylus boivini* (CAS 127770; CT); *Bunopus crassicauda* (CAS 140598A; CT); *Calodactylodes aureus* (MCZ R-3918; CT); *Carphodactylus laevis* (MCZ R-35114; CT); *Chatogekko amazonicus* (MTR 12682A; CT); *Chondrodactylus anguilfer* (CAS 126466; CT); *Chondrodactylus bibronii* (CAS 173299; CT); *Christinus marmoratus* (CAS 75014; CT); *Cnemaspis boulengeri* (MCZ R-16665; CT); *Cnemaspis gracils* (CAS 113988; CT); *Cnemaspis spinicollis* (CAS 103312; CT); *Coledactylus brachystoma* (UMMZ 103051; CT); *Coleonyx variegatus* (YPM 14383; CT); *Colopus wahlbergii* (CAS 125901; CT); *Correlophus ciliates* (JFBM 15825; Sk); *Crenadactylus ocellatus* (CAS 95287; CT); *Crossobamon eversmanni* (CAS 180001; CT); *Cryptactites peringueyi* (CAS 186375; CT); *Cyrtodactylus ayeyarwadyensis* (CAS 221985; CT); *Cyrtopodion scabrum* (CAS 218186; CT); *Dactylocnemis pacificus* (CAS 95146; CT); *Delma borea* (USNM 128679; CT); *Dierogekko insularis* (r161070; CT); *Diplodactylus pulcher* (CAS 75182; CT); *Dixonius siamensis* (CAS 95254; CT); *Ebenavia inunguis* (CAS 66195; CT); *Elasmodactylus tetensis* (AMB 6180; CT); *Eublepharis macularius* (CMNH 67524l; CT); *Euleptes europaea* (MCZ R-4463; CT); *Eurydactylodes agricolae* (CAS 232001; CT); *Garthia gaudichaudii* (UMMZ 111574; CT); *Geckolepis maculate*

(CAS 126344; CT); *Gehyra mutilate* (CAS 251893; CT); *Gehyra oceanica* (MCZ R-66501; CT); *Gehyra vorax* (CAS 74742; CT); *Gekko gecko* (SHSVM-H 0001-2014; CT); *Gekko smithii* (CAS 9595; CT); *Gekko vittatus* (CAS SUI 20857; CT); *Goggia lineata* (CAS 193627; CT); *Gonatodes albogularis* (FMNH 55929; CT); *Goniurosaurus araneus* (JFBM 15830; Sk); *Gymnodactylus geckoides (*CAS 49397; CT); *Haemodracon riebeckii* (MCZ A-27255; CT); *Hemidactylus frenatus* (CAS 215743; CT); *Hemidactylus turcicus* (TNHC 85380; CT); *Hemiphyllodactylus typus* (CAS 174223; CT); *Hemitheconyx caudicinctus* (CAS 165588; CT); *Heteronotia binoei* (CAS 74923; CT); *Holodactylus africanus* (CAS 198932; CT); *Homonota fasciata* (CAS 84771; CT); *Homopholis wahlbergii* (CAS 248630; CT); *Hoplodactylus duvaucelii* (BMNH 62.9.2.18; DI); *Kolekanos plumicaudus* (CAS 248782; CT); *Lepidoblepharis xanthostigma* (CAS 178104; CT); *Lepidodactylus lugubris* (CAS 224273; CT); *Lialis burtonis* (FMNH 166958; CT); *Lucasium steindachneri* (CAS 75185; CT); *Luperosaurus corfieldi* (CAS 182570;CT); *Lygodactylus capensis* (CAS 167621; CT); *Matoatoa breviceps* (AMNH R-159476; CT); *Mediodactylus kotschyii* (CAS 101566; CT); *Microgecko persicus* (UMMZ 122007; CT); *Mniarogekko jalu* (CAS A-27255; CT); *Mokopirirakau granulatus* (CAS 47982; CT); *Nactus pelagicus* (CAS 119003; CT); *Narudasia festiva (*CAS 186278*;* CT); *Naultinus elegans* (CAS 47976; CT); *Nebulifera robusta* (UMMZ 131647; CT); *Nephrurus levis occidentalis* (CAS 254620; CT); *Oedodera marmorata* (AMS 161264; CT); *Oedura tyroni* (CAS 75669; CT); *Ophidiocephalus taeniatus (*SAMA 45176; CT); *Orraya occultus* (QMJ 60717; CT); *Pachydactylus bicolor* (CAS 223912; CT); *Paradelma orientalis* (CAS 77652; CT); *Paragehyra gabriellae* (UMMZ 216284; CT); *Paroedura picta* (JFBM 15826; Sk); *Paroedura stumpffi* (CAS 66192; CT); *Perochirus*

ateles (CAS 206241; CT); *Phelsuma lineata* (FMNH 260100; CT); *Phyllodactylus baurii* (CAS 9501; CT); *Phyllopezus lutzae* (MCZ R-46191; CT); *Phyllurus platurus* (MCZ R-130254; CT); *Pletholax gracilis (*MCZ R-187676; CT); *Pristurus carteri* (CAS 193627; CT); *Pseudogekko smaragdinus* (CAS 62344; CT); *Pseudogonatodes barbourin* (MCZ R- 14385: CT); Pseudothecadactylus australis (MCZ R-35162; CT); *Ptenopus carpi* (CAS 214548; CT); *Ptychozoon kuhli* (UMMZ 65570; CT); *Ptyodactylus hasselquistii* (CAS 228536; CT); *Pygopus lepidopodus* (CAS 135450; CT); *Quedenfeldtia trachyblepharus* (CAS 123275; CT); *Ramigekko swartbergensis* (CAS 180418; CT); *Rhacodactylus auriculatus* (CAS 205486; CT); *Rhoptropella ocellata* (CAS 193865; CT); *Rhoptropus afer* (CAS 193865; CT); *Rhynchoedura ornata* (UMMZ 124484; CT); *Saltuarius salebrosus* (CAS 74742; CT); *Saurodactylus fasciatus* (CAS 92404; CT); *Sphaerodactylus ariasae* (USNM 541810; CT); *Stenodactylus doriae* (CAS 250946; CT); *Strophurus strophurus* (CAS 254623; CT); *Tarentola mauritanica* (CAS 87112; CT); *Tenuidactylus fedtschenkoi* (CAS 182955; CT); *Teratoscincus przewalskii* (CAS 171013; CT); *Thecadactylus rapicauda* (CAS 95146; CT); *Toropuku stephensi* (CAS 47986; CT); *Tropiocolotes triolitanus* (CAS 123467; CT); *Underwoodisaurus milii* (CAS 74744; CT); *Urocotyledon inexpectata* (UMMZ 168104; CT); *Uroplatus phantasticus* (CAS 250492; CT); and *Woodworthia maculatus* (CAS 228536; CT)

APPENDIX D: Character Matrix

"Matrix in file "Diurnality_6gene.part1.Yule.trees.OUT.tre""

Type of matrix: Standard Categorical Data (compacted)

Number of characters: 26

Number of taxa: 144

Aeluroscalabotes_felinus -00000000000000000000--1

Afroedura_karroica -00000000000000000000---

Kolekanos_plumicaudus -00000000000000000000---

Afrogecko_porphyreus -00000000000000000000---

Ramigekko_swartbergensis -00000000000000000000---

Agamura persica -00000000000000000000---

Ailuronyx -00000000000000000000---

Alsophylax_pipiens -00000000000000000000---

Amalosia_rhombifer -00000000000000000000---

Amphisbaena ??????????????????????????

Anolis_caronlinensis ??????????????????????????

Aprasia_parapulchella -0000000000000000-00000---

Aristelliger_georgeensis -00000000000000000000--

Asaccus -00000000000000000000---

Asiocolotes_levitoni -00000000000000000000---

Aspidoscelis_tigris ??????????????????????????

Bavayia -00000000000000000000---

Blaesodactylus_antongilensis -0(1&2)(1&2)(1&2)(1&2)(1&2)(1&2)000000000000000---

Bunopus -0000000000000000000000---

Calodactylodes 0000000000000000000000--?

Carphodactylus_laevis -0(0&3)33330300011001000010---

Chatogekko_amazonicus -00000000000000000-00000---

Chondrodactylus_angulifer -0001111100000000000000---

Chondrodactylus -(0&2)222222200000000002000---

Christinus_marmoratus -0000000000000000000000---

Cnemaspis_A -0000000000000000000000---

Cnemaspis_C -0000000000000000000000---

Cnemaspis_B -0000000000000000000000---

Coleodactylus_brachystoma -00000000000000000-00000---

Coleonyx_variegatus -0000000000000000000000---

Colopus_wahlbergii -0000000000000000000000---

Correlophus_ciliatus -0000000000000000000000---

Crenadactylus_ocellatus -0000000000000000000000---

Crossobamon_orientalis -0000000000000000000000---

Cryptactites_peringueyi -0000000000000000000000---

Cyrtodactylus_ayeyarwadyensis -00000000000000000000000---

Cyrtopodion_scabrum -0000000000000000000000---

Dactylocnemis_pacificus -0000000000000000000000---

Delma -0000000000000000000000---

Dibamus_bouretti ??????????????????????????

Dierogekko_insularis -0000000000000000000000---

Diplodactylus -00000000000000000000---

Dixonius_siamensis -00000000000000000000---

Ebenavia_inunguis -00000000000000000000---

Elagaria_kingii ??????????????????????????

Elasmodactylus_tetensis -00000000000000000000---

Eublepharis_macularius -00000000000000000000???

Euleptes_europaea -00001000000000000000---

Eumeces ??????????????????????????

Eurydactylodes_agricolae -0000000000000000-00000---

Gallus ??????????????????????????

Garthia_gaudichaudii -00000000000000000000---

Geckolepis_maculata -00000000000000000000---

Gehyra_sp -1111111000000000000000---

Gehyra_mutilata -00000000000000000000---

Gekko_gecko 10000000000000000000---

Gekko_vittatus -00000000000000000000---

Goggia_lineata -00000000000000000000---

Gonatodes_albogularis -00000000000000000000---

Goniurosaurus_araneus -00111110000000000000---

Gymnodactylus -00000000000000000000---

Haemodracon_riebeckii -00(0&1)(0&1)11(0&1)000000000000000---

Heloderma_suspectum ??????????????????????????

Hemidactylus_frenatus -00000000000000000000---

Hemidactylus_turcicus -1111111000000000000000---

Hemiphyllodactylus -00000000000000000000---

Hemitheconyx_caudicinctus -00001100000000000000---

Hesperoedura_reticulata ??????????????????????????

Heteronotia_binoei -00000000000000000000---

Holodactylus_africanus -00001100000000000000---

Homonota_fasciata -00000000000000000000---

Homopholis -(0&1)1111110000000(0&1)00(0&1)0000---

Hoplodactylus_duvaucelii -00000000000000000000---

Lepidoblepharis_xanthostigma -00000000000000000000---

Lepidodactylus_lugubris -00000000000000000000---

Lialis_burtonis -000000000-000000000000---

Lucasium_damaeum -00000000000000000000---

Luperosaurus -00000000000000000000---

Lygodactylus -000000000-000000000000---

Matoatoa_brevipes 03333(0&3)00000000000000000---

Mediodactylus -00000000000000000000---

Microgecko_persicus 100000000000000000000---

Mniarogekko_jalu -00000000000000000000---

Mokopirirakau_granulatus -00000000000000000000---

Nactus_pelagicus -00000000000000000000---

Narudasia_festiva -00000000000000000000---

Naultinus_elegans -00000000000000000000---

Nebulifera_robusta -00000000000000000000---

Nephrurus_levis -00000000000000000000---

Oedodera_marmorata -00000000000000000000---

Oedura -0000000000000000000---

Ophidiocephalus_taeniatus -00000000000000000000---

Orraya occultus -00003(0&3)0000000000000000---

Pachydactylus -0000000000000000000---

Paniegekko_madjo ??????????????????????

Paradelma_orientalis -00000000000000000000---

Paragehyra_gabriellae -00000000000000000000---

Paroedura_sp -0(0&3)33333000000000000000---

Paroedura_picta -111111110000000000000---

Perochirus_ateles -00000000000000000000---

Phelsuma -0000000000000000000---

Phyllodactylus -00000000000000000000---

Phyllopezus_lutzae -0000(0&1)00000000000000000---

Phyllurus_platurus -(0&3)(0&3)333330000000000000000---

Pletholax_gracilis -00000000000000000000-0-

Podarcis_sicula ??????????????????????

Pristurus_carteri -0000000000000000-00000---

Pseudogekko_smaragdina -00000000000000000000---

Pseudogonatodes_guianensis -0000000000000000-00000---

Pseudothecadactylus -03333200000000000000---

Ptenopus_carpi -00000000000000000000---

Ptychozoon_kuhli -00000000000000000000---

Ptyodactylus -0000000000000000-00000---

Pygopus_lepidopodus -00000000000000000000---

Python_molurus ????????????????????????

Quedenfeldtia_trachyblepharus -0000110000000000000000---

Ramphotyphlops_braminus ????????????????????????

Rhacodactylus -00000000000000000000---

Rhineura_floridana ????????????????????????

Rhoptropella_ocellata -00000000000000000000---

Rhoptropus_afer -00000000000000000000---

Rhynchoedura_ornata 1000000000-000000000000---

Saltuarius -0333333000000000000---

Saurodactylus_fasciatus -00000000000000000000---

Sphaerodactylus 00000000000000000-00000---

Sphenodon_punctatus ????????????????????????

Stenodactylus_doriae -00000000000000000000---

Strophurus_strophurus -00000000000000000000---

Tarentola_mauritanica 1000000000000000000000---

Tenuidactylus_rohtasfortai -00000000??????????????---

Teratoscincus_przewalskii -00000000-0000000000000---

Teratoscincus_roborowskii -00011100-0000000000000?--

Thecadactylus_rapicauda -000001100000000000000000---

Toropuku_stephensi	-00000000000000000000---
Trachydosaurus_rugosus	????????????????????????????
Trioceros_jacksonii	????????????????????????????
Tropiocolotes_tripolitanus	-00000000000000000000---
Tukutuku_rakiurae	????????????????????????????
Underwoodisaurus_milii	-000111100000000000000---
Urocotyledon_inexpectatus	-00000000000000000000---
Uroplatus_phantasticus	-000011000000000000000---
Uvidicolus_sphyrurus	????????????????????????????
Woodworthia_maculata	-00000000000000000000---
Xantusia_vigilis	????????????????????????????

APPENDIX E: Specimen examined for interspecies size variation

Codes for Institutional Collections: AMB, Aaron M. Bauer, personal collection, Villanova, PN, USA; AMNH, American Museum of Natural History, New York, NY, USA; AMR, Australian Museum, Darlinghurst, NSW, AUS; BMNH, The Natural History Museum, London, ENG**;** CAS, California Academy of Sciences, San Francisco, CA, USA; CMNH, Cleveland Museum of Natural History, Cleveland, OH, USA**;** FMNH, The Field Museum of Natural History, Chicago, IL, USA; JFBM, Bell Museum of University of Minnesota, St Paul, MN, USA; MCZ, The Museum of Comparative Zoology, Cambridge, MA, USA; MTR, Miguel T. Rodrigues, personal collection, São Paulo, SP, BRA**;** QMJ, Queensland Museum, South Brisbane, QLD, AUS; SAM, South Australian Museum, Adelaide, SA, AUS **;** SHSVMH-H, The Sam Houston State Vertebrate Museum, Herpetology Collection, Huntsville, TX, USA; TNHC, Texas Natural History Collection, University of Texas, Austin, TX, USA; UMMZ, University of Michigan Museum of Zoology, Ann Arbor, MI, USA; USNM, National Museum of Natural History, Smithsonian Institution, Washington D.C., USA; WAM, Western Australian Museum, Northbridge, WA, AUS; YPM, Peabody Museum of Natural History, Yale University, New Haven, CT, USA.

Preparation type is indicated according to the following key: C&S = cleared and stained, DI = digital images of specimens, Sk = dry skeleton, and CT = high-resolution X-ray computed tomography.

List of specimens examined (including collection number; preparation; cranial sculpturing score; skull length):

Aeluronyx seychellensis (BMNH 69.5.14.49; Sk; 0; 25.413); *Aeluronyx seychellensis* (CAS 8421; C&S; 0; 19.859); *Aeluroscalabotes felinus* (FMNH 166958; CT; 0; 25.81); *Aeluroscalabotes felinus* (UC MVZ 111777; C&S; 0; 22.08); *Afroedura africana* (CAS 126206; C&S; 0; 14.037); *Afroedura karroica* (CAS 198274; CT; 0; 12.99); *Afroedura transvaalica* (BMNH 1960.1.7.6; Sk; 0; 14.401); *Afrogecko porphyreus* (CAS 175312; CT; 0; 10.75); *Afrogecko swartbergensis* (CAS 180419; C&S; 0; 18.311); *Agamura persica* (BMNH 86.9.21.16; Sk; 0; 19.815); *Agamura persica* (CAS 140562; CT; 0; 18.34); *Ailuronyx seychellensis* (CAS 167459; CT; 0; 26.87); *Alsophylax pipiens* (CAS 143679; CT; 0; 8.49); *Altiphylax levitoni* (121037A; CT; 0; 11.04); *Amalosia rhombifer* (CAS 100919; CT; 0; 11.97); *Apraisia parapulchella* (WAM 62884; CT; 0; 0); *Aristelliger goergeensis* (CAS 176485; 0; CT; 26.33); *Aristelliger lar* (AMNH; Sk; 0;23.98) *Aristelliger nelsoni (A)* (-; CT; 0; 26.73); *Aristelliger praesignis praesignis* (AMNH; Sk; 0; 20.251); *Aristelliger praesignis praesignis* (AMNH; Sk; 0; 21.035); *Aristelliger praesignis praesignis* (BMNH; Sk; 0; 21.407); *Aristelliger praesignis praesignis* (BMNH; Sk; 0; 21.622); *Asaccus elisae* (BMNH; Sk; 0; 17.049); *Asaccus elisae* (CAS 218137; CT; 0; 14.35); *Bavayia montata* (AMS R 77666; C&S; 1; 20.17); *Bavayia robusta* (AMB 7335; CT; 0; 14.72); *Bavayia sauvagii* (CAS 165907; C&S; 1; 14.4); *Blaesodactylus antongilensis* (UMMZ 192320; CT; 1; 22.17); *Blaesodactylus boivini* (CAS 127770; CT; 1; 18.45); *Bunopus crassicauda* (CAS 140598A; CT; 0; 12.82); *Bunopus crassicauda* (CAS 140599; C&S; 0; 12.349); *Bunopus species* (BMNH

1971.1222; Sk; 0; 13.263); *Calodactylodes aureus* (BMNH 7.4.29.1166; Sk; 0; 23.026); *Calodactylodes aureus* (MCZ R-3918; CT; 0; 18.7); *Carphodactylus laevis* (MCZ R-35114; CT; 3; 27.49); Chatogekko amazonicus (AMNH; C&S; 0; 5.631); *Chatogekko amazonicus* (AMNH; C&S; 0; 5.824); *Chatogekko amazonicus* (MTR 12682A; CT; 0; 4.993); *Chondrodactylus anguilfer* (CAS 126466; CT; 1; 21.85); *Chondrodactylus angulifer* (AMNH R-143808; Sk; 1; 23.651); *Chondrodactylus angulifer* (BMNH 1910.4.20.2; Sk; 1; 20.832); *Chondrodactylus bibronii* (CAS 173299; CT; 2; 22.96); *Christinus marmoratus* (CAS 75014; CT; 0; 12.79); *Christinus marmoratus* (R67263; Sk; 0; 12.158); *Cnemaspis boulengerii* (MCZ R-16665; CT; 0; 15.3); Cnemaspis gracils (CAS 113988; CT; 0; 10.21); *Cnemaspis spinicollis* (CAS 103312; CT; 12.79); *Coledactylus brachystoma* (UMMZ 103051; CT; 0; 5.51); *Coleodactylus brachystoma* (MZUSP; C&S; 0; 6.191); *Coleonyx variegatus abbotti* (BMNH 2040; Sk; 0; 14.425); *Coleonyx variegatus* (AMNH R-141105; SK; 0; 15.527); *Coleonyx variegatus* (AMNH R-69090; Sk; 15.503); *Coleonyx variegatus* (AMNH R-74613; Sk; 0; 16.412); *Coleonyx variegatus* (AMNH R-89271; Sk; 0; 16.882); *Coleonyx variegatus* (YPM 14383; CT; 0;0); *Colopus wahlbergii* (CAS 125901; CT; 0; 9.48); *Correlophus ciliates* (JFBM 15825; Osteo; 0; 0); *Crenadactylus ocellatus* (CAS 95287; CT; 0; 9.07); *Cristhinus marmoratus* (R67263; Sk; 0; 12.092); *Crossobamon eversmanni* (CAS 180001; CT; 0; 11.55); *Cryptactites peringueyi* (CAS 186375; CT; 0; 7.32); *Cyrtodactylus ayeyarwadyensis* (CAS 221985; CT; 0; 20.6); *Cyrtodactylus consobrinus* (BMNH 1904.7.19.48; Sk; 0; 31.713); *Cyrtopodion scabrum* (CAS 218186; CT; 0; 13.77); *Dactylocnemis pacificus* (CAS 95146; CT; 0; 15.876); *Delma borea* (USNM 128679; CT; 0; 8.70); *Delma molleri* (AMNH 24852; Sk; 0; 8.427); *Dierogekko insularis*

(r161070; CT; 0; 10.27); *Diplodactylus pulcher* (CAS 75182; CT; 0; 10.96); *Dixonius siamensis* (CAS 95254; CT; 0; 8.1); *Ebenavia inunguis* (CAS 66195; CT; 0; 7.67); *Elasmodactylus tetensis* (AMB 6180; CT; 0; 19.71); *Eublepharis macularis* (AMNH R-89837; Sk; 0; 37.063); *Eublepharis macularis* (AMNH R-89838; Sk; 0; 33.11); *Eublepharis macularis* (BMNH 87.11.2.3; Sk; 0; 21.461); *Eublepharis macularius* (CMNH 67524; CT; 0; 30); Euleptes europaea (MCZ R-4463; CT; 1; 9.72); *Eurydactylodes agricolae* (CAS 232001; CT; 0; 0); *Garthia gaudichaudii* (UMMZ 111574; CT; 0; 9.02); *Garthia penai* (-; C&S; 0; 8.54); *Geckolepis maculata* (CAS 126344; CT; 0; 13.1); *Gehyra marginata* (BMNH 1910.4.26.9; Sk; 1; 23.939); *Gehyra mutilate* (CAS 251893; CT; 0; 10.5); *Gehyra oceanica* (AMNH R-27048; Sk; 0; 17.928); *Gehyra oceanica* (MCZ R-66501; CT; 0; 18); *Gehyra vorax* (CAS 74742; CT; 1; 13.25); *Gekko gecko* (AMNH R-118697; Sk; 1; 40.474); *Gekko gecko* (AMNH R-140787; Sk; 1; 40.501); *Gekko gecko* (AMNH R-141120; Sk; 36.668); *Gekko gecko* (SHSVM-H 0001-2014; CT; 0; 40); *Gekko smithii* (CAS 9595; CT; 1; 42.98); *Gekko vittatus* (CAS SUI 20857; CT; 0; 28.38); *Goggia lineata* (CAS 193627; CT; 0; 7.08); *Gonatodes albogularis* (AMNH; Sk; 0; 9.236); *Gonatodes albogularis* (FMNH 55929; CT; 0; 9.4); *Gonatodes antillensis* (AMNH; C&S; 0; 10.201); *Goniurosaurus araneus* (JFBM 15830; Osteo; 1; 8.8); *Gymnodactylus geckoides* (CAS 49397; CT; 0; 9.64); *Haemodracon riebeckii* (MCZ A-27255; CT; 1; 2.63); *Hemidactylus bowringii* (AMNH R-77529; Sk; 0; 13.703); *Hemidactylus brooki* (BMNH 1978.1472; Sk; 0; 12.4); *Hemidactylus fasciatus* (BMNH 1911.5.291; Sk; 0; 21.719); *Hemidactylus frenatus* (AMNH R-71551; Sk; 0; 13.601); *Hemidactylus frenatus* (AMNH R-71589; Sk; 0; 15.513); *Hemidactylus frenatus* (CAS 215743; CT; 0; 0); *Hemidactylus giganteus* (BMNH 1908.1.29.6; Sk; 1; 30.944);

Hemidactylus lemurinus (BMNH 1977.99; Sk; 0; 17.824); *Hemidactylus mabouia* (AMNH R-102426; Sk; 1; 16.991); *Hemidactylus turcicus* (AMNH R-153733; Sk; 1; 8.385); *Hemidactylus turcicus* (TNHC 85380; CT; 1; 15.51); *Hemiphyllodactylus typus* (CAS 174223; CT; 0; 9.91); *Hemitheconyx caudicinctus* (AMNH R-104409; Sk; 1; 25.23); *Hemitheconyx caudicinctus* (BMNH 1911.7.11.1; Sk; 1; 29.68244); *Hemitheconyx caudicinctus* (CAS 165588; CT; 1; 24.66); *Hemitheconyx taylori* (BMNH 1937.12.5.37; Sk; 1; 24.488); *Heteronotia binoei* (CAS 74923; CT; 0; 12.03); *Holodactylus africanus* (CAS 198932; CT; 1; 19.04); *Homonota andicola* (-; C&S; 0; 12.269); *Homonota borelli* (-; C&S; 0; 9.466); *Homonota darwinni* (-; C&S; 0; 10.471); *Homonota fasciata* (-; C&S; 0; 11.09); *Homonota fasciata* (CAS 84771; CT; 0; 8.83); *Homonota underwoodi* (-; C&S; 0; 11.65); *Homonota uruguayensis* (-; C&S; 0; 10.649); *Homopholis wahlbergii* (CAS 248630; CT; 1; 18.93); *Hoplodactylus cf maculatus* (AMNH R-31547; Sk; 0; 15.981); *Hoplodactylus duvaucelii* (BMNH 61.3.20.11; Sk; 1; 33.611); *Hoplodactylus duvaucelii* (BMNH 62.9.2.18; DI; 0; 0); *Hoplodactylus pacificus* (AMB 482; C&S; 1; 18.505); *Kolekanos plumicaudus* (CAS 248782; CT; 0; 11.1); *Lepidoblepharis xanthostigma* (CAS 178104; CT; 0; 8.51); *Lepidoblepharis xanthostigma* (USNM; C&S; 0; 7.451); *Lepidodactylus lugubris* (CAS 224273; CT; 0; 10.17); *Lialis burtonis* (AMNH R-103872; Sk; 0; 17.808); *Lialis burtonis* (AMNH R-20883; Sk; 0; 24.834); *Lialis burtonis* (FMNH 166958; CT; 0; 28.8); *Lialis burtonis* (USNM 213030; C&S; 0; 17.969); *Lucasium damaeum* (AMB 54; C&S; 1; 15.047); *Lucasium steindachneri* (CAS 75185; CT; 0; 13.14); *Luperosaurus corfieldi* (CAS 182570; CT; 0; 20.81); *Lygodactylus capensis* (CAS 167621; CT; 0; 9.23); *Matoatoa breviceps* (AMNH R-159476; CT; 3; 8.32); *Mediodactylus kotschyii* (CAS

101566; CT; 0; 12); *Microgecko persicus* (UMMZ 122007; CT; 0; 6.72); *Mniarogekko jalu* (CAS A-27255; CT; 0; 29.09); *Mokopirirakau granulatus* (CAS 47982; CT; 0; 21.773); *Nactus pelagicus* (CAS 119003; CT; 0; 15.63); *Nactus pelagicus* (UC MCZ 77610 77615; C&S; 0; 14.062); *Narudasia festiva* (CAS 186278; CT; 0; 8.59); *Naultinus elegans* (AMB 395; C&S; 0; 20.342); *Naultinus elegans* (CAS 47976; CT; 0; 17.986); *Naultinus grayii* (AMB 1766; C&S; 3; 19.782); *Nebulifera robusta* (UMMZ 13164; CT; 0; 21.15); *Nephrurus deleani* (AMB 48; C&S; 0; 20); *Nephrurus deleani* (USNM 292074; Sk; 0; 21.537); *Nephrurus deleani* (USNM 292075; Sk; 0; 20.303); *Nephrurus levis occidentalis* (CAS 254620; CT; 0; 26.22); *Nephrurus levis* (AMNH R-86394; Sk; 0; 20.833); *Nephrurus levis* (BMNH 1908.5.28.24; Sk; 0; 25.122); *Nephrurus milii* (BMNH 1904.10.7.35; Sk; 1; 25.365); *Nephrurus milii* (BMNH 5.10.16.106; Sk; 1; 23.135); *Oedodera marmorata* (AMS 16126; CT; 0; 14.23); *Oedura tyroni* (CAS 75669; CT; 0; 19.314); *Ophidiocephalus taeniatus* (SAMA 45176; CT; 0; 7); *Orraya occultus* (QMJ 60717; CT; 3; 26.25); *Pachydactylus bibonii* (BMNH 1910.4.20.9; Sk; 0; 23.388); *Pachydactylus bicolor* (CAS 223912; CT; 0; 19.43); *Pachydactylus namaquensis* (CAS 186342; C&S; 0; 19.518); *Pachydactylus rangei* (UC MVZ 110498; C&S; 0; 17.884); *Paradelma orientalis* (CAS 77652; CT; 0; 12.46); *Paragehyra gabriellae* (UMMZ 216284; CT; 0; 19.01); *Paroedura stumpffi* (CAS 66192; CT; 3; 17.72); *Perochirus ateles* (CAS 159768; C&S; 0; 15.045); *Perochirus ateles* (CAS 206241; CT; 0; 18.59); *Phelsuma cepediana* (AMNH R-141104; Sk; 0; 8.794); *Phelsuma lineata* (FMNH 260100; CT; 0; 11.78); *Phelsuma madagascariensis* (CAS 13961; C&S; 0; 19.774); *Phyllodactylus baurii* (CAS 9501; CT; 0; 10.3); *Phyllodactylus hasselquistii* (BMNH; Sk; 0; 19.538); *Phyllodactylus hasselquistii* (UC MVZ; C&S; 0; 20.187);

Phyllodactylus pollicaris (-; C&S; 0; 17.781); *Phyllodactylus tuberculosus* (AMNH; Sk; 0; 15.176); *Phyllodactylus tuberculosus* (BMNH; Sk; 0; 23.913); *Phyllodactylus wirshingi* (CAS; C&S; 0; 17.31); *Phyllodactylus xanti* (AMNH; Sk; 0; 12.724); *Phyllopezus lutzae* (MCZ R-46191; CT; 1; 18.1); *Phyllurus platurus* (AMS no data; C&S; 3; 24.68); *Phyllurus platurus* (MCZ R-130254; CT; 3; 27.43); *Pletholax gracilis* (MCZ R-187676; CT; 0; 7.61); *Pristurus carteri* (BMNH; Sk; 0; 17.908); *Pristurus carteri* (CAS 193627; CT; 0; 13.83); *Pristurus insiguis* (BMNH; Sk; 0; 15.544); *Pseudogekko brevipes* (CAS 128978; C&S; 0; 12.142); *Pseudogekko smaragdinus* (CAS 62344; CT; 0; 15.15); *Pseudogonatodes barbourin* (MCZ R- 14385; CT; 0; 5.33); *Pseudogonatodes guianensis* (MZUSP; C&S; 0; 6.557); *Pseudothecadactylus australis* (MCZ R-35162; CT; 3; 26.86); *Pseudothecadactylus lindneri* (AMB 1765; C&S; 0; 25.63); *Ptenopus carpi* (CAS 214548; CT; 0; 13.05); *Ptenopus garrulus* (UC MVZ 142062; C&S; 0; 10.051); *Ptychozoon kuhli* (UMMZ 65570; CT; 0; 21.64); *Ptyodactylus hasselquistii* (CAS 228536; CT; 0; 22.54); *Pygopus lepidopodus* (AMNH R-140843; Sk; 0; 20.6); *Pygopus lepidopodus* (CAS 135450; CT; 0; 19.74); *Pygopus nigriceps* (AMNH R-24915; Sk; 0; 16.93); *Quedenfeldtia trachyblepharus* (CAS 123275; CT; 1; 11.516); *Quedenfeldtia trachyblepharus* (UC MVZ; C&S; 1; 10.196); *Ramigekko swartbergensis* (CAS 180418; CT; 0; 16.45); *Rhacodactylus auriculatus* (CAS 205486; CT; 0; 25.32); *Rhacodactylus ciliates* (BMNH 85.11.16.7; Sk; 0; 32.726); *Rhacodactylus trachyrhynchus* (BMNH 86.3.11.4; C&S; 0; 37.96); *Rhoptropella ocellate* (CAS 193865; CT; 0; 9.56); *Rhoptropus afer* (AMB 1872; C&S; 0; 13.536); *Rhoptropus afer* (BMNH 1937.12.3.60; Sk; 0; 14.013); *Rhoptropus afer* (CAS 193865; CT; 0; 13.28); *Rhynchoedura ornate* (UMMZ 124484; CT; 0; 10.51); *Saltuarius salebrosus* (CAS

74742; CT; 3; 35.36); *Saurodactylus fasciatus* (CAS 92404; CT; 0; 6.497); *Saurodactylus mauritanicus* (BMNH; Sk; 0; 8.038); *Sphaerodactylus ariasae* (USNM 541810; CT; 0; 4.53); *Sphaerodactylus glaucus* (UC MVZ; C&S; 0; 6.993); *Sphaerodactylus glaucus* (UC MVZ; C&S; 0; 7.308); *Sphaerodactylus klauberi* (UPRRP; C&S; 0; 7.278); *Sphaerodactylus richardsoni* (BMNH; Sk; 0; 10.019); *Sphaerodactylus torrei* (AMNH; Sk; 0; 9.178); *Stenodactylus arabicus* (BMNH 1978.1349; Sk; 0; 9.595); *Stenodactylus doriae* (BMNH 1971.1191; Sk; 0; 18.242); *Stenodactylus doriae* (CAS 250946; CT; 0; 19.145); *Stenodactylus khobarensis* (BMNH 171.1733; Sk; 0; 13.343); *Stenodactylus petrii* (BMNH 1917.3.31.1; Sk; 0; 9.1); *Strophurus strophurus* (CAS 254623; CT; 0; 14.93); *Tarentola Americana* (AMNH; Sk; 1; 22.93); *Tarentola annularis* (BMNH; Sk; 0; 22.827); *Tarentola boreneensis gigas* (BMNH; Sk; 1; 20.687); *Tarentola mauritanica* (AMNH; Sk; 1; 17.216); *Tarentola mauritanica* (CAS 87112; CT; 1; 14.83); *Teniudactylus caspius* (BMNH 90.9.22.0.13; Sk; 0; 15.508); *Tenuidactylus fedtschenkoi* (CAS 182955; CT; 0; 16.91); *Teratoscincus microlepis* (AMNH; Sk; 0; 13.898); *Teratoscincus microlepis* (BMNH; Sk; 0; 16.918); *Teratoscincus przewalskii* (CAS 17101; CT; 0; 22.35); *Teratoscincus scincus* (BMNH; Sk; 0; 19.522); *Thecadactylus rapicaud* (AMNH; Sk; 1; 19.709); *Thecadactylus rapicauda* (AMNH; Sk; 1; 23.883); *Thecadactylus rapicauda* (AMNH; Sk; 1; 24.758); *Thecadactylus rapicauda* (BMNH; Sk; 1; 27.076); *Thecadactylus rapicauda* (CAS 95146; CT; 1; 23.49); *Toropuku stephensi* (CAS 47986; CT; 0; 18.825); *Tropiocolotes triolitanus* (CAS 123467; CT; 0; 10.07); *Tropiocolotes triplolitanus* (BMNH 97.10.28.7; Sk; 0; 9.024); *Underwoodisaurus milii* (CAS 74744; CT; 1; 23.21); *Urocotyledon inexpectata* (UMMZ 168104; CT; 0; 9.68); *Uroplatus fimbriatus* (AMNH R-2235; Sk; 0; 37.448); *Uroplatus fimbriatus*

(BMNH 61.3.20.9; Sk; 0; 48.5); *Uroplatus phantasticus* (CAS 250492; CT; 1; 54.8); *Woodworthia maculatus* (CAS 228536; CT; 0; 16.127)

VITA

Education

Aug. 2018 Iowa State University in Ames, Iowa
Enrolled in Ecology, Evolution and Organismal Biology Ph. D program

Aug. 2016 – Aug. 2018 Sam Houston State University in Huntsville, TX
Masters of Science – Biology

Jan. 2014 – Dec. 2015 Sam Houston State University in Huntsville, TX
Bachelors of Science - Psychology with minor in Biology

Jan. 2013 – May 2013 Montgomery County Community College in Rockville, MD
Non-degree

Aug. 2011 – May 2012 Collin County Community College in McKinney, TX
Non-degree

Aug. 2008 – May 2013 Blinn College in Bryan, TX
Associates of Arts - Biology

Technical Skills

Experience with digital X-ray systems (Amphibian and reptile division at the Smithsonian Institution National Museum of Natural History).
Experience fixing and preserving herpetological specimens.
Experience with classic histological sectioning and staining methods.

Software Abilities

Three-dimensional analysis software including Avizo, Avizo lite, Amira, Dragonfly, and Volume Graphics Studios.
IBM SPSS predictive analytics.
Phylogenetic analysis software including Mesquite, Winclada, FigTree, and TNT.
Sequence alignment software such as M.U.S.C.L.E., T-Coffee, MAFFT, as well as corresponding software, including: Geneious and C.I.P.R.E.S.
Adobe Creative Suite Programs.
ImageJ

Publications

Bauer, A. M., Beach-Mehrotra, M., Bermudez, Y., Clark, G., Daza, J. D., **Glynne, E.**, Hagyari, D., Harnden, J. M., Holovacs, N., Kanasiro, A., Lofthus, A. J., Pierce, Z. W., Aaliyah, R., Syed, S., Vallejo-Pareja, M. C., and B. A. Walker. The tiny skull of the Peruvian gecko *Pseudogonatodes barbouri* [Gekkota: Sphaerodactylidae]. (Accepted 2/1/2018 for South American Journal of Herpetology).

Publications – In Preparation

Glynne, E., Daza, J. D., Bauer, A. M. Bone sculpturing in Gekkota. (Anatomical Record).
Glynne, E., Daza, J. D., Bauer, A. M. Skull anatomy of the Thickhead Rock Gecko (*Bunopus crassicauda* NIKOLSKY 1907, Gekkonidae, Sauria) using a High-Resolution CT Scan. (Asian Herpetological Research Journal).
Glynne, E., Daza, J. D., Bauer, A. M. Alternative configurations of the lacrimal foramen in geckos. (Biological Journal of the Linnean Society).

Scholarships, Grants, and Awards

2018 Ecology and Evolutionary Biology Fellowship at Iowa State University
2017 Travel grant from Gans Collections and Charitable Fund to attend JMIH 2017.
2017 Travel grant from Royal Microscope Society to attend T.o.S.c.A.- North America.
2017 Travel grant from Dean of Science at Sam Houston State University.
2015 Travel grant from Gans Collections and Charitable Fund to attend JMIH 2015.
2015 Fall, Dean's List of Academic Honors

Conferences & Presentations

The Society for Integrated & Comparative Biology (SICB), San Francisco Marriott Marquis in San Francisco, California. January 3-7, 2017, poster presentation: Kanasiro, A., Glynne, E., Daza, J. D., Bell, C. J., Maisano, J. A., Gamble, T., and Bauer, A. M. 2018. Learning to Fly: skeletal evolution in gliding geckos.

Joint Meeting of Ichthyologists and Herpetologists (JMIH), Renaissance Hotel in Austin, Texas. July 12-16, 2017, poster presentation: Glynne, E., Daza J. D., and Bauer, A. M. 2017. Alternative configurations of the lacrimal foramen in geckos.

Tomography for Scientific Advancement (ToSCA), University of Texas in Austin, Texas. June 6-8, 2017, poster presentation: Glynne, E., Daza, J. D., and Bauer, A. M. 2017. Establishing the variation of dermal sculpturing within Gekkota.

Joint Meeting of Ichthyologists and Herpetologists (JMIH), Marriott Hotel in New Orleans, Louisiana. July 6-10, 2016, attendee.

58th annual meeting of Society for the Study of Amphibians and Reptiles at University of Kansas, Lawrence, Kansas, July 30- August 2, 2015, poster presentation: Glynne, E., Daza J. D., Bauer, A. M. 2015. Gekkota Skulls: taking the rough with the smooth.

Workshops

Using Volume Graphics Studio. Workshop at University of Texas in Austin. Austin, Texas. June 5, 2017, attendee.

Using Aviso. Workshop at University of Texas in Austin. Austin, Texas. June 5, 2017, attendee.

Tree Analysis using New Technology (TNT) Workshop with J. Salvador Arias at Sam Houston State University. Huntsville, Texas, December 12-14, 2016, attendee.

The Austin Working Group advancing contrast-enhanced CT Imaging in the Biological Sciences at The University of Texas at Austin and the High-Resolution X-ray CT Facility, April 2-3, 2015, attendee.

Society and Organization Memberships

2017 – Present	(Member)	Society for Integrative and Comparative Biology
2017 – Present	(Member)	American Society of Ichthyologists and Herpetologists
2017 – Present	(Member)	Herpetologists League
2017 – 2018	(President)	Biological Sciences Graduate Student Organization
2016 – 2017	(Member)	
2016 – Present	(Member)	Texas Academy of Science
2015 – Present	(Member)	Society for the Study of Amphibians and Reptiles

Museum Experience

National Museum of Natural History, Smithsonian Institution (Washington, DC). Digital X-rays using a MCI's Philips MOD 301/4 X-ray tube machine for 100 gecko specimens, Jul. 31- Aug. 4, 2017.

National Museum of Natural History, Smithsonian Institution (Washington, DC). Digital X-rays using a MCI's Philips MOD 301/4 X-ray tube machine for 400 gecko specimens, Mar. 13-17, 2017.

Sam Houston State University. Herpetological specimen identification and cataloging.

National Museum of Natural History, Smithsonian Institution (Washington, DC). Digital X-rays using a MCI's Philips MOD 301/4 X-ray tube machine for 200 gecko specimens and 50 skinks, Dec. 14-21, 2014.

Teaching Experience

Sam Houston State University — Jan. 2017 – May 2017
Graduate Teaching Assistant – Contemporary Biology

Sam Houston State University — Aug. 2016 – Dec. 2016
Graduate Teaching Assistant – Zoology & Botany

Sam Houston State University — Aug. 2014 – May 2015
Undergraduate Teaching Assistant – Zoology

Volunteer Experience

February 17, 2018. Girls in STEM event hosted by Houston Museum of Natural Sciences: participant, hosted a table with the B.S.G.S.O. to educate about the biodiversity and effect of invasive species.

November 4, 2017. Girls in STEM Event at Klein ISD: assisted with booth set up and tear down, spoke with girls grades 3 – 8 to educate about biological sciences as well as being a woman in STEM.

July 7, 2017: Assisted Texas Invasive Species Institute with a public education event: assisted with set up and tear down of booth, informed attendees about biodiversity of Texas as well as informed regarding invasive species.

August 19, 2017. Assisted with Graduate Orientation at S.H.S.U.: welcomed new graduate students and assisted with checking them in as well as with the set up and tear down of the event.

February 18, 2017. Girls in STEM event hosted by Houston Museum of Natural Sciences: participant, hosted a table with the B.S.G.S.O. to educate about the biological sciences.

December 2, 2016. Participant of a Women in Stems Panel hosted by S.H.S.U.: 8th graders visited with us and asked us questions regarding college experience and being a woman in STEM.

Field Experience

Puerto Rico, USA. May 11– 21, 2016. Led by Dr. Juan D. Daza. Herpetological survey of amphibians and reptiles from Puerto Rico and Culebra Island.

Zimbabwe, Africa. May 31 – June 30, 2015. Led by Dr. Monte Thies and Dr. Jeffrey Wozniak.